Complementarity underlies forest function: diversity as a facet of compensation and stability

Sarah Gould Bruner

Submitted in partial fulfillment of the
requirements for the degree of
Doctor of Philosophy
under the Executive Committee
of the Graduate School of Arts and Sciences

COLUMBIA UNIVERSITY

2024

© 2024

Sarah Gould Bruner

All Rights Reserved

Abstract

Complementarity underlies forest function: diversity as a facet of compensation and stability

Sarah Gould Bruner

Forests face an unprecedented range of disturbances from climate change, introduced pests and pathogens, and novel species, which frequently interact causing severe consequences to forest communities and ecosystem function. Understanding the mechanisms by which forests recover from disturbance and maintain stability of function is not only an issue of ecological interest, but one of pressing human need, as forest functioning is involved in maintaining a suite of ecosystem services that provide for humanity, including the global carbon and water cycles. Using an experimental manipulation of tree species diversity within an oak-dominated temperate northeastern deciduous forest, this dissertation broadly asks: how do forest community biomass and diversity influence stability and magnitude of forest community growth and water use? All three chapters are based on data from the same forest, where four treatments had previously been established by trunk girdling, which kills a tree by severing the cambium and sapwood, but leaves it standing, similar to the effect of many pathogens on trees. The treatments represent a range of species richness (2-10 species), biomass (5.5×10^4 kg/ha to 7.1×10^5 kg/ha), and level of disturbance, with experimental plots losing anywhere from zero to 94% of their living biomass. **Chapter 1** focuses on competitive release after the loss of a dominant species using an annual census of trees over the last 10 years. Community level growth rates showed that diversity positively influenced biomass recovery rate. **Chapter 2** addresses the role of the tree community's biomass and diversity on soil water content using soil moisture sensors, which have recorded data hourly for two years, as well as the trees' water stress, by using foliar stable carbon

isotope ratios. Here, diverse communities have higher and more stable levels of soil water as well as trees that are less water stressed. Using the same long term data as Chapter 1, **Chapter 3** assesses whether growth in the tree communities has been more stable over the past 10 years, and investigates whether this can be explained by shorter term fluctuations in tree growth measured by automated point dendrometers. While more diverse communities are more stable in their growth rates over time, this was strongly dependent on how much of the original community had been mechanically girdled. Species showed complementarity in phenology of tree growth at the seasonal scale, but our models could not directly link this intra-annual complementarity in more diverse communities to the stability seen over 10 years. Taken together, results from these three chapters suggest that diversity plays a role in mediating recovery of function from disturbance, which has implications for both the global carbon and water cycles.

Table of Contents

List of Charts, Graphs, Illustrations iii

Acknowledgments v

Dedication vii

Introduction 1

Chapter 1: Stand diversity mediates rate of biomass recovery after loss of the dominant tree genus in a temperate forest 5

1.1 Introduction 5

1.2 Methods 8

1.3 Results 13

1.4 Discussion 16

1.5 Tables and Figures 21

Chapter 2: Tree diversity increases soil water drying rate constants, but raises and stabilizes soil water minima 27

2.1 Introduction 27

2.2 Methods 30

2.3 Results 38

2.4 Discussion 43

2.5 Tables and Figures 49

Chapter 3: Diversity stabilizes forest growth rates via phenological complementarity: A long-term experimental test of the portfolio effect in oak-dominated forests 62

3.1 Introduction 62
3.2 Methods 65
3.3 Results 71
3.4 Discussion 73
3.5 Conclusions 77
3.6 Tables and Figures 79
References 85
Appendix A: Supplementary Information for Chapter 1 99
Appendix B: Supplementary Information for Chapter 2 101
Appendix C: Supplementary Information for Chapter 3 103

List of Charts, Graphs, Illustrations

Chapter 1

Table 1.1 *Linear mixed effects models for effects of biomass and species richness on relative plot growth and the interaction between species and treatment on relative tree growth*.....21

Table 1.2 *Summary of effects of oak girdling treatment on biomass compensation* 21

Figure 1.1 Schematic of treatment layout at Black Rock Forest 22

Figure 1.2 Non-metric dimensional scaling for species biomass at the experimental forest plots at Black Rock Forest, NY 23

Figure 1.3 Plot biomass and growth following oak girdling. 24

Figure 1.4 Partial residual plots from two separate linear mixed effects models showing the effects of plot aboveground biomass and species richness on relative plot growth 25

Figure 1.5 Coefficient plot of the effect of the interaction between species and treatment on tree relative growth. ...26

Chapter 2

Table 2.1 *Metrics derived from analyses of terrestrial lidar point clouds using the lidR R package*.....49

Table 2.2 *AIC for linear mixed effects models with minimum soil water as the response variable* 50

Table 2.3 *AIC for linear mixed effects models with drying rate decay constant (drying rate constant) as the response variable*.....51

Table 2.4 *AIC for linear mixed effects models with soil water loss as the response variable*.....52

Table 2.5 *Results for multiple linear models with either the coefficient of variation (CV) of minimum soil water or soil water loss as the response variable.* 53

Figure 2.1 Experimental layout and conceptual diagram of analyses 54

Figure 2.2 Forrest community biomass and species distribution and principal component biplot of stand metrics 57

Figure 2.3 Partial residual plots from separate linear mixed effects models showing effects on minimum soil water, drying rate constant, and soil water loss 58

Figure 2.4 Coefficient of variation (CV) for minimum soil water (a) and soil water loss (b) against the dominance diversity axis.....60

Figure 2.5 Relationship between mean leaf $\delta^{13}C$ for 2020-2022 and mass-weighted Shannon diversity of the tree community. 61

Chapter 3

Table 3.1 *Number of trees with dendrometers, by species.* 79

Table 3.2 *Linear mixed effects models for individual tree relative growth based a zero-growth model for hourly or daily measurements.* 80

Figure 3.1 Relationship between the coefficient of variation (CV) of a forest communities' annual relative growth and the number of species in the community 81

Figure 3.2 Day of year for start of the growing season for each species in 2021 and 2022. 82

Figure 3.3 Effect of vapor pressure deficit on growth phenology of different species 83

Figure 3.4 Relationship between relative growth and hour of day, by species as measured by automated point dendrometers. 84

Appendices

Figure S1.1 Relationships between the percentage of the original plot's biomass lost due to girdling with number of years to biomass compensation and percentage of biomass gained 99

Figure S1.2 Total biomass accumulation for all species in the years following the girdling treatments, 2010-2020. 100

Figure S2.1 Non-metric dimensional scaling (NMDS) for species biomass at the experimental forest plots at Black Rock Forest, NY in 2007 and in 2020 101

Figure S2.2 Ratio of carbon-13 to carbon-12 ($\delta^{13}C$) by species and position on hill slope 102

Figure S3.1 Annual growth of different species as measured by dendrometers. 103

Figure S3.2 Effect of vapor pressure deficit on growth (mg/day) phenology of different species 104

Figure S3.3 Relationship between relative growth, hour of day and VPD, by species, as measured by automated point dendrometers. 105

Acknowledgments

Any dissertation is a journey. My advisors, Kevin and Shahid, have championed me along it with endless enthusiasm. I would like to thank Kevin and Shahid, who are both not only amazing scientists with profound knowledge in their respective fields, but also wonderful human beings. They have pushed me to deepen my science without losing my humanity. Also, they are a lot of fun. My committee, Duncan, Jan, and Bill, have encouraged me to think precisely about the natural world, even when I have put them on some very tight timelines.

The "distracted, but enthusiastic" members of the Naeem-Palmer lab, Sebastian, Krishna and Ivan as well as Steph, Patrick, Roi, Suzanne, Mukund, and Anouch, make science not only something we are all interested in, but a truly enjoyable process. My thanks additionally to Ya-Hsuan, my brother Aaron, and Isobel in particular for coming through at key moments to discuss the finer details of communication with the written word. Krishna has advised, supported, and encouraged me at every step, turn, and climb – even from half way across the world – and for her wisdom and humor I am grateful.

My experiment would not be up and running if not for the help of my brother Jeremy, Ivan, and Jeremy H.; or maybe it would, but I would be a little sadder. And, of course, truly none of this work would have been possible without the immense help and support of the Black Rock Forest staff: Bill, Katie, Aaron, Matt M., Matt B., and Aidan. I have spent some truly enjoyable days in the field with all of them. Black Rock Forest is always a beautiful place, but during 2020 and 2021, when New York City was shut down from the COVID-19 pandemic, it was also a place of refuge for me. Thank you to the Black Rock staff for keeping it alive as a place of learning and respite.

Lastly, it is well possible I would have dissolved into an incoherent pile of goo without the good humor, patience, and steadfast support of Akio, who will never accept his own awesomeness.

Dedication

For Z, friend and writing gnome.

Introduction

Over a century of ecological research has defined stability as a multidimensional construct (Hillebrand et al., 2018; Kéfi et al., 2019) and, while theory predicts a suite of underlying mechanisms, how best to quantify them in real world communities remains an area of active research (Dallas & Kramer, 2022; Gonzalez & Loreau, 2009; Wang et al., 2021). Organisms face a broad range of disturbances, from both biotic and abiotic factors in their environment. The community of organisms comprising an ecosystem determines its ability to retain function over time (Cardinale et al., 2012), though the way this is measured and reported is highly variable (Donohue et al., 2016). Species diversity, while infrequently the dominant contributor to stability, plays a nonetheless important – and quantifiable – role (Pennekamp et al., 2018). Though much of the empirical work describing biodiversity-stability relationships has been conducted in grasslands, the theory that underpins the connection between species and stability of community functioning should be applicable to ecosystems worldwide (Loreau & de Mazancourt, 2013).

The assessment of stability is critically dependent on temporal scale, as short-term losses or gains may not represent the overall trends of longer time periods. In the absence of long-term manipulative studies (e.g. Tilman, Reich, & Knops, 2006), trees can offer a way to connect long and short timescale responses to environmental fluctuations within a single organism. Trees are some of the longest-lived individual organisms, recording centuries of historical climate in their annual growth (Rao et al., 2020), yet also respond to environmental conditions over the course of the season or even the day (Krejza et al., 2022). Global climatic drivers, catalyzed by human activities, are rapidly shifting from historical norms, while humanity itself is critically dependent on the continued stable functioning of forests themselves: forests represent a significant portion

of the global carbon sink and human societies rely on them for continued provisioning of potable water (Gentine et al., 2019; Tague et al., 2019). As we enter an era of novel plant and climate interactions, it becomes increasingly challenging to predict how forests will respond to new species introductions, or loss of existing species to pests, pathogens, and changes in climate. Since continued functioning of the world's forests is critical for global water and biogeochemical cycling (Bonan, 2008), habitat for species (Laurance et al., 2002), and human livelihoods (Foley et al., 2005), understanding why stability is an emergent property of some communities but not others remains a focus not just for theoretical, but also applied scenarios.

While much is understood about individual tree response to perturbations such as drought, relatively little may be known about the effects of the same disturbance at the stand level (Clark et al., 2016). The mechanics by which drought or pests cause mortality has been well studied in individual trees, but how an ecosystem might respond to broad-scale mortality of trees is what this dissertation research seeks to address. Temperate forests are often dominated by a single or several congeneric species which strongly influence ecosystem functioning (Ellison, 2019). Loss of such species, often termed "dominant species," is therefore likely to have complex, potentially dramatic impacts on forests, but the duration and magnitude of these impacts likely depends on how remaining non-dominant, or subordinate, species influence community function (Chaves & Smith, 2021; Mariotte et al., 2013; Pan et al., 2016). While forests provide a number of services to humanity, this study focuses on two processes, both quantifiable at multiple scales and both relevant to provisioning and sustaining service to humanity: the magnitude and stability of growth and the feedback between the tree community and soil water. Understanding the mechanisms by which the ecosystem functions of forests alter

in response to changes in community composition is a critical ecological component for predicting the future of our forests and the stability of the ecosystem services they provide.

Focusing on an experimental manipulation of tree species diversity and biomass within a temperate forest in the northeastern United States, this dissertation examines how tree diversity affects stand growth at longer time scales, stand water use at short time scales, and how species-specific growth may impact stability of community growth. The experimental forest communities in this study represent a range of diversity as well as different degrees of disturbance as, in order to manipulate diversity, trees were trunk-girdled. Girdling kills a tree by severing the cambium and sapwood, but leaves it standing, similar to the effect of many pathogens on trees. Chapter 1 examines the role of subordinate species in forest community biomass recovery after the loss of a dominant species. Chapter 2 looks at the effect of tree diversity on soil water as well as on the water stress within the tree community. Chapter 3 explores a potential mechanism underlying long term community stability: the differential response of different tree species to environmental conditions. Taken together, these chapters show that diversity plays a role in the ecosystem processes of recovery after loss of a dominant species, and ecohydrology, either by higher and more stable growth rates, more consistent soil water environment, or complementary growth strategies.

While this study broadly examines the influence of tree diversity on forest function and thus has relevance to other ecosystems, it is also place-based ecology. It focuses on a particular forest within New York State and, specifically, the potential devastating consequences of large scale mortality of the dominant tree taxa. Unfortunately, this possibility is not remote or even uncommon: such devastation is not localized to temperate forests within the northeastern United States, but is becoming an increasingly widespread global phenomenon. As humanity continues

to alter the climate and often homogenize global communities, understanding how forest communities respond to change becomes critical for predicting both the future of the forests themselves and the services they provide.

Chapter 1: Stand diversity mediates rate of biomass recovery after loss of the dominant tree genus in a temperate forest

Sarah G. Bruner, Shahid Naeem, Jan U. H. Eitel, Kevin L. Griffin, Duncan N. L. Menge, Mukund P. Rao, Katherine Terlizzi, William S. F. Schuster.

1.1 Introduction

The prevailing characteristics of many ecosystems are governed by one or a few congeneric species. The mechanism for this control varies from predation (e.g., keystone predators (Paine, 1966)), to niche construction which influences other species (e.g. ecosystem engineers (Erwin, 2008; Jones et al., 1994)), to competitive dominance where a particular taxon contributes the majority of biomass in a community (e.g. dominant or foundation taxa (Dayton, 1972; Ellison et al., 2005; Grime, 1998)). By contributing the preponderance of biomass, dominant species define the form and function of their ecosystems: the physical structure, ecosystem functioning, biogeochemistry, and biodiversity of their communities (Avolio et al., 2019; Dayton, 1972; Ellison, 2019; Grime, 1998; M. D. Smith & Knapp, 2003). Though dominant species are both abundant locally and common regionally, they are nonetheless often at risk of being rapidly lost due to shifts in the environment and introduced pests and pathogens (Gaston, 2010).

The loss of dominant species, not surprisingly, can dramatically and rapidly alter an ecosystem's properties, but the duration and extent of such impacts are infrequently studied (Avolio et al., 2019). The magnitude of the effect of dominant species loss depends on the physiology, morphology, and ecology of the non-dominant species that remain (Chaves & Smith, 2021; Mariotte et al., 2013; Pan et al., 2016). These subordinate species may experience

competitive release after dominant species loss which can result in compensatory growth by the remaining species, defined here as the extent to which the community regains biomass relative to pre-loss levels (Adler & Bradford, 2002). As species contributions to ecosystem function can be biomass dependent (Gaston, 2010; Grime, 1998), compensation is a key component of functional recovery. Studies in grasslands have demonstrated increased growth at the community level from various mechanisms attributable to increased levels of diversity: niche complementarity, species identity, and overyielding (Gonzalez & Loreau, 2009; Marquard et al., 2009). Such diversity effects, however, are sensitive to environmental factors like precipitation and nutrient availability (Hallett et al., 2014; Hautier et al., 2014), which makes predicting both biomass recovery dynamics and the future of a community post dominant species loss challenging, particularly at temporal scales appropriate for long-lived species such as trees (Jucker et al., 2014) and at spatial scales relevant to management (Gonzalez et al., 2020; Wang & Loreau, 2014).

The amount of biomass lost within a system greatly influences compensation timescales, with forests being the most impacted (Fu et al., 2017) due to the sheer magnitude of biomass lost. The slow decline and emergence of another dominant taxon is often part of natural succession dynamics within a forest, yet the dramatic loss of dominant tree species is not uncommon. Some well-known examples include: the decimation of American chestnuts (*Castanea dentata*), western North American oaks (*Quercus* spp.), northern-hemisphere elms (*Ulmus* spp.), and ʻōhiʻa (*Metrosideros polymorpha*) by pathogens (Asner et al., 2018; Brasier & Buck, 2001; Ellison et al., 2005; Pellegrini et al., 2021), and eastern and Carolina hemlock (*Tsuga canadensis* and *T. caroliniana*) by the wooly adelgid (*Adelges tsugae*) (Orwig et al., 2002), as well as rapid decline of quaking aspen (*Populus tremuloides*) (Smith et al. 2011) after fire suppression and climate-sensitive species such as yellow cedar (*Callitropsis nootkatensis*) following snow to rain

transitions (Buma et al., 2017). Unsurprisingly, the real-world dynamics of dominant tree species loss have been little studied experimentally due to the substantial effort necessary in eradicating large numbers of trees and continued censusing of the remaining community, as well as long temporal scales required to assess recovery (Avolio et al., 2019). Though trees may take decades to reach the canopy, trajectories for biomass recovery may still be inferred at smaller timescales (Bahamondez & Thompson, 2016), though very short study periods, previous land use history, and recovery of multiple ecosystem functions may complicate predictions (Meli et al., 2017; Norden et al., 2015; Royo et al., 2016). Whether and by what mechanism the subordinate species might compensate for the loss of aggregate forest function, including biomass, remains an open question, yet understanding compensatory dynamics is critical for predicting the short- and long-term consequences of dominant species loss for forests.

Though the positive effects of biodiversity and detrimental effects of depauperate communities on productivity have been comparatively well explored (Cardinale et al., 2012), biodiversity's influence on compensation when the majority of biomass has been lost is less well understood. Studies with short-lived species suggest characteristics of subordinate species (e.g. conservative resource acquisition, high functional diversity, and resistance to climatic perturbations) may mediate the system's biomass recovery from disturbance (Lipoma et al., 2016; Mariotte et al., 2013). Whether this finding holds true for long-lived species such as forest trees, remains largely unexplored. Here, using a long-term (15 year) experimental reduction of the dominant species, oaks (*Quercus spp.*), in a temperate forest within the northeastern United States, we explored whether species richness, species identity, and aboveground biomass of the non-dominant species influenced the rate of biomass recovery after significant reductions in the presence of the dominant oaks. If competitive release is occurring for subordinate species

following the removal of the dominant oaks, a community's growth should be inversely related to initial aboveground biomass; i.e., communities which lost a large number of oaks and thus have a low initial biomass should grow faster than undisturbed plots. We tested whether growth rates among replicate plots were positively associated with diversity of the remaining community because of either a) selection effects, i.e., a greater probability that one or more species in a diverse subordinate species pool would compensate for dominant species loss or b) complementarity, where a more diverse pool of subordinate species is indicative of greater complementarity between species which leads to greater efficiency of resource use. Collectively, our findings support the argument that the biodiversity of non-dominants will determine the rate of ecosystem recovery after dominant species loss.

1.2 Methods

Site characteristics

Black Rock Forest (BRF) is located in the Hudson Highlands region of southeast New York State, USA (41°24′ N, 74°01′ W). While the mean annual air temperature is 9.7 ºC, air temperature is quite seasonal, with mean monthly temperatures ranging from 24 ºC to -2.1 ºC (NOAA, 2020). Mean annual precipitation is 1.3 m and the topography is relatively sloped (10-30º). Soils are moderately to excessively drained, rocky and shallow, with 0-60 cm to lithic bedrock (approximately 60% of site) and 35-90 cm to fragipan (approximately 35% of site) (Soil Survey Staff, USDA 2022). This deciduous temperate forest is dominated by oak species (*Quercus spp.)* which make up approximately 70% of the canopy trees (Schuster et al., 2008). Oak species present include white oak (*Quercus alba*), red oak (*Q. rubra*), chestnut oak (*Q. montana*), and black oak (*Q. velutina*). Common subordinate species are red maple (*Acer*

rubrum), sugar maple (*A. saccharum*), black birch (*Betula lenta*), American beech (*Fagus grandifolia*), and black gum (*Nyssa sylvatica*). Before BRF was established as a research forest in 1927, much of the area had been repeatedly logged for approximately the previous 200 years.

Experimental setup

Twelve 75 m by 75 m experimental plots, assigned to one of four treatments, were laid out in a three by four grid on the north slope of Black Rock Mountain in 2006 (Fig. 1.1). The layout is a semi-randomized block design grouped by slope position (low, middle and high), where each treatment is repeated once within each of the slope positions, for a total of three replicates per treatment. In 2008, each plot received one of three oak-loss treatments: 0% of the trees girdled (control), 50% (by stem number) of oak trees girdled, and 100% of oaks girdled. Trees were girdled using a chainsaw cutting 3-5 cm into the trunk of the tree to sever phloem transport (Noel, 1970), mimicking the mechanism by which many pathogens block the vertical flow of nutrients. Girdled trees were left standing if greater than 10 cm at 1.3 m (diameter at breast height (DBH)) and felled if they were smaller. Trees that continued to leaf out were girdled a second time in 2010. Each plot was divided into nine 25 m by 25 m subplots; all live oak trees within a plot and all live trees within the central subplot have been censused annually since 2006 (except for 2014) to establish species identity, record sprouting, assess tree health (alive or dead via leaf presence), and measure the DBH of living trees. New trees were added to the census once they reached 1 cm DBH.

Calculations and Statistical Analyses

All analyses were conducted on the central 25 m by 25 m subplot (hereafter, plot) of the 0%, 50%, and 100% oak girdled plots to create a 50 m buffer between plots (Fig. 1.1). Trees which died before 2020 were excluded from the analysis as were trees less than 10 cm DBH to

focus on the existing trees which represent the rate of living aboveground biomass recovery, instead of the processes of mortality and recruitment. All analyses were performed using R Statistical Software (v4.1.3; R Core Team 2022).

Community composition and biomass accumulation

The tree communities, which may be represented by the biomass of each species forming one axis within multidimensional space, can be shown in two dimensions using Non-Metric Multidimensional Scaling (NMDS). NMDS was run on the census data for species biomass for all years 2007-2020 individually, to establish that there were no systematic differences between treatments before the experiment began in 2008, to determine if the girdling resulted in differences between treatments, and to see if those differences persisted until 2020. NMDS minimizes the difference between observed (multi-dimensional) and fitted (two-dimensional) rank-order, but usually several potential solutions exist. NMDS analyses used multiple iterations with previous best solutions to avoid local minima and were performed with the *vegan* package (Oksanen et al., 2010). Best solutions were compared to each other via Procrustes root-mean-square error to ensure they were similar.

Aboveground tree biomass was calculated using species-specific allometric equations based on a living tree's DBH (Brenneman et al. 1978; Monteith, 1979; Whittaker and Woodwell, 1968) and summed by plot for plot biomass for all surviving trees over 10 cm DBH. To roughly approximate how long it would take for each of the treatment plots to recover the biomass it had in 2007 prior to girdling (biomass compensation), a plot's rate of biomass accumulation post-girdling (2010-2020) was used. The length of time it would take a plot to attain the living biomass it had had in 2007 was calculated based on the intercept of an experimental plot's biomass in 2010 (post girdling) and the linear model for its biomass accumulation between 2010-

2020, with year as the independent variable. For the experimental plots, the biomass lost was calculated as the percent decrease of living biomass from 2007 to 2010 for each plot. Biomass lost was compared to both the time to biomass compensation as well as the biomass accumulation 2010-2020 as a percentage of the same plot's biomass in 2010.

Relative growth calculations

Relative annual aboveground biomass growth (relative growth) of both individual trees and plots was calculated as:

$$relative\ growth = \frac{\ln(B_{t+\Delta t}) - \ln\ (B_t)}{\Delta t}$$

Where $B_{t+\Delta t}$ equals biomass at the current time and B_t is the biomass from the previous census. Δt is the difference in years between censuses. Relative growth was restricted to post-treatment years (2010-2020) and mean plot relative growth rates between different treatments were statistically compared using Kruskal-Wallis and *pgirmess* package (Giraudoux, 2022) due to small sample size.

Competitive release

If competitive release is occurring, relative plot growth should decrease with increased plot aboveground biomass. To test this hypothesis, we used a linear mixed effects model (*lme4* package, Bates et al., 2015) with relative annual aboveground biomass growth within plots (relative plot growth) as the dependent variable. Aboveground plot biomass from the previous annual census and tree species richness within plots were treated as fixed effects and plot identity as a random intercept (Table 1.1). Previous year's aboveground biomass was used instead of the current year's, since the competitive effects of crowding on current growth was determined by the previous year's biomass within a plot. As relative growth is based on an annual census, the random effect of plot identity was used to account for repeated measures as well as potential

delayed effects from the initial girdling treatment that might be plot-specific. Both relative plot growth and aboveground biomass were log-transformed to linearize the relationship and normalize residuals of the model.

Biodiversity effect

Non-dominant tree species richness differs among plots, but is relatively static over time. Therefore, to examine the effect of species richness on relative plot growth, we used a second linear mixed effects model, similar to one described above, but with year as the random effect (instead of plot identity) (Table 1.1). The model used plot relative growth as the dependent variable and independent variables of previous year's biomass (log-transformed) and species richness (both fixed effects) and year (the random effect). For each of the models (competitive release and biodiversity effect), slopes for fixed effects were extracted using the *lme4* package (Bates et al., 2015), where a negative slope for previous plot biomass and a positive slope for species richness would support the hypotheses of competitive release and a biodiversity effect, respectively. To examine the relative influence of fixed and random effects, marginal pseudo R^2 were generated with the *MuMIn* package (Bartoń, 2022). The *jtools* package (Long, 2022) was used to adjust observed data for covariates in the partial residual plots.

Non-dominant compensatory growth

To examine species relative growth rates between plots, we selected tree species which had at least five individual trees in both control and one treatment plot. This subset was used in a linear mixed effects model with individual tree annual aboveground biomass relative growth (relative tree growth) as the dependent variable, the biomass of the tree from the previous year as a fixed effect, and random effects of individual tree (to account for repeated measures) as well as the interaction between species and treatment (Table 1.1). Tree growth and tree's previous year

biomass were log-transformed, to linearize their relationship and improve model fit. Prior to log-transforming, the minimum value was adjusted to one and the value required to do this was added to all data. Plots for effects of species and treatment on growth were created using the *merTools* package (Knowles and Frederick, 2020).

1.3 Results

Community composition

Oak reduction led to a substantial alteration in relative live aboveground biomass of species between 2007 and 2020: the NMDS shows the tree communities of the different treatments were indistinguishable at the outset, as the triangles defined by the treatments overlap, but the communities were readily differentiated in 2020, where the triangles are distinct (Fig. 1.2). The corner of each triangle is one of the treatment replicates and the triangle represents how the treatment occupies the two-dimensional space defined by the relative biomass of all species. In 2020, the most abundant trees were (in descending order), *Acer rubrum* (red maple), *Quercus rubra* (red oak), *Betula lenta* (black birch), *Nyssa sylvatica* (black gum), *Acer saccharum* (sugar maple), and *Quercus montana* (chestnut oak). These species, with the addition of *Acer pensylvanicum* (which only occurred in a single plot), make up the majority of the dispersion along NMDS axis 1 in 2020 (Fig. 1.2). Since the NMDS process of dimension reduction is separate for each year, the axes of Figure 1.2 are not directly comparable between 2007 and 2020, except for scale.

Biomass accumulation

The effect of the girdling treatments in 2008 and 2010 was also readily apparent in the reduction in aboveground biomass (Fig. 1.3a, Table 1.2). By 2020, the effect of the girdling

treatment was still evident: the total aboveground biomass showed a negative relationship with the percentage of oaks girdled, though only the 100% oak girdled was statistically different from the 0% oak girdled (Kruskal-Wallis test, $p < 0.05$, Fig. 3b). The rate of relative plot growth in the 100% oak girdled plots decreased between 2010-2020 (Fig. 1.3c) and by 2020 was still positively associated with the percentage of oaks girdled, though again only the 100% oak girdled was statistically different from the 0% oak girdled (Kruskal-Wallis test, $p < 0.05$, Fig. 1.3d). Linear models approximated the slope of biomass accumulation well for all plots (minimum $R^2 = 0.98$). One 50% oak girdled plot had already attained the aboveground biomass it had in 2007 by 2020 (Table 1.2). For the other plots with oaks girdled, rough estimates using models assuming linear growth showed a minimum of 16 years and maximum of 57 years until pre-treatment biomass would be reached (Table 1.2). Length of time until recovery of biomass to projected levels had a strong positive, linear correlation with the percent of the original biomass that died due to girdling ($R^2 = 0.96$; $p < 0.05$) (Fig. S1.1a). The percentage of biomass that had been regained by 2020 relative to the reduced amount in 2010 was exponentially related to percent girdled (linearized relationship, $R^2 = 0.91$; $p < 0.05$) (Fig. S1.1b).

Competitive release

In the linear mixed effects model examining the effect of aboveground biomass on relative plot growth, aboveground biomass had a negative effect on relative plot growth, with a slope of -1.16 ($p < 0.05$, Fig. 1.4a), as expected. The fixed effects of the previous year's plot aboveground biomass and plot species richness explained 81% of the variance, with previous aboveground biomass predicting the majority ($R^2 = 0.80$). This model used starting plot biomass as a random effect to account for the repeated measures and, as species richness does not vary

much within a single plot year to year, species richness was not expected to have an effect and it did not ($p > 0.05$).

Biodiversity effect

In the linear mixed effects model that looked at the influence of species richness on relative plot growth with year as a random effect, since diversity varies between plots within a year, species richness had a small, positive effect on growth (slope = 0.04, $R^2 = 0.04$, $p < 0.05$**,** Fig. 1.4b). Within the same model, previous plot aboveground biomass had a negative, and stronger, effect on growth, with a steeper slope and explaining more of the variance (slope = -1.0, $R^2 = 0.79$, $p < 0.05$).

Non-dominant compensatory growth

In the linear mixed effects model examining the effect of the interaction of tree species and treatment on individual tree relative biomass growth, only five species had five or more individual trees in both the control and at least one other plot: red maple, sugar maple, black birch, black gum, and a single oak species, red oak (Supplementary Fig. S1.2). Most species (red maple, sugar maple, black birch, and red oak) showed a trend towards increased relative growth as percentage of oaks girdled increased (Fig. 1.5). In the 50% oak girdled plots, red oak, red maple, and sugar maple had increased relative growth compared to the control. The two maple species and black birch had error bars that did not overlap between the 0% and 100% oak girdled plots. Sugar maple in both the 50% and 100% oak girdled plots showed significantly increased relative growth compared to the mean relative growth for all trees; i.e., the error bars did not overlap with zero. Red oak was the only species that showed a relative growth significantly above the mean in the control plots.

1.4 Discussion

Ten years after the reduction of the dominant oak species, tree communities are still responding with increased growth (Fig. 1.3c), a feature of competitive release. This, along with the negative influence of aboveground biomass on growth (Fig. 1.4a), both support the argument that non-dominants were suppressed by competition from the dominant oak taxa, as expected, though the current analyses do not distinguish between removal of the oak species specifically and biomass independent of species. Species richness, however, positively influences the rate of biomass accumulation (Fig. 1.4b), an effect observed for growth in naturally assembled forests (van der Plas, 2019), and likely attributable to either selection for or complementarity within compensatory growth among non-dominants. Though the effects of aboveground biomass and species richness differ in magnitude, their significance reflects the importance of the subordinate community in mediating biomass recovery after dominant species loss. Thus, compensatory growth, or recovery of lost biomass or lost functioning attributable to dominant species loss, reflects the combination of competitive release of non-dominants and a biodiversity effect. This can only be true, however, if the non-dominant species pool contains species that, through selection or complementarity, can exhibit compensatory growth above what competitive release provides.

Oak girdling drastically altered the experimental forest plots: communities that were indistinguishable before the experiment had distinct species compositions in 2020 (Fig. 1.2) and, between the control and the 100% oak girdled plot, different growth and biomass (Figs. 1.3b and 1.3d). In all but one of the treatment plots, recovery of forest biomass is still underway (Fig. 1.3a; Table 1.1). The data imply the remaining tree community will likely compensate for the biomass loss of its dominant species within the next 50 years (Table 1.1), though the species

composition will remain altered (Fig. 1.2), which may affect habitat for other species (Leidinger et al., 2021). Increased growth in the treatment plots suggests the residual trees are experiencing competitive release and taking advantage of the newly available resources, such as light, water, and nutrients. Loss of living aboveground biomass positively influenced growth; the most severely impacted plot, even though it lost 94% of its original biomass, more than tripled its biomass in 10 years solely from growth of the existing tree community. The enormity of such biomass reductions is the signature of dominant species loss, yet it also demonstrates the possibly transient nature of such impact when non-dominants have the potential to promote recovery.

Higher growth rates where oaks have been girdled do not fully offset the magnitude of dominant species death, as plots with the most living biomass lost still have the longest times to recovery (Table 1.1), as would be expected for logistic growth. Growth rates also diminish over time (Fig. 1.3c), a finding consistent with the observation that community biomass often reduces tree growth, which is the basis for thinning to increase tree growth and vigor in forest management (Mayor & Roda, 1993) via reduced competition for resources (Bréda et al., 1995). Studies in grasslands also show increased growth of subordinate species after a dominant has been removed (Munson & Lauenroth, 2009), though even these fast-growing species do not show full compensation at most experimental timescales (Avolio et al., 2019; Chaves & Smith, 2021), unless another co-dominant species is present (Pan et al., 2016). Since biomass losses are often more extreme in forests relative to grasslands, as well as longer generation times for trees, full biomass recovery is likely to take longer in forest systems (Fu et al., 2017).

While aboveground biomass is the dominant influence on growth in our statistical model, and a demonstration of competitive suppression, species richness also influenced total

aboveground biomass in each plot (Fig. 1.4b). Positive relationships between biodiversity and the magnitude of biomass production are seen in experimental systems (Cardinale et al., 2012) and in the majority of naturally assembled temperate forests, though biodiversity effects are often outweighed by both composition and abiotic drivers (van der Plas, 2019). After reductions in dominant taxa, species richness within the residual community appears to serve as a "safety net" for biomass accumulation; in a depauperate system, few species remain to capitalize on the increase in resource availability. Our results suggest that a larger pool of subordinate species, i.e., greater species richness within the non-dominant community, likely decreases recovery time. As our experiment did not consist of replicate plots of tree species grown as monocultures as well as species mixtures, disentangling selection from complementarity is not possible as is often done in stratified, randomized biodiversity manipulation experiments (e.g., Loreau M. and Hector. A., 2001).

When 50% of the oaks were girdled, the remaining oaks showed competitive release similar to other species. Red oak, when present, showed the most positive growth (Fig. 1.5), similar to trends found in long term plots within the same forest (Schuster et al., 2008). Though mature oaks dominate the growth response in the 50% oak girdled plots, within the same long term plots sugar maple canopy trees increased between 1936 and 2006 and the understory has shifted towards the more shade-tolerant maples (Schuster et al., 2008), perhaps due to oaks' inability to tolerate low light levels. In our data, both red and sugar maple have increased growth in the 100% oak girdled plots relative to the control, though only sugar maple shows a positive response distinguishable from zero in the girdling treatments (Fig. 1.5). This, along with the understory data, suggests that maples may be the next dominant species within the forest.

Forest functions are likely to be altered along with the compositional change from oak dominance, since species are not likely to replace each other in all aspects of their physiology, function, and response to environment (Gaston, 2010). Oaks attain a large size, are long-lived, and decay slowly (Tirmenstein, 199; Perez et al., 2022); alteration of these characteristics with potential replacements is likely to affect carbon cycling, sequestration, and stability of the ensuing system. Modelled forest communities where dominant red oak is replaced by red maple show overall reduced carbon pools, even after 300 years (Crowley et al., 2016). Maples have lower rates of gas exchange (Abrams, 1998), are more shallow rooted (Lyford, 1980; Lyford & Wilson, 1964), and more sensitive to environmental variability and water stress than oaks (Yi et al., 2017a), suggesting a maple-dominated forest may be less drought resistant (Harrison et al., 2020) and sequester less carbon than the current forest. Because dominant species represent the majority of the system's biomass, differences in functioning with replacement species will be amplified, likely resulting in overall change of forest form and function.

While our experimental system examines the effects of sudden, dramatic loss of oak species, longer term regeneration failure is occurring across the globe (van de Gevel et al., 2012). This decline is not well understood, but variously attributed to browsing (Götmark et al., 2005; Singh et al., 1997), lack of protection status or insufficient management (Dias et al., 2016; Zavaleta et al., 2007), and the cessation of controlled burns (Brose, 2014; Dey, 2014). Many of these drivers relate to oaks' poor growth in low light conditions relative to other species (Modrow et al., 2020), which, in certain systems, may be compounded by physiological alteration by pathogenic mildew (Demeter et al., 2021). As oaks decline worldwide (Dey, 2014), the physiology and morphology of the remaining trees will dictate the relative ability of the forest system to recover. Given the prevalence of global change factors that are putting dominant

species at risk (Avolio et al., 2019; Gaston, 2010), the value of biodiversity becomes more important: should dominant species be lost, more remaining species allow for better probability of recovery of function. Greater diversity provides an increased chance that, under uncertain and unpredictable climate conditions, one species from the community will perform well (Cardinale et al., 2012). Non-dominant forest tree diversity, which may be overlooked when focusing on the decline of dominant species, is likely to be important as a reservoir of species which will maintain the functioning of the community in the event of dominant species loss.

1.5 Tables and Figures

Table 1.1 *Linear mixed effects models for effects of biomass and species richness on relative plot growth and the interaction between species and treatment on relative tree growth*

Dependent variable	Fixed effects	Random effects	Hypothesis
relative plot growth	previous plot biomass, species richness	plot identity	competitive release
relative plot growth	previous plot biomass, species richness	year	biodiversity effect
relative tree growth	previous tree biomass	tree identity, species:treatment	non-dominant compensatory growth

Table 1.2 *Summary of effects of oak girdling treatment on biomass compensation*

Treatment[a]	Biomass lost (%)[b]	Years to compensation[c]	Biomass gained 2010-2020 (kg m^{-2} $year^{-1}$)	Biomass gained 2010-2020 (%)[d]
0	0	N/A	9	17
0	0	N/A	10	16
0	0	N/A	13	16
50	28	10	10	40
50	31	17	9	27
50	55	34	16	35
100	80	36	17	111
100	86	44	10	139
100	94	57	14	257

[a] percentage of oak trees girdled between 2008 and 2010
[b] living biomass lost 2008-2010 due to girdling as a percentage of a plot's biomass in 2007
[c] compensation means the aboveground biomass of that plot will be equal to what it was in 2007 (pre-girdling) from a starting point of 2010 (post-girdling)
[d] amount of biomass accumulation 2010-2020 as a percentage of that plot's biomass in 2010

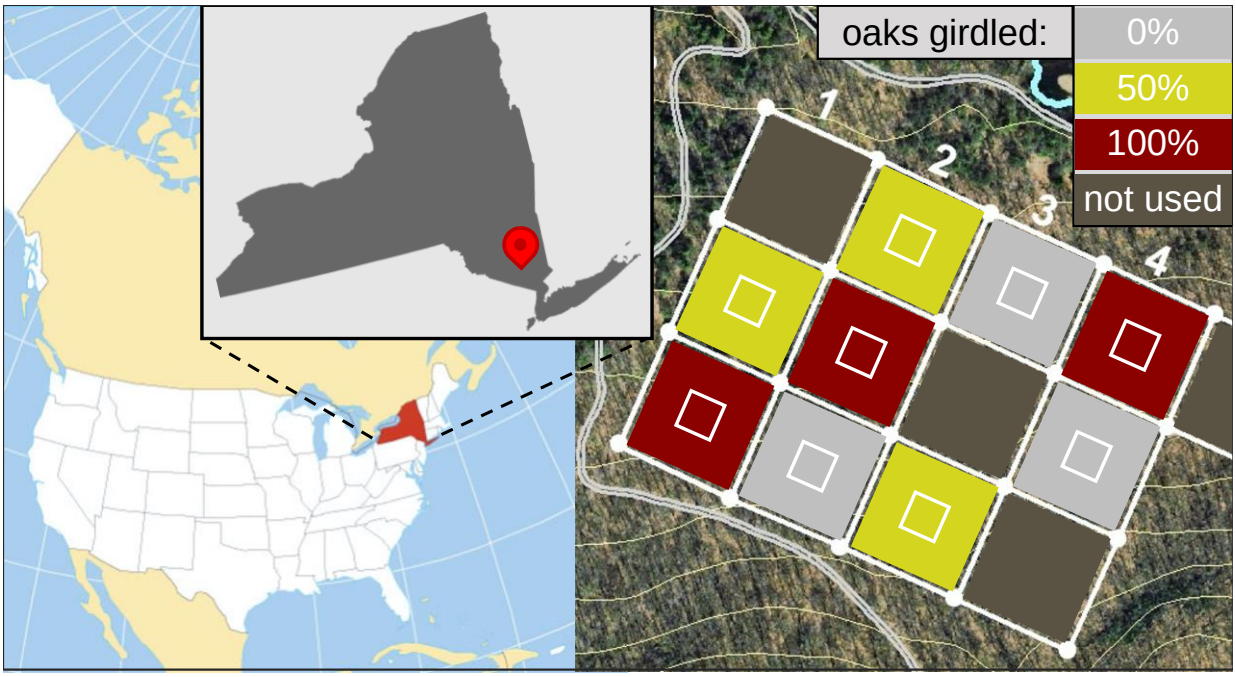

Figure 1.1 Schematic of treatment layout at Black Rock Forest

Layout of experimental treatments at Black Rock Forest (red marker), located in the Hudson Highlands of New York State within the United States. In 2008 and 2010, oak trees (*Quercus* spp.) were girdled according to one of three treatments: (1) 100% (red), (2) 50% (yellow), and (3) 0% (grey) of oaks girdled. Each treatment has three replicates. Each plot measures 75 m x 75 m, but only data from the central subplot of 25 m x 25 m were used (smaller square within each treatment plot).

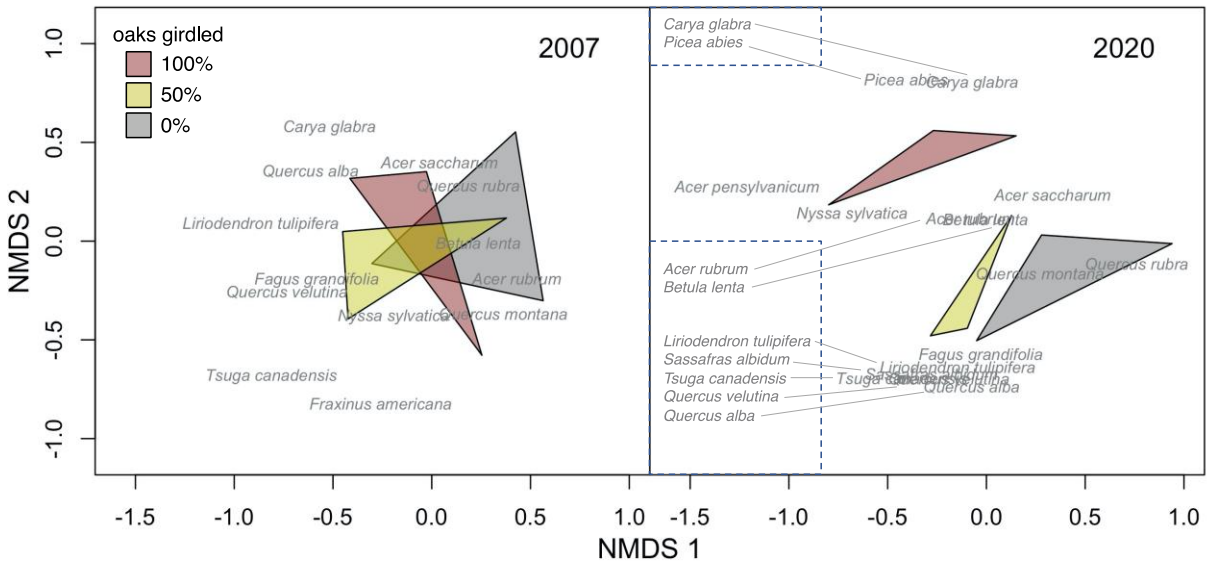

Figure 1.2 Non-metric dimensional scaling for species biomass at the experimental forest plots at Black Rock Forest, NY

Non-metric dimensional scaling (NMDS) for species biomass at the experimental forest plots at Black Rock Forest, NY in 2007 and in 2020. In 2008 and 2010, selective girdling of trees was carried out according to one of three treatments: (1) 100% (red), (2) 50% (yellow), and (3) 0% (grey) of oaks girdled. Each treatment had three plot replicates, which are the corners of each correspondingly colored triangle. In 2007, the colors refer to the treatment that would be applied in 2008 and 2010. As these triangles overlap, no systematic differences exist in the communities prior to the girdling. By 2020, each treatment occupies a distinct space defined by its constituent species' relative biomass. This suggests that the plots' communities have not yet recovered from the girdling treatment. For ease of reading, overlapping species names in 2020 are separated out on the left side with lines connecting to their original location.

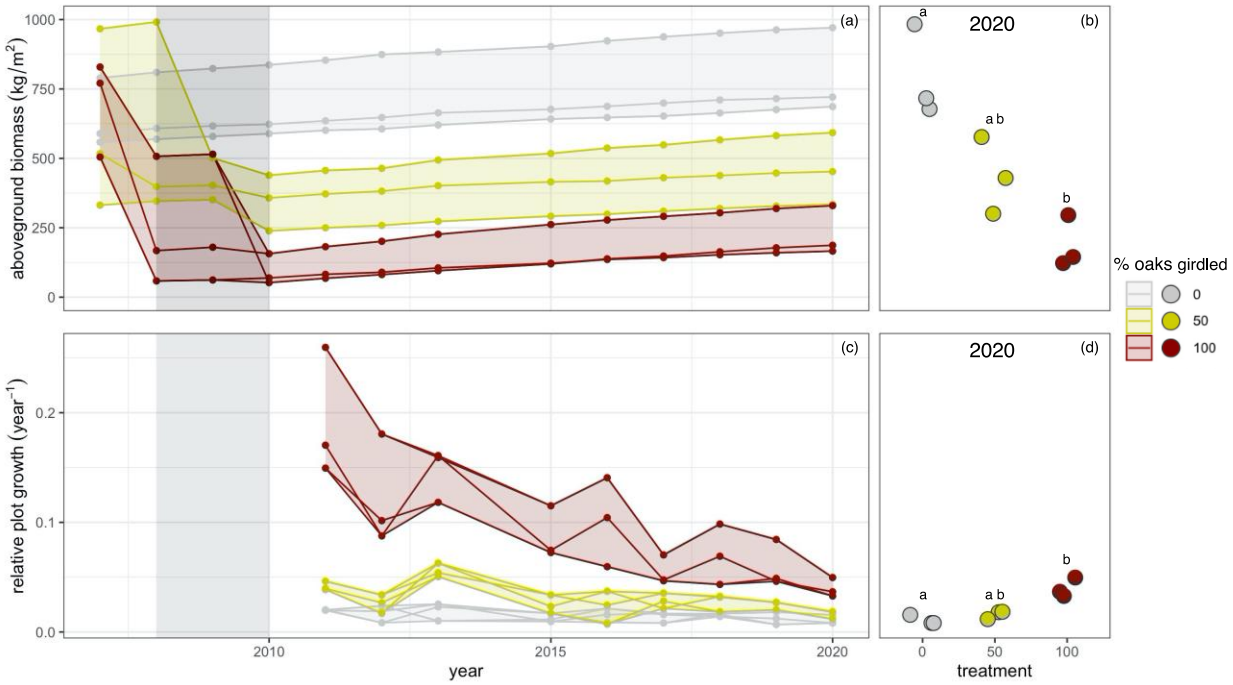

Figure 1.3 Plot biomass and growth following oak girdling.

In 2008-2010, selective girdling of the dominant genera of oaks trees was carried out according to one of three treatments: (1) 100% (red), (2) 50% (yellow), and (3) 0% (grey) of oaks girdled. Total living aboveground biomass (kg/m^2) 2007-2020 (a) and relative plot growth post girdling (year^{-1}) 2010-2020 (c) of treatment plots. Each treatment had three replicates (lines) and was censused annually (dots), except 2014. Grey rectangle indicates period during which trees where girdled (2008- 2010). Letters indicate significant differences by Kruskal-Wallis test ($p < 0.05$) for total living aboveground biomass (b) and relative plot growth (d) in 2020. For 2010-2020, only trees greater than 10 cm DBH and those that were alive for the duration of the experiment were included in calculations to focus on growth of the living community without recruitment or mortality.

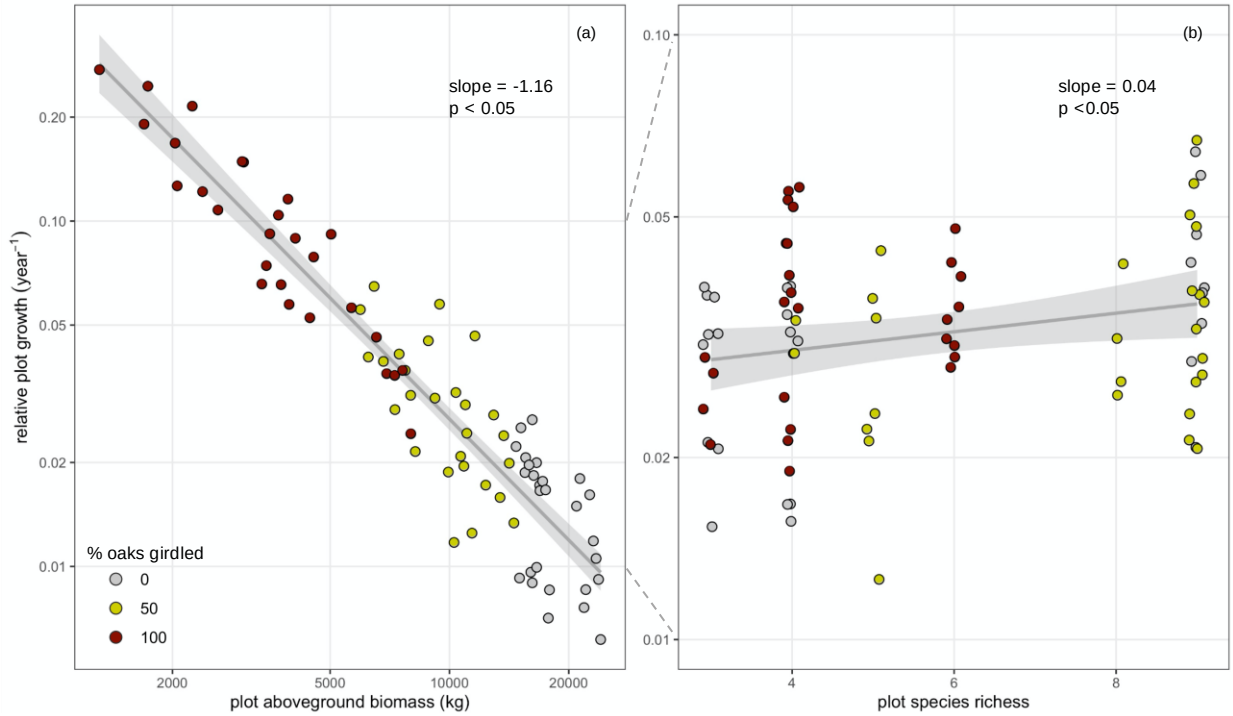

Figure 1.4 Partial residual plots from two separate linear mixed effects models showing the effects of plot aboveground biomass and species richness on relative plot growth

Partial residual plots from two separate linear mixed effects models showing the effects of plot aboveground biomass (kg) (a) and species richness (b) on relative plot growth (kg/year). Both models use fixed effects of the previous year's aboveground biomass and species richness; (a) includes a single random effect on intercept of plot identity, to account for repeated measures within the same plot and starting conditions, and (b) a single random effect of year on intercept, since differences of species richness occur between plots within a single year. Line is the linear fit between x and y variables and the shaded area is 95% confidence interval, which only shows the variance of the fixed effects. Note that while the y-axis is relative plot growth for both (a) and (b), the points should not be expected to line up as the data take into account the partial residuals from the variable not plotted. Additionally, though the y-axes on both panels are plotted on the log-scale, the ranges vary. X-axis for (a) is log scale; (b) is not and points have been jittered along this axis. Each point is one plot for one year in the period 2010-2020.

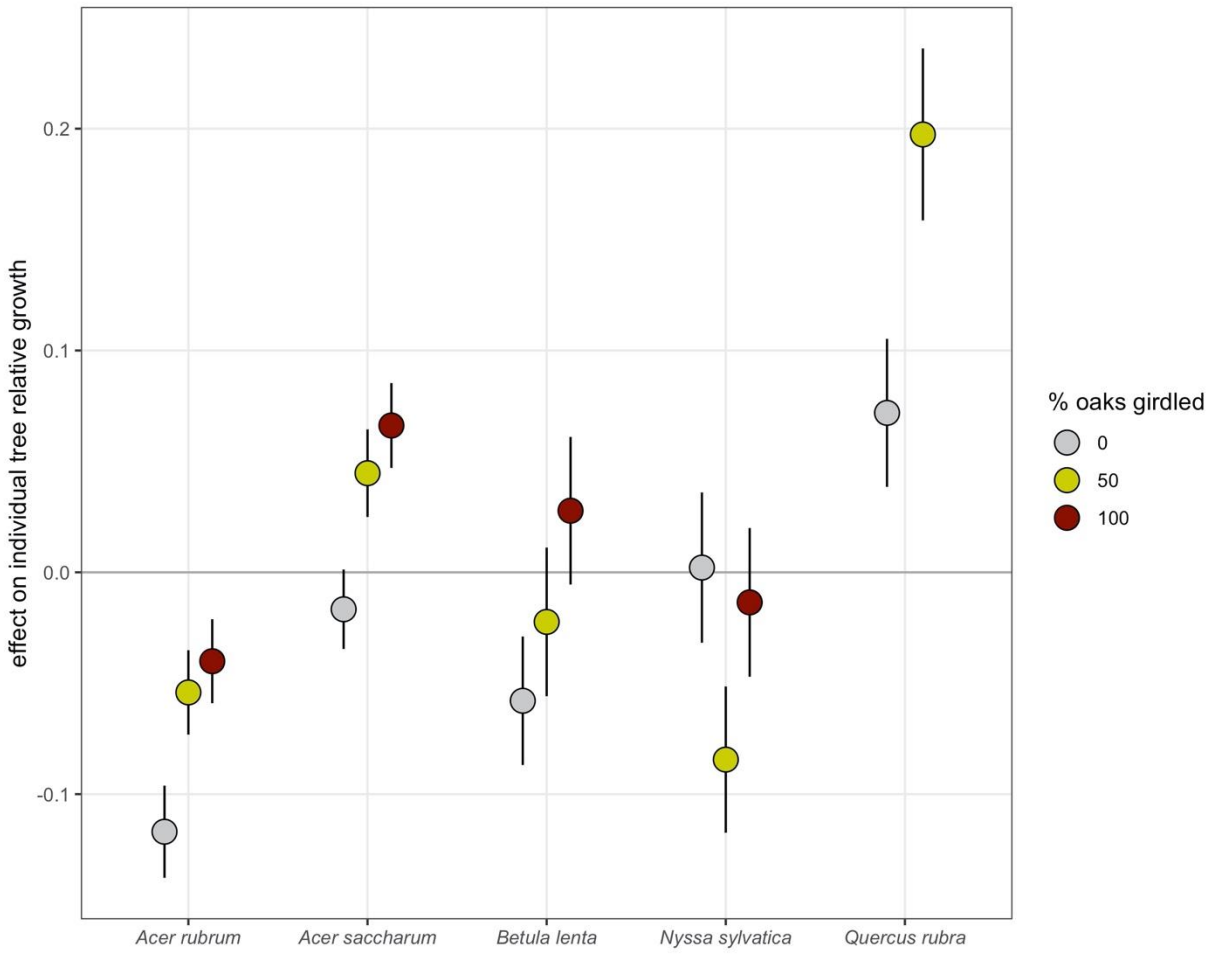

Figure 1.5 Coefficient plot of the effect of the interaction between species and treatment on tree relative growth.

The effect of interaction between species and treatment on relative tree growth from a linear mixed model with tree relative growth as the response variable, a fixed effect of the tree's previous year's biomass, and random intercepts of individual tree (to account for repeated measures), and the interaction between treatment and species. Zero line represents the mean relative growth for all trees. Only species that had five or more trees in more than a single treatment and were included in the model. Points represent mean interaction effect on relative growth and the bar is +/- one standard deviation.

Chapter 2: Tree diversity increases soil water drying rate constants, but raises and stabilizes soil water minima

Sarah G. Bruner, Shahid Naeem, Jan U. H. Eitel, Kevin L. Griffin, Duncan N. L. Menge, Katherine Terlizzi, William S. F. Schuster

2.1 Introduction

The balance of water within soils dictates a large portion of plant function: at the global level, it organizes biomes, while at the community level it exerts control over many vegetation-mediated ecosystem processes, such as primary productivity (Green et al., 2019). Soil moisture can drive both broad and local patterns in plant species composition, absolute and relative abundance, and other dimensions of biodiversity (Gaston, 2000; Naeem et al., 2016). Plants, in turn, influence soil moisture through both their structure, via physical properties like shading, and their physiology, especially through the process of transpiration (D'Odorico et al., 2010). Though soil moisture is largely governed by precipitation and the chemical and physical properties of the soil, such as porosity, depth, and particle size and type, which all affect water retention, infiltration, and evaporation, water movement out of soils by plants is also integral to the soil water balance equation (Hunt et al., 2023). While the effects of soil water on individual plants' physiology and plant community composition, distribution, abundance and function have been extensively researched, by contrast, the influence of plant diversity on soil moisture has received little attention (Gottschall et al., 2022).

The body of research examining diversity's effect on ecosystem function has mainly focused on biomass production. Since plant productivity is intimately tied to soil water use through photosynthesis (Leuning, 1995), diversity should likewise influence soil water. More

diverse systems tend to be both more productive and more stable in their productivity over time (Duffy et al., 2017; Isbell et al., 2015), likely due to either or both niche complementarity (i.e., how organisms with different functional traits may use resource pools more completely over time and space) or selection effects (i.e., the presence of high-impact or dominant species due to random selection from the species pool). The species differences that drive increased productivity and stability of production at longer timescales should be tied to species-specific photosynthetic rates (Niinemets, 2007), which from daily to yearly time scales directly influence soil water content (Daly et al., 2004). Complementarity of physical structure between plant species, such as optimization of light capture by leaves within canopies or differing root morphologies, may also influence water use through increased evaporative surface or access to water throughout the soil profile (Dimitrakopoulos & Schmid, 2004; Pretzsch, 2014). Root distribution, however, is notoriously hard to measure, and empirical evidence for vertical niche differentiation by roots is mixed, even when increases in diversity correspond to increases in productivity (Bakker et al., 2018; Kesanakurti et al., 2011; Ravenek et al., 2014).

Though diversity has a positive and stabilizing effect on many ecosystem functions, biomass is often the greater influence, and the overall quantity of water used by vegetation is largely biomass dependent (Hagger et al., 2019). Trees are usually the dominant contributor to biomass within an ecosystem and the effect of tree water use is readily visible within soil water content readings (Elliott et al., 2017). Though a tree stand can be described by species, biomass, and community diversity metrics derived from them, direct quantification of the community's architecture is possible through structural assessment techniques such as light detection and ranging (lidar), while carbon isotope discrimination provides a proxy for ecophysiological function. The three dimensional information from lidar enables evaluation of plant architectural

information such as vegetation area index (VAI) as well as its canopy roughness (rugosity), together describing the total evaporative surface and its connection to the atmosphere, which may be indicative of the tree community's influence on soil water. The effect of soil water on trees, in turn, can be described by carbon isotope ratios. During dry conditions, trees may close their stomata, ceasing transpiration while photosynthesis continues and relying on carbon dioxide already present within the leaf for carbon assimilation (Farquhar et al., 1989). Since photosynthesis discriminates against carbon-13, a higher ratio of carbon-13 to carbon-12 (usually expressed as $\delta^{13}C$) is indicative of water scarcity in plants (Grossiord, Granier, et al., 2014). $\delta^{13}C$ can therefore provide a link between soil water content and its effect on plant physiology and rates of transpiration and photosynthesis.

In this study, we examined how tree diversity, biomass, physical structure, and physiology of the tree community affected minimum soil water content, soil water dry down rates, and the magnitude of water lost from the soil, as well as the stability of these variables. Using a tree dominance and diversity experiment located in the northeastern region of the United States, we asked the questions: 1) How does soil water availability (i.e., minimum soil water content, drying rate constant, and the magnitude of soil water loss) differ between tree communities varying in biomass and species composition? 2) Which aspects of the community (biomass, structure, diversity) have the greatest influence? 3) How do biomass and diversity relatively affect leaf carbon isotope discrimination? We hypothesized that species rich communities would have: 1) lower minimum soil water and 2) greater soil water loss, both because of the likelihood that a species able to utilize soil water under given (or dry) conditions will be present in the community as well as 3) larger drying rate constants due to either temporal complementary of transpiration or spatial complementarity of root architecture. Additionally, 4)

these features of soil water availability would be more stable over time in more diverse plots, since different species are theoretically able to utilize soil water under a wider range of environmental conditions than depauperate communities. We expected biomass would also decrease soil water minima and increase drying rate constants, but did not expect that biomass would influence ecohydrological stability, since, in our system, biomass is correlated with dominance by oak (*Quercus*) species and members of the same genus likely regulate transpiration and photosynthesis similarly in response to environmental conditions. Additionally, communities with lower minimum soil water and faster drying rate constants would have higher values of $\delta^{13}C$, indicating water scarcity. Much work on the relationship between biodiversity and ecosystem function (BEF) in forests has focused on biomass production and related processes, such as carbon sequestration; this study expands the BEF concept to ecohydrology, an important dimension of forest functioning with implications for the resilience and resistance of forests to climate change as species composition alters due to shifting weather patterns and introduction of non-native species.

2.2 Methods

Site characteristics

Black Rock Forest (BRF) is located in the Hudson Highlands region of southeast New York State, USA (41°24′ N, 74°01′ W). Air temperature is seasonal, with mean monthly temperatures ranging from 24 ºC to -2.1 ºC (NOAA, 2020), with the annual mean at 9.7 ºC. Mean annual precipitation is 1.3 m and soils are medium-texture loamy till, relatively sloped (10-30 %), moderately to excessively draining, shallow, and rocky throughout. Lithic bedrock at 0-60 cm underlays approximately 60% of site with the remainder being fragipan at 35-90 cm (Soil

Survey Staff, USDA 2022). BRF is a temperate deciduous forest where oak species (*Quercus spp.*) make up approximately 70% of the canopy trees (Schuster et al., 2008), with other common species being red maple (*Acer rubrum*), sugar maple (*A. saccharum*), black birch (*Betula lenta*), American beech (*Fagus grandifolia*), and black gum (*Nyssa sylvatica*). Oak species present include white oak (*Quercus alba*), red oak (*Q. rubra*), chestnut oak (*Q. montana*), and black oak (*Q. velutina*). Before BRF was established as a research forest in 1927, much of the area had been repeatedly logged for approximately the previous 200 years.

Experimental setup

Twelve 75 m by 75 m experimental plots were laid out in a three by four grid on the north slope of Black Rock Mountain in 2006 (Fig. 2.1a). The layout is a semi-randomized block design grouped by slope position (low, mid and high), where each treatment is repeated once within each of the slope positions. In 2008, each plot received one of four treatments: 0% of the trees girdled (control), 50% (by stem number) of oak trees girdled, 100% of oak trees girdled, and 100% of all non-oak trees girdled. Trees were girdled using a chainsaw cutting 3-5 cm into the bark of the tree to sever phloem transport (Noel, 1970), mimicking the mechanism by which many pathogens block the flow of nutrients through the phloem and cambium. Girdled trees were left standing if greater than 10 cm in diameter at breast height (DBH) and felled if they were smaller. A small number of tree (<5%) continued to leaf out after the girdling in 2008; these were girdled a second time in 2010.

Field measurements

In the summer of 2019, within each plot, a soil moisture sensor (METER Group TEROS 12) was inserted horizontally into the wall of a hole at 10 cm depth and within the mineral soil. Holes were backfilled with original excavated material. 10 cm is a common depth for soil moisture

sensors (e.g. (Majone et al., 2013; Robertson et al., 2018) and pervasive rockiness of the soil precluded consistent placing at greater depths. The sensor measured soil temperature as well as soil volumetric water content (VWC or soil moisture) and took readings every five minutes. These were averaged once an hour and recorded on a data logger (METER Group EM50 and ZL6). A single data logger was shared between two plots and cables leading to the sensors were dug into the ground to discourage disruption from animals. Since the maximum length for the sensor cable is 35 m before the signal starts to degrade, after installation the sensors were located approximately 30 m in from the edge of the plot and 5 m from its midpoint (Fig. 2.1a). In April of 2020, a weather station (METER Group ATMOS 41) measuring precipitation and other environmental variables including air temperature, relative humidity, and wind speed was installed at the top of the slope containing the experimental treatments.

When trees were fully leafed-out, the plots were scanned using terrestrial light detection and ranging (lidar, BLK360, G1 Leica™) and the canopy was imaged with a hemispherical lens (Yasuhara Madoka 180) using a self-levelling gimbal (Zhiyun WEEBILL). While taking measurements, each piece of equipment was positioned on top of the location of the soil moisture sensor within each of the plots. We took lidar scans in August of 2020 and May, June, and July of 2021 and hemispherical images a single time in August of 2020 and early September of 2021. These campaigns yielded 48 spherical scans and 24 canopy images. The centers of the lidar scans and the location of the hemispherical lens were 1.3 m and 2 m above the forest floor, respectively.

In late August of 2020-2022, leaves were collected from each plot for isotopic analysis from the three trees closest to the soil moisture sensors which were also larger than 10 cm DBH. Full sun leaves from the top of the canopy were retrieved via shotgun sampling and 4-6 leaves

per tree were placed inside individual paper bags and dried. Leaves were then sent to the University of Washington for isotopic analysis of the ratio of carbon-13 (^{13}C) to carbon-12 (^{12}C) (reported as $\delta^{13}C$) relative to a standard (Pee Dee Belemnite), where:

$$\delta^{13}\mathrm{C} = \left(\frac{\left(\frac{^{13}C}{^{12}C}\right)_{sample}}{\left(\frac{^{13}C}{^{12}C}\right)_{standard}} - 1 \right) \times 1000$$

In April of 2023, all trees within a 10 m radius from each of the soil moisture sensors (tree community) were censused for DBH and species identity, to estimate the effect of the surrounding tree community on soil moisture. Within a 5 m radius, these measurements were taken for all trees 1 cm DBH and over; between 5-10 m radius, only trees over 10 cm DBH were censused.

Data Processing

All data processing and statistics were done in R version 4.1.3, with the exception of the lidar data processing, which was conducted using R version 4.2.1 (R Core Team 2022).

Soil moisture

Only soil moisture data for 2020 and 2021 were used, as they represented the years in which the greatest number of data loggers were functioning and also had a full complement of corresponding structural metrics. A "rain event" was considered to be any precipitation greater than 1 mm/hour; rain events less than 12 hours apart were considered to be the same event. For each plot, hourly soil moisture measurements were cropped to include only the times between rain events (dry periods or dry downs) and further cropped to exclude wet-up periods, so that dry periods only included maximum to minimum soil moisture. Dry periods less than three days were excluded from further analysis. The dry periods were grouped into leaf-on (May–August)

and leaf-off (November–March) and each was given an identification number (dry period ID). Since we were interested in how plant physiology affects soil water, but could not assess our plots with and without vegetation, we used soil water content (SWC) during the leaf-off period to standardize SWC during the leaf-on period, as follows:

$$standardized\ leaf\text{-}on\ SWC_{pt} = leaf\text{-}on\ SWC_{pt} \times \left(\frac{mean\ leaf\text{-}off\ SWC_{all\ plots}}{mean\ leaf\text{-}off\ SWC_{p}} \right)$$

Where *leaf-on* SWC_{pt} is the soil water content of plot *p* at time *t* during the leaf-on period, *mean leaf-off* SWC_p is the mean SWC of plot *p* during the entire leaf-off period, and *mean leaf-off* $SWC_{all\ plots}$ is the mean of SWC for all plots at all times during the leaf-off period. This measurement attempts to assess what the SWC of the plot would be taking into account inherent differences in the soil properties particular to each plot.

For each dry period, each plot's minimum and maximum standardized soil moisture were obtained and the difference between them (soil water loss) calculated. An exponential decay curve was fitted to each plot's standardized soil moisture measurements within each dry period using the following equation:

$$y(t) = y_{min} + (y_{max} - y_{min})e^{-\lambda t}$$

where soil moisture VWC (y) begins at y_{max} and decays towards y_{min} at a rate determined by λ (the drying rate decay constant) as the soil dries (Fig. 2.1c). Base R stats package's self-starting asymptotic regression function *SSasymp* and nonlinear least-squares parameter estimates, *nls*, were used to automate curve fitting (via the *data.table* package; Dowle & Srinivasan, 2021) for each plot for each dry down. The drying rate decay constant (λ) was extracted for use as a response variable in later analyses. Dry periods that failed in the *nls* decay curve fitting were plotted for visual inspection and fit was attempted using manually determined starting values.

Linear models were also fit to the same periods as the exponential decay model and the two were compared by Akaike Information Criterion (AIC).

Tree community metrics

Using the tree census information along with allometric equations (Brenneman et al., 1978; Monteith, 1979; O'dell, 2020; Telfer, 1969; Whittaker & Woodwell, 1968), we calculated total tree community biomass (biomass); the percentage of biomass made up of *Quercus* species (percent oaks), *Acer* species (percent maples), and *Betula lenta* (percent birch); the number of species (species richness); and the Shannon diversity weighted by biomass (diversity). Diversity was calculated as follows:

$$diversity = -\sum_{i=1}^{S} p_i \, lnp_i$$

Where *S* is the total number of species in the community and p_i the proportion of mass belonging to the *i*th species. We used a biomass-weighted version of Shannon diversity as the size of trees differed by large amounts (1 cm DBH to > 80 cm DBH) and we assumed that their potential influence on water depended on their relative biomass.

Canopy images

Hemispherical photos were read into R and analyzed using the *hemiphot* package in R (ter Steege, 2018) to extract LAI for each tree community. Separate parameters were manually set for each imaging field campaign, to maximize leaf coverage without creating false canopy closure in densely leaved areas. Each photo from a field campaign was visually examined for changing light conditions, and those which appeared slightly different from average were checked to make sure the prevailing parameters captured leaf coverage well.

Lidar Metrics

We used the lidR package (Roussel et al. 2020, Roussel and Auty 2022) to convert point clouds to the metrics of rumple, cover fraction, top rugosity (rugosity), vertical standard deviation, entropy, vegetation area index (VAI), vertical complexity index (Table 2.1). We used the default settings in the package as recommended by NEON, with the exception that the scans were clipped to 40 m radius circles. Small radii often cut trees, but occlusion increases as one moves away from the center of the scan sphere. Occlusion was not accounted for in our analyses and future work would likely benefit from exploration into how different radii influence the results.

Statistical analysis

Relationships between variables

Since many of the lidar-derived metrics are collinear, broadly describing leaf coverage within the stand volume, we employed a principal component analysis (PCA) for dimensional reduction, calculating a separate PCA for each lidar campaign. Lidar scans were done monthly, yet other stand metrics were assessed annually, so the mean of the first and second principal components per year (lidar PC1 and PC2) were used for later analysis. A second PCA (overall PCA) evaluated the relationship between the lidar PCs and the other predictor variables of: community biomass, species richness, diversity, LAI, and percent oak, maple, and birch as well as annual means for lidar derived VAI and rugosity. A Pearson correlation was also used to examine the relationship between the variables in the second overall PCA. Those variables with a high degree of correlation (>40% and $p < 0.05$) were not used together in subsequent models. Additionally, neither rugosity nor VAI were used together with the lidar PCs.

Soil water availability: minimum soil water, drying rate constant, and soil water loss

To examine the relative effects of tree community biomass, canopy coverage, and species diversity and structural composition on soil water availability, we used linear mixed effects models with either the minimum soil water, drying rate constant (drying rate decay constant, λ), or soil water loss as the response variable. Multiple models were compared for each response variable. The overall methods were identical for each response variable and are as follows: each considered model included at least a single aspect of its composition (species richness, diversity, or percent oaks, maples, or birch) or the tree community's biomass as a fixed effect. As predictors that were correlated were excluded from the same model, as previously mentioned, this eliminated almost all combinations, with three exceptions: biomass and species richness, biomass and percent birch, and diversity and percent birch. Other potential fixed effects included: LAI, rugosity, VAI, lidar PC1, and lidar PC2. Predictor variables were mean-centered and standardized, as they had large differences in magnitude. All models included dry period ID as a random effect so that data points were compared for a given dry period's environmental conditions and to account for repeated measures within a plot. Position on the mountain slope was also included, when possible, to account for suspected wetter conditions at the base and dryer conditions higher up. The resulting models were compared by AIC to determine parsimony. Models with a difference of over seven from the most parsimonious model (ΔAIC) were not considered (Burnham & Anderson, 2004), unless they contained an aspect of biomass or community composition that was not present in more parsimonious models. Standardized slopes for fixed effects were extracted using the *lme4* package (Bates et al., 2015) and marginal and conditional pseudo R^2 were generated with the *MuMIn* package (Bartoń, 2022). The *jtools* package was used (Long, 2022) to adjust observed data for covariates in the partial residual plots.

Stability of minimum soil water, drying rate constant, and soil water loss

The coefficient of variation (CV), i.e., the standard deviation divided by the mean, was used to determine stability of the minimum soil water, drying rate constant, and soil water loss. For each of these metrics, all years and all measurements for a plot were used to provide a single CV. Because this yields of total of 12 points for each metric, simple linear regressions were performed with a single mean for all years for each of the above-mentioned predictor variables (biomass, diversity, species richness, percent oaks, percent maples, percent birch, LAI, rugosity, VAI, lidar PC1 and PC2, and overall PC1 and PC2).

Tree water stress ($\delta^{13}C$)

Though $\delta^{13}C$ was collected annually 2020-2022, lidar metrics and hemispherical canopy photos were only taken in 2020 and 2021, several soil moisture sensors were not functioning in 2022, and the tree community was censused a single time in 2023 (before the growing season). Therefore, to look at the relationship between $\delta^{13}C$ and potential predictors, means for all years for each variable were used in linear models. This gives a single $\delta^{13}C$ value for each of the three trees within a plot and a single value for each predictor describing plot characteristics (biomass, diversity, species richness, percent oaks, percent maples, percent birch, LAI, rugosity, VAI, lidar PC1 and PC2, and overall PC1 and PC2.) As this reduces the data to 36, linear models had a single predictor.

2.3 Results

Tree community composition and structure

Girdling altered the tree community (Supplementary Fig. S2.1) and in 2023 the plots still differed by biomass and species composition: oak trees (*Quercus spp.*) comprised the largest

amount of biomass and oak-dominated plots tended to have lower diversity (Fig. 2.2a), whereas maples tended to occur in plots with higher diversity (Fig. 2.2a, Fig. 2.2b). The biomass of oak species was between zero and 100% of the entire tree community, while maples made up a maximum of 59% (minimum 0%). Mass-weighted Shannon diversity ranged from 0.05 to 1.6; if diversity had not been weighted by mass, the Shannon diversity would have ranged from 0.5 to 2.

In the PCA of lidar metrics, the first two principal components described 82% of the variance in the data (Fig. 2.2c). For the first principal component, all loadings were positive and a similar magnitude (range 0.2) and so we call this the structural similarity axis. For the second principal component, VAI and rugosity were the upper and lower bounds, respectively, for all variables (range 1.1). Since this axis represents the spread of the different metrics, we name it the structural dissimilarity axis. We acknowledge these are not precise term, but give them as general descriptors to facilitate later discussion. The PCA of only lidar metrics shows the relationship between lidar-derived variables, but for many, it is not as intuitive as something like LAI. The PCA of all variables shows how the lidar-derived metrics fit within the context of more traditional forest assessment metrics. The PCA of all variables described less of the total variance (66.8%, Fig. 2.2d), however, than the PCA of lidar metrics alone. The first principal component was defined by biomass, percent oak, and rugosity on one end, and diversity, species richness, and percent maple on the other. Since the former group are metrics broadly describing dominance within the forest community and the latter group ones which describer diversity, we call this the dominance-diversity axis. VAI, structural dissimilarity, and structural similarity made up the majority of the second principal component (architectural axis); however, structural dissimilarity was more correlated with the diversity end of dominance-diversity axis, whereas

structural similarity, fell towards the dominance end. LAI influenced both the diversity end and the architectural axis.

Precipitation and soil moisture processing

Precipitation totaled 14.1, 45.3, and 24.0 cm for the analyzed leaf-on period for 2020, 2021, and 2022, respectively. The weather station logged 36 individual precipitation events: 10 in 2020, 13 in 2021, and 13 in 2022. SWC had a mean of 0.18 (± 0.06), 0.25 (± 0.06), 0.19 (± 0.08) m^3/m^3 in 2020, 2021, and 2022, respectively.

During the leaf-on period, the weather station recorded 36 periods with no rain, for a possible 432 dry periods for all plots. Due to occasional sensor failure, 335 dry periods were available for analysis. Of these, fitting the exponential decay model to SWC was successful for 70%, leaving 235 dry periods for later analysis. For the models that failed automatic curve-fitting, 13 were data deficient; others would fit a linear model, but could not be fit using manual starting points for R's built in non-linear least squares estimates for parameters of the exponential decay function.

When fitting the soil moisture dry downs to both linear and exponential decay functions, comparisons showed that, in 5% of the models, AIC was lower for the linear model fit, but for all of these the ΔAIC was less than two, showing essentially no difference between the linear and exponential fits (Burnham & Anderson, 2004). When exponential decay was the better fit, the majority of the models (85%) showed essentially no support for the linear model (ΔAIC>10). Exponential decay was used for all models.

Tree community influence on soil water

Including slope position as a random effect did not improve fit in any models for any feature of soil moisture. All linear mixed-effects models (Tables 2.2, 2.3, 2.4), however, have a

much higher conditional than marginal R^2 (mean difference = 0.64 ±0.06), suggesting that the single random effect of dry period was important in determining the analyzed aspects of soil moisture.

Minimum soil water

The linear mixed-effects model for the minimum soil water as the response variable was most parsimoniously predicted by percent oak with a single random effect of dry period ID (Table 2.2, Fig. 2.3a). The only other model with ΔAIC < 7 contained both percent oak and VAI as predictors, but only percent oak was significant. Though models with biomass and diversity had little support by AIC (ΔAIC > 10), these predictors were nonetheless significant within the models that included them: biomass had a small, negative relationship with minimum soil water and diversity a slight positive one (Table 2.2, Fig. 2.3b and 2.3c). A Kruskal-Wallis test showed no difference in minimum soil water by slope position; including slope position as a random effect did not improve models, with the exception of the least parsimonious model listed in Table 2.2 with predictor variables of percent birch and diversity (ΔAIC = 3.3).

Drying rate constant

For models using the drying rate constant as the response variable, inclusion of slope position as a random effect did not improve model fit and resulted in a singular fit for most models. A Kruskal-Wallis test found no difference in drying rate constants by slope position; based on this, only dry period ID was included as a random effect. The model with the single fixed effect of percent maple was the most parsimonious by AIC; all models with a ΔAIC < 7 from this model contained either percent maple, percent oak, or diversity as predictors (Table 2.3). Percent maple, diversity, and the dominance-diversity axis were all positively correlated with drying rate constant, whereas percent oak was negatively correlated (Fig. 2.3d, 2.3e, and

2.3f). Tree community biomass had no effect on the drying rate constant ($p > 0.05$). Out of the eight models considered, the four with two predictors all had percent maple as one of the fixed effects and the second predictor was not significant ($p < 0.05$) (Table 2.3).

Soil water loss

For the linear mixed effects models with soil water loss as the response variable, including slope position as a random effect did not improve fit. A Kruskal-Wallis test also showed no difference in soil water loss between slope positions. The model including the architecture axis was the most parsimonious (Table 2.4) and it had a negative relationship with soil water loss (Fig. 2.3g), meaning more soil water was lost during dry periods in plots that had similar architecture, as quantified by the lidar PCA. Other models with a $\Delta AIC < 7$ tended to include variables that were descriptive of the architecture axis: of the 10 models, five included birch, five LAI, and five VAI as significant predictors, though none of these were present alone (Table 2.4). Biomass and diversity were present in models, though they were not significant predictors.

Stability of soil water minima, drying rate constants, and loss

Drying rate constant CV had no relationship with any of the predictor variables. Minimum soil water CV was negatively correlated with the dominance-diversity axis (Fig. 2.4a, $p < 0.05$), and the variables that fall towards the diversity end of that axis: structural dissimilarity, diversity, percent maple, percent birch, and LAI (Table 2.5). Minimum soil water CV biomass had a negative relationship with variables on the dominance side of the dominance diversity axis: structural similarity, biomass, percent oak, and rugosity (Fig. 2.4a and Table 2.5). Soil water loss CV was positively correlated with the dominance-diversity axis (Fig. 2.4b, $p < 0.1$), diversity, species richness, and LAI and negatively correlated with structural similarity and

rugosity (Table 2.5). Note that percent maple, percent birch, and LAI all have a single outlier in the data; removing these points changed the R^2, slope, and significance of the relationship, but never the direction.

Tree community influence on water stress ($\delta^{13}C$)

Foliar $\delta^{13}C$ did not differ between species or slope position (Kruskal-Wallis test, $p > 0.05$, Supplementary Fig. S2.2). Higher, i.e., less negative, values of $\delta^{13}C$ are indicative of water stress. Linear models showed $\delta^{13}C$ to be negatively correlated with both species richness and diversity (separate models, both $p < 0.05$) (Fig. 2.5) and to have no relationship with biomass, drying rate constant, minimum soil water, or percent oaks, maples, or birch. In a linear mixed effects model with species identity as a random effect, diversity was marginally significant ($p < 0.1$) and had a negative relationship with $\delta^{13}C$.

2.4 Discussion

Broadly, this study demonstrates that diversity, weighted by biomass, influences forest ecohydrology. We evaluated the hypotheses that more diverse tree communities would have: 1) lower minimum soil water, 2) higher soil drying rate constants, 3) greater soil water loss and, while all three of these would also be true for high biomass communities, diverse ones would also have greater stability of these metrics. Diverse tree communities tended to have larger drying rate constants; though soil water minimums were more stable, they were also higher than those in less diverse communities, in contrast to expectations (Fig. 2.3c, 2.3f, and 2.4a). While high biomass communities did have lower and more variable minimum soil water, surprisingly, biomass in absence of diversity had no effect on the drying rate constant.

High biomass and high diversity communities differed in composition: maples and birch were present in greater numbers in diverse communities and their percentages were indicative of diversity within the PCA, even though oaks are the dominant contributor of biomass within most of the experimental communities (Fig. 2.2a and 2.2d). As oaks differ from maples and birch structurally as well as physiologically, the individual tree communities represent a range of hydraulic strategies. In response to dry conditions, oaks do not down-regulate photosynthesis but maintain high rates of transpiration; by contrast, maples and birch reduce transpiration as soils dry by controlling their stomatal aperture to maintain a consistent amount of water within the leaf (Meinzer et al., 2013; Thomsen et al., 2013). If environmental conditions are such that maples and birch cease transpiration, but oaks continue, soil water minimums would be lower where oaks dominate. Since minimums would therefore depend on the length of the dry period, they also likely would be more variable, as observed (Fig. 2.3d and 2.4a). Conversely, if the physiological thresholds for transpiration in maples and birch are routinely being reached during each dry period, earlier cessation of transpiration could result in not only higher, but more stable soil water minimums (Fig. 2.3f and 2.4a). If, however, community transpiration is proportional to biomass, then the effect of the more abundant oaks continually drying out the soil should dictate the minimum soil water signal in the majority of communities. As the drying effect of oaks is less apparent in diverse tree communities, this suggests some community property that opposes oaks' drying effect is also operating.

Soil drying rate constants differed by community and were positively influenced by percent maple and diversity (Fig. 2.3d and 2.3f). While this could be a result of transpiration rates varying by species, as oaks and maples differ in their rates of water use, some studies show red oak to have higher transpiration than red maple (e.g Catovsky, Holbrook, & Bazzaz, 2002;

Nagel et al., 2002) while others find the opposite (Elliott et al., 2017; Meinzer et al., 2013). In our study, neither biomass nor percent oak influenced the drying rate constant, suggesting either some property of maples or an aspect of the communities they represent increases the rate constant. Timing of photosynthesis, at both diurnal and annual timescales, differs by species, particularly in response to environmental conditions (Niinemets, 2007; Thomsen et al., 2013; Yi et al., 2017b); larger drying rate constants in diverse tree communities could therefore be a result of temporal complementary of transpiration or spatial complementarity of root architecture and corresponding water use. Complementarity of transpiration rates, however, suggests more uniform water use over time and no relationship exists between CV of drying rate constants and diversity. Alternately, larger drying rate constants could be related to greater canopy openness due to increased soil evaporation from tree communities with fewer large oak canopies, yet this would likely also make for lower minimums as well, an effect which was not observed. Additionally, VAI showed no relationship with diversity and LAI had a positive relationship, showing little support for an environment with increased evaporation. Note that these analyses refer to the drying rate constant, while the overall rate at which the soil dries is also determined by the minimum SWC.

Our experiment saw effects of diverse communities on soil water, yet, unfortunately, cannot distinguish whether these relationships are due to tree species' physiology and selection effects or a product of the community as a whole, such as complementary of photosynthesis over time or root architecture over space. The tree's leaves themselves, however, tended to have lower $\delta^{13}C$ in more diverse tree communities (Fig. 2.5). As the leaves sampled for $\delta^{13}C$ came from full sunlight at the top of the canopy within a relatively small area, environmental variables such as light intensity, temperature, and carbon dioxide concentrations should be similar, suggesting

either increased soil water supply or lessened physiological demand of trees within diverse tree communities (Ferrio et al., 2003; Grossiord, Granier, et al., 2014). Since $\delta^{13}C$ did not differ by species sampled (Supplementary Fig. S2.2) and comparisons of leaf carbon isotopes in other maple and oak species also show no inherent differences between species (Chevillat et al., 2005; Garten & Taylor, 1992), this implies some property of the community is likely responsible for greater water availability. In species that have not ceased transpiration, the higher and more stable soil water minima found in diverse communities (Fig. 2.3c and 2.4a) could correspond to lower $\delta^{13}C$. Alternatively, lower $\delta^{13}C$ in diverse communities might be the result of reduced competition with different species using water sources at different depths within the soil profile (Grossiord, Gessler, et al., 2014; Werner et al., 2012) or facilitation via movement of water from deeper soil by deeper rooted species to shallower soils via hydraulic redistribution (Grossiord, 2019; Prieto, Armas, & Pugnaire, 2012).

Biomass effects on forest function are common, yet biomass did not influence water availability to trees, neither was it a driver of the drying rate constant (Fig. 2.3e), nor did it override the influence of diversity on soil water minimums in diverse tree communities (Fig. 2.3c). In our tree communities, biomass is strongly correlated with a high percentage of oak species and negatively correlated with percentage maple species and diversity (Fig. 2.2). These characteristics define opposite ends of the first principal component (Fig. 2.2d) or dominance-diversity axis, and the duality defines almost all of the relationships (positive or negative) with the assessed soil water features (Tables 2.2, 2.3, and 2.5). Structure was also divided by the dominance-diversity axis; tree communities high in biomass and oaks were more structurally more similar to each other, whereas higher diversity had higher structural dissimilarity (Fig. 2.2d). In the PCA, VAI is the divider between the dominance and diversity, as well as structural

similarity and dissimilarity (Fig. 2.2d), suggesting that the volume of vegetation is not influenced by the other measured variables. LAI was more associated with diversity metrics, but may not be readily interpretable, since oak trees dominating the high biomass tree communities tended to be taller than the secondary growth from post-girdling (personal observation). The farther leaves are from the lens, the smaller they appear; conversely, shorter trees with the same leaf size will cover a larger portion of the hemispherical image, which could result in LAI not directly correlated with actual leaf area. This effect, however, should not affect lidar estimates of VAI, which showed no correlations with LAI.

Our results suggest trees in diverse communities may be buffered against stress from low water availability by higher and more stable soil water minimums, as reflected in the trees' lower $\delta^{13}C$ values. Empirical evidence as to whether more diverse forests are more resistant to drought is mixed (Grossiord, 2019; Liu et al., 2022); our results provide some indication as to why drought resistance may depend on the species involved. Though oak species are generally considered more resistant to drought, maples are considered more resilient (Kunz et al., 2018; Thomsen et al., 2013); both resistant and resilient species are critical for continued function of the forested ecosystem over longer timescales, especially given the uncertainty of future climate which will likely differ from what the forest has experienced presently or in the recent past. With natural ecosystems ever more dependent on what we choose to protect, better understanding what aspects of tree physiology and community diversity are responsible for resistance and resilience of forests is crucial for preserving their function. This study makes an initial foray into understanding the link between tree diversity and forest ecohydrology by quantifying the effects of tree biodiversity on soil water. Further investigation into which aspects of tree physiology are

responsible for diversity driven soil water differences could help to establish a mechanism for forests' resistance and resilience to extreme climate events.

2.5 Tables and Figures

Table 2.1 *Metrics derived from analyses of terrestrial lidar point clouds using the lidR R package.*

See text and references for detail on algorithms used for deriving these forest structural metrics from point cloud data.

Metric	**definition**
rumple	Ratio of outer canopy surface area to ground surface area
cover fraction	Inverse of the number of deep gaps in the canopy height model relative to total number of canopy height model pixels
top rugosity	The standard deviation of pixel values in canopy height model; a measure of outer canopy roughness
vertical standard deviation	Standard deviation of height values for all points in the point cloud
entropy	Diversity and evenness of point cloud heights
vegetation area index	VAI; the sum of leaf area density values for all horizontal 1 m slices
vertical complexity index	VCI; fixed normalization of entropy

Table 2.2 *AIC for linear mixed effects models with minimum soil water as the response variable*

Models with ΔAIC<7 from the most parsimonious model are shown as well as the most parsimonious models containing either biomass and species richness, or diversity. Variables with a significance of p > 0.05 are in grey and slopes with p > 0.05 are not listed. R^2m and R^2c are marginal and conditional R^2, respectively. All predictors have been standardized.

Minimum soil water

Fixed effects	Random effect	Slope	R^2m	R^2c	ΔAIC
% oak	dry period ID	-0.34	0.106	0.867	0
% oak, VAI	dry period ID	-0.33	0.106	0.867	6.7
% oak, species richness	dry period ID	-0.34	0.106	0.866	7.6
biomass, % birch, LAI, VAI	dry period ID	-0.17, 0.07, 0.20, -0.09	0.121	0.863	11.8
% birch, diversity	dry period ID	0.15, 0.16	0.055	0.809	90.5

Table 2.3 *AIC for linear mixed effects models with drying rate decay constant (drying rate constant) as the response variable*

Only models with ΔAIC<7 from the most parsimonious model are shown. Variables with a significance of p > 0.05 are in grey and slopes with p > 0.05 are not listed. R^2m and R^2c are marginal and conditional R^2, respectively. All predictors have been standardized.

Drying rate constant

Fixed effects	Random effect	Slope	R^2m	R^2c	ΔAIC
% maple	dry period ID	0.14	0.021	0.609	0
% oak	dry period ID	-0.12	0.015	0.593	3.1
diversity	dry period ID	0.10	0.010	0.589	5.3
% maple, VAI	dry period ID	0.15	0.024	0.610	5.4
dominance-diversity axis	dry period ID	0.10	0.010	0.589	5.5
% maple, structural dissimilarity	dry period ID	0.15	0.022	0.607	6.1
% maple, % birch	dry period ID	0.14	0.022	0.607	6.2
% maple, species richness	dry period ID	0.14	0.022	0.608	6.4
community biomass	dry period ID	–	0.010	0.589	6.7

Table 2.4 *AIC for linear mixed effects models with soil water loss as the response variable.*

Only models with ΔAIC<7 from the most parsimonious model are shown. Variables with a significance of p > 0.05 are in grey and slopes with p > 0.05 are not listed. R^2m and R^2c are marginal and conditional R^2, respectively. All predictors have been standardized.

Soil water loss

Fixed effects	Random effect	Slope	R^2m	R^2c	ΔAIC
architecture axis	dry period ID	-0.16	0.024	0.672	0
% birch, LAI, VAI	dry period ID	-0.10, -0.11, -0.10	0.040	0.680	2.5
% birch, LAI, structural similarity	dry period ID	-0.10, -0.15, -0.10	0.040	0.678	2.8
% birch, VAI	dry period ID	-0.12.-0.12	0.028	0.678	3.2
architecture axis, dominance-diversity axis	dry period ID	-0.16	0.029	0.673	3.4
% birch, LAI	dry period ID	-0.14	0.030	0.668	3.5
% birch, VAI, species richness	dry period ID	-0.11, -0.14, -0.10	0.033	0.681	5.9
biomass, LAI, VAI	dry period ID	-0.13, -0.10	0.036	0.673	6.2
% birch, VAI, diversity	dry period ID	-0.11, -0.13	0.032	0.680	6.7
biomass, LAI	dry period ID	-0.17	0.027	0.662	6.8

Table 2.5 *Results for multiple linear models with either the coefficient of variation (CV) of minimum soil water or soil water loss as the response variable.*

Predictors have been centered and standardized to facilitate comparison between slopes. Only models with p < 0.20 are shown. Grey-shaded cells fall on the dominance side of the dominance-diversity axis.

predictor	**response**	**R^2**	**Slope**
CV of minimum soil water	dominance-diversity axis	0.54 **	-0.05 **
	structural similarity	0.24	0.03
	biomass	0.35 **	0.04 **
	% oak	0.65 **	0.05 **
	rugosity	0.47 **	0.05 **
	structural dissimilarity	0.18	-0.03
	diversity	0.16	-0.03
	% maple	0.39 **	-0.04 **
	% birch	0.19	-0.03
	% birch (without outlier)	0.26	-0.07
	LAI	0.49 **	-0.05 **
	LAI (without outlier)	0.24	-0.04
CV of soil water loss	dominance-diversity axis	0.28 *	0.05 *
	structural similarity	0.17	-0.04
	rugosity	0.26 *	-0.05 *
	diversity	0.39 **	0.06 **
	species richness	0.49 **	0.06 **
	LAI	0.25 *	0.05 *
	LAI (without outlier)	0.44 **	0.09 **

* $p < 0.1$, ** $p < 0.05$

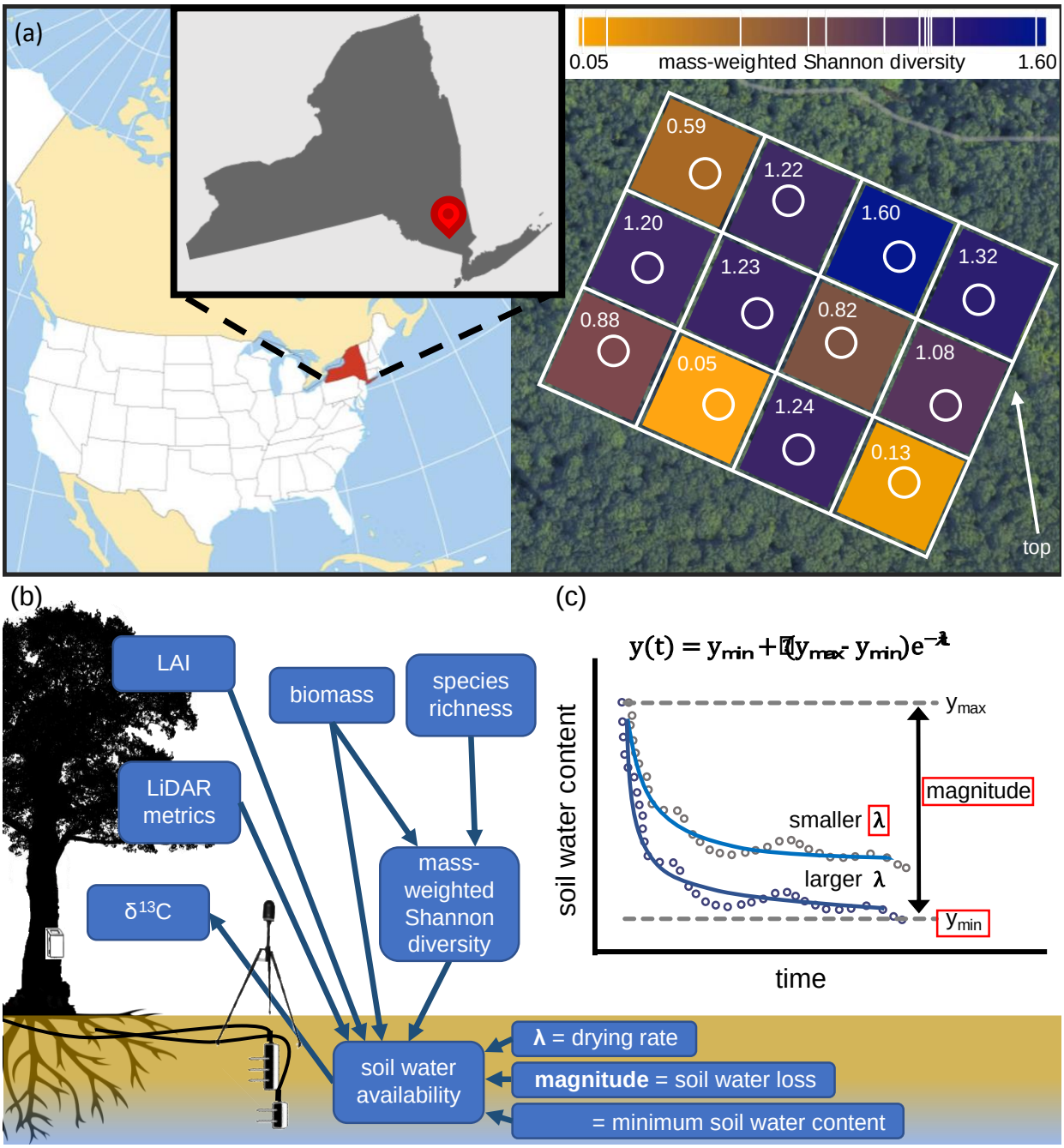

Figure 2.1 Experimental layout and conceptual diagram of analyses

Schematic of treatment layout at Black Rock Forest (red marker), located in the Hudson Highlands of New York State within the United States (a). Each plot is 75 m x 75 m; the arrow shows the direction up the hill slope. White circles represent approximate locations of the 10 m radius tree communities surrounding each soil moisture sensor. The number within each plot

designates the tree community's mass-weighted Shannon-diversity and each white line on the colored scale represents a plot. A conceptual diagram of the relationship between variables (b) and a schematic of fitted soil water dry down curve with response variables outlined in red (c).

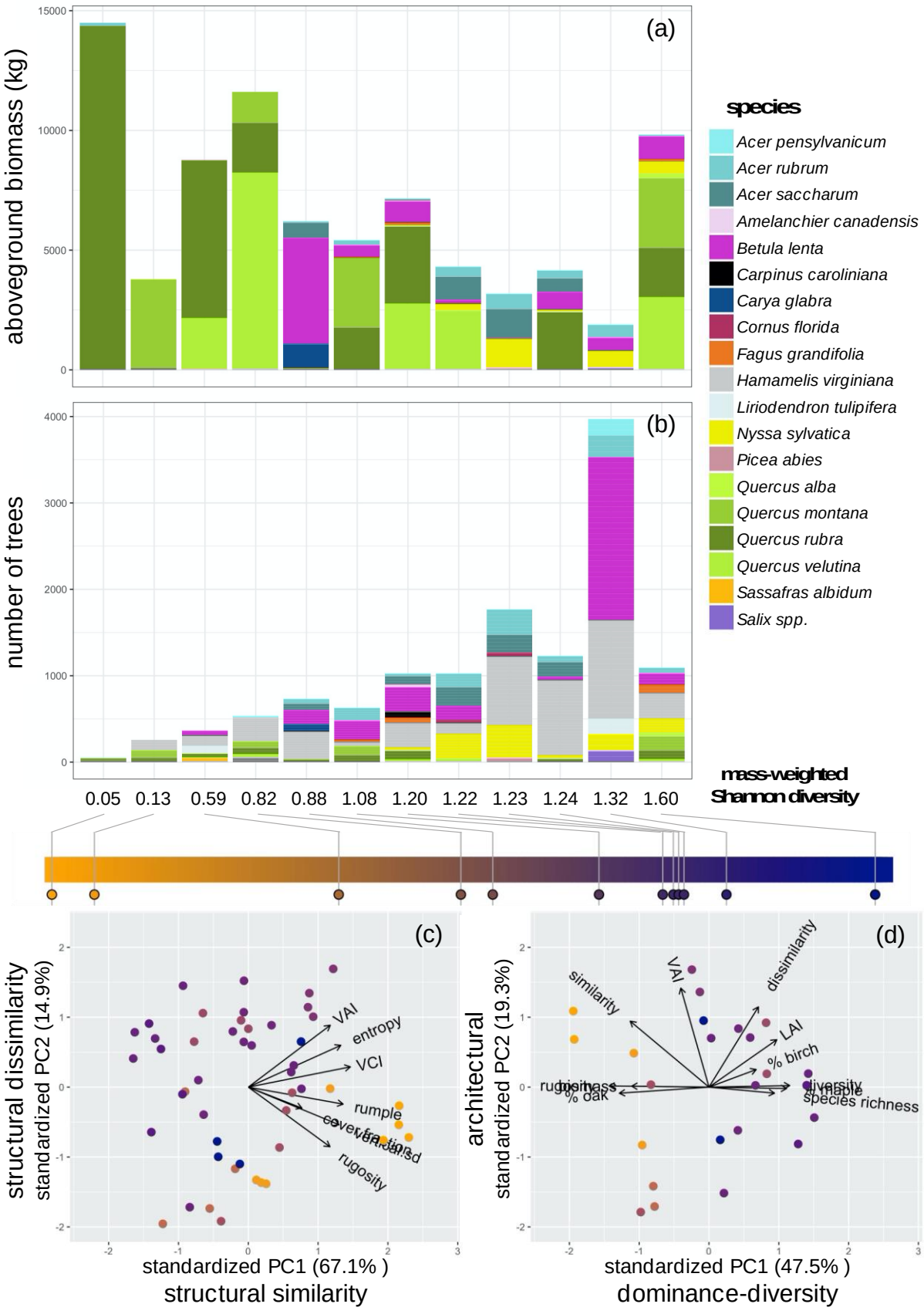
(a)
aboveground biomass (kg)
15000
10000
5000
0
(b)
number of trees
4000
3000
2000
1000
0
species
Acer pensylvanicum
Acer rubrum
Acer saccharum
Amelanchier canadensis
Betula lenta
Carpinus caroliniana
Carya glabra
Cornus florida
Fagus grandifolia
Hamamelis virginiana
Liriodendron tulipifera
Nyssa sylvatica
Picea abies
Quercus alba
Quercus montana
Quercus rubra
Quercus velutina
Sassafras albidum
Salix spp.
0.05 0.13 0.59 0.82 0.88 1.08 1.20 1.22 1.23 1.24 1.32 1.60
mass-weighted Shannon diversity
(c)
structural dissimilarity
standardized PC2 (14.9%)
VAI
entropy
VCI
rumple
rugosity
standardized PC1 (67.1%)
structural similarity
(d)
architectural
standardized PC2 (19.3%)
similarity
VAI
dissimilarity
LAI
% birch
% oak
% maple
species richness
standardized PC1 (47.5%)
dominance-diversity

Figure 2.2 Forrest community biomass and species distribution and principal component biplot of stand metrics

Stacked bar charts showing total aboveground biomass separated by species (a) and number of trees per species (b), ordered by mass-weighted Shannon diversity for each experimental plot. Color bar shows the gradient of diversity; each circle and line represent a plot. First and second principal components from two separate principal component analyses showing relationships between lidar-derived stand metrics (c) and all predictor variables (d). In (d), similarity and dissimilarity refer to the first and second principal components, respectively, derived from (c). Points are colored by diversity.

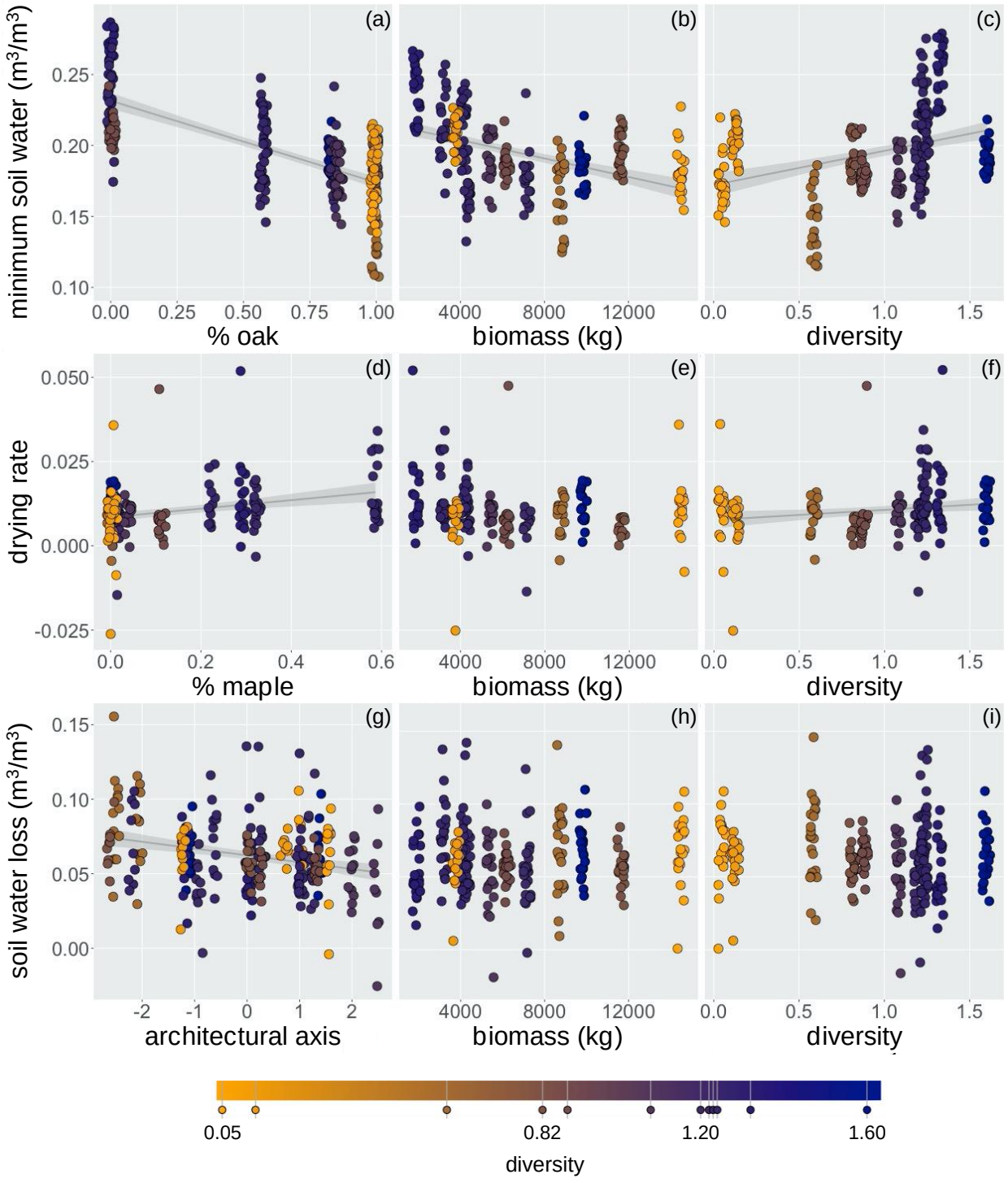

Figure 2.3 Partial residual plots from separate linear mixed effects models showing effects on minimum soil water, drying rate constant, and soil water loss

Partial residual plots from separate linear mixed effects models showing effects on minimum soil water (a, b, c), drying rate constant (d, e, f), and soil water loss (g, h, i). Leftmost column (a, d, g)

shows the effect from the most parsimonious model; middle column and right column show the effect of the biomass (b, e, h) and diversity (c, f, i), respectively, from the most parsimonious model that included these variables. All models use a random effect on intercept of dry period ID, to account for environmental conditions within a dry period and repeated measures within the same plot. Line is the linear fit between x and y variables and the shaded area is 95% confidence interval, which only shows the variance of the fixed effects; line is not shown if $p < 0.05$. Note that while the y-axis for each is the same, the points should not be expected to line up as the data take into account the partial residuals from the variables not plotted and also may be negative when the data underlying them is not. A single, high drying rate constant point lies outside the plotting area of d, e, and f; the outlier belongs to a single, high volume rain event, but the relationship and significance are the same when it is excluded. All points have been jittered along the x-axis. Model comparison was done on standardized variables, but this figure shows actual values, for ease of interpretation.

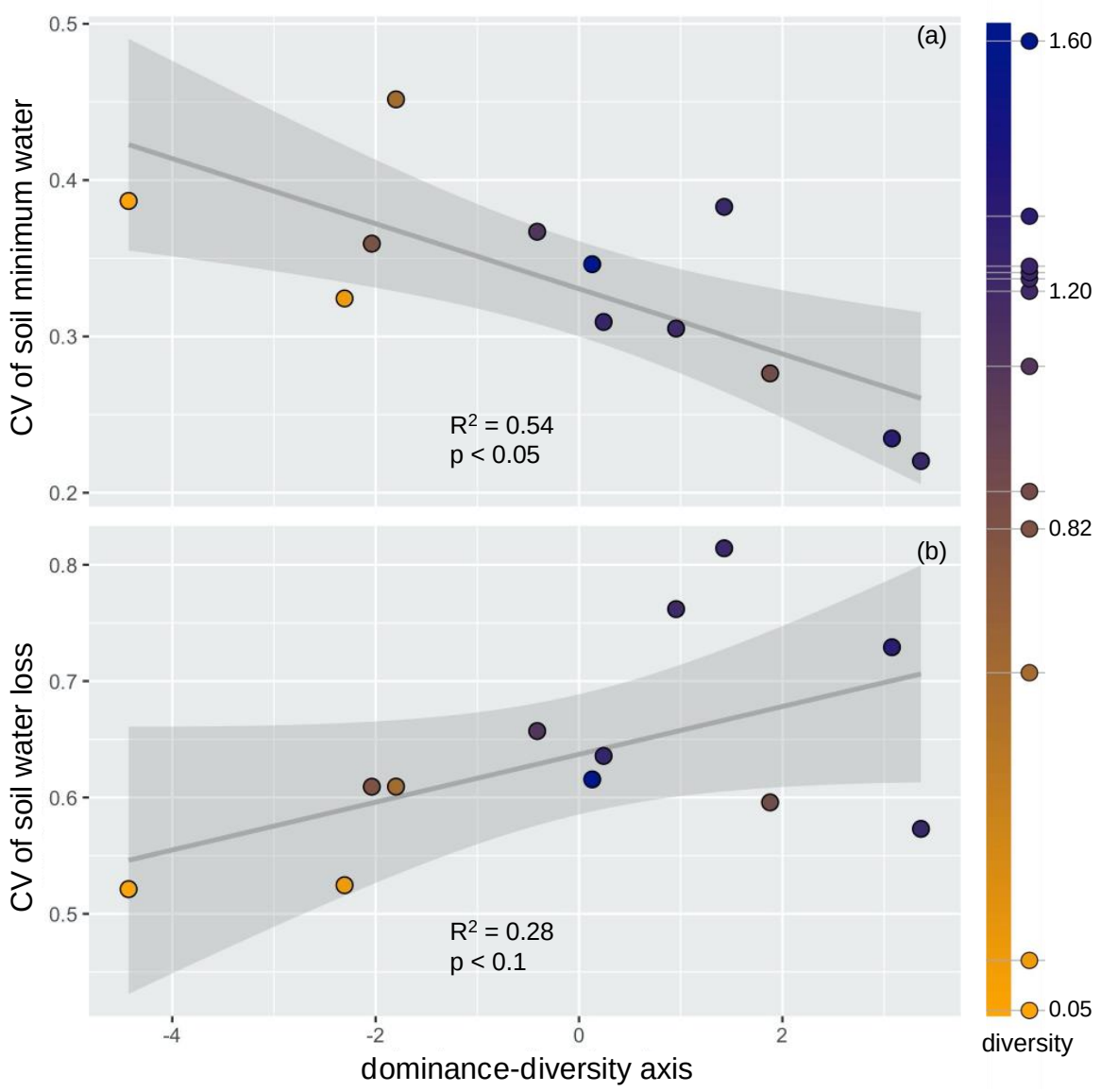

Figure 2.4 Coefficient of variation (CV) for minimum soil water (a) and soil water loss (b) against the dominance diversity axis.

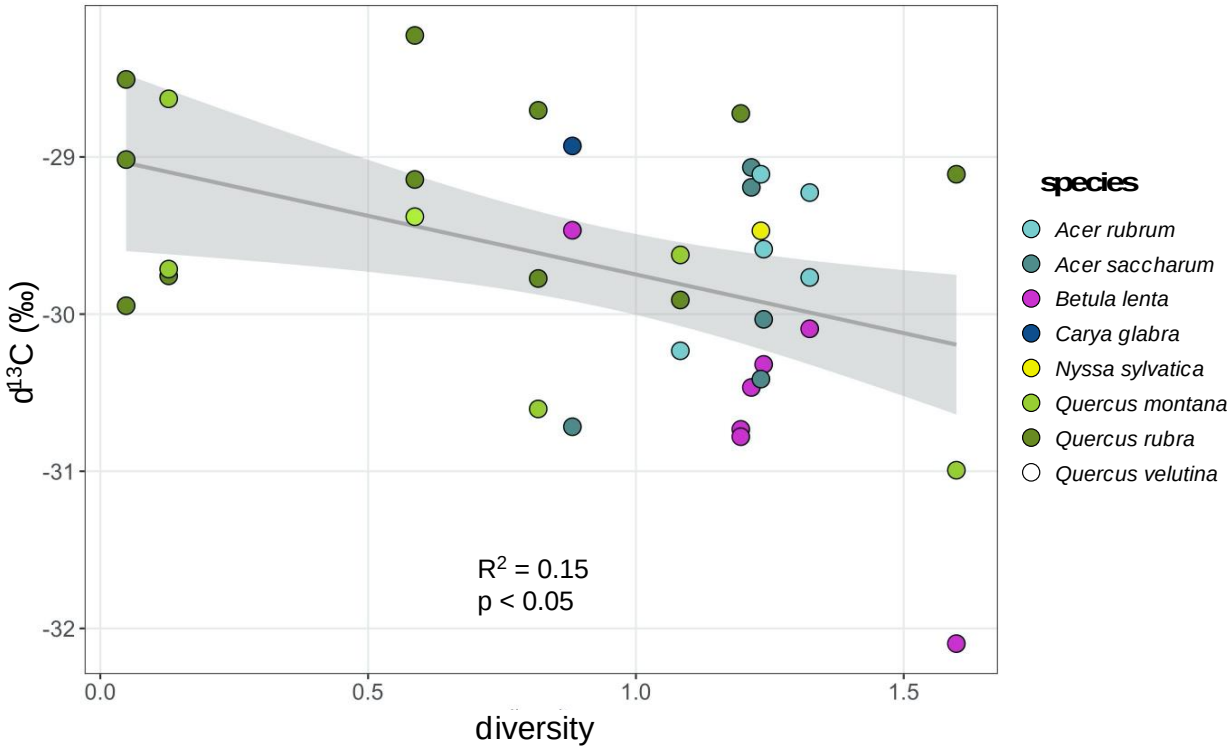

Figure 2.5 Relationship between mean leaf $\delta^{13}C$ for 2020-2022 and mass-weighted Shannon diversity of the tree community.

Chapter 3: Diversity stabilizes forest growth rates via phenological complementarity: A long-term experimental test of the portfolio effect in oak-dominated forests

Sarah G. Bruner, Shahid Naeem, Jan U. H. Eitel, Kevin L. Griffin, Duncan N. L. Menge, Katherine Terlizzi, William S. F. Schuster

3.1 Introduction

Three decades of empirical and theoretical study has found a positive relationship between biodiversity and ecosystem functioning (BEF), and, while the scientific community acknowledges both selection and niche complementarity as drivers, the physiological mechanisms underpinning complementarity remain unclear (Cardinale et al., 2012; Dallas & Kramer, 2022; Kéfi et al., 2019; Naeem et al., 2012). When BEF relationships are a result of complementarity, i.e., either facilitation by species, differential resource use, or both, occurring throughout time and/or space, an increase in the stability of function with greater diversity is both predicted by theory and has been demonstrated empirically (Wang et al., 2021). One potential explanation is the asynchronous response of different species to environmental conditions over time (Loreau & de Mazancourt, 2013), known as the "portfolio effect." The portfolio effect describes the tendency of an entire system to vary less than its constituent species due to statistical averaging (Doak et al., 1998; Schindler et al., 2015; Tilman et al., 1998), similar to the stabilizing effect of asset diversity on financial portfolios (Markowitz, 1952). The portfolio effect has been demonstrated empirically over several scales, from communities (Tilman et al., 2006), to populations (Schindler et al., 2010), to within populations (Abbott et al., 2017). Though

these studies and others demonstrate the emergent property of stability increasing with diversity, quantifying the underlying mechanism of differential response within non-simulated communities has remained a challenge.

When analyzing the portfolio effect, most studies have focused on fluctuations of abundances over time, particularly using herbaceous plant species (e.g., Dallas & Kramer, 2022; Valencia et al., 2020). Changes in abundance, however, are challenging to assess for longer-lived, high biomass organisms such as trees, which may take decades for new recruitment to compensate for the loss of a single mature tree. Such timescales typically fall outside of the range of most scientific study. Yet tree growth is remarkably sensitive to environmental conditions: analysis of tree growth rings has provided insights into centuries of historical climate (Babst et al., 2019; Rao et al., 2020), while species-specific changes in tree stem radii in response to temperature and soil and atmospheric aridity can be measured in as little as sub-hourly timescales (Cocozza et al., 2018; Griffin et al., 2021; Zweifel et al., 2021). Positive diversity-stability relationships have been documented in forests (Jia et al., 2021), as well as a global pattern relating hydraulic traits to drought resilience (Anderegg et al., 2018). The underlying dynamic ecophysiological processes responsible for the emergent property of stability should be quantifiable via asynchronous response as tree species react in different ways to environmental drivers.

Forests face an ever-increasing number of disturbances, from both the physical environment as well as from other organisms. New pests and pathogens, as well as changing weather regimes, can either be devastating to or accommodated by a forest, depending on the forest community's ability to retain function over time (Cardinale et al., 2012). As the global environment undergoes unprecedented changes, understanding and quantifying the variability

and stability of forest growth is critical for predicting and managing forests and their functions. Automated point dendrometers (hereafter, dendrometers), which can measure temporal changes in the radius of tree stems, offer a way of understanding whether species complement each other in their growth habits through time and, because of their sensitivity, at what scale: seasonal, intra-seasonal, or daily. Dendrometers can detect onset and cessation of growth (Eitel et al., 2023), fluctuations in stem size due to drought (Neuwirth et al., 2021; Salomón et al., 2022), and diel patterns of growth and stem dehydration and hydration (Chan et al., 2016; Krejza et al., 2022). During the growing season, water evaporating from the leaves' stomata during daytime photosynthesis sets up a pressure gradient over the length of the tree which is measurable as the non-lignified tissues in the stem contract due to water loss. Evaporation is driven by atmospheric vapor pressure deficit (VPD), a measure of how much water the air is able to hold. VPD increases in hot and/or dry weather and is a major limiter on forest function (Brum et al., 2023; Fu et al., 2022; Lammerant et al., 2023). Effects of VPD should likewise be visible in the dendrometer signal as tree stems dehydrate during the day and rehydrate and grow at night (Peters et al., 2023; Zweifel et al., 2021).

This study quantitatively assesses the applicability of the portfolio effect by examining how forest community stability at longer timescales is a function of individual tree responses at daily, intra-seasonal, and seasonal timescales. Stability is inherently multidimensional (Donohue et al., 2013; Hillebrand et al., 2018; Kéfi et al., 2019), but here we focus on variation of function over time, commonly described by the coefficient of variation (CV), where a lower CV is understood to indicate greater stability of the given function. Using a selective tree species removal experiment located within a temperate north-eastern United States deciduous forest, we ask:

1) At the decadal timescale, how does diversity affect the CV of relative growth in a forest community?
2) Over the course of day, the growing season, or at low versus high VPD, do different species show complementarity in relative stem growth?

We hypothesize: 1) Higher tree species diversity will increase stability of a forest community's growth rate because of complementarity between species growth and that 2) this will be visible in the dendrometer signal under low versus high VPD, as species have different physiological optima. Answers to these questions will help improve knowledge as to whether and at what timescale complementarity occurs and thus the mechanism(s) underpinning the portfolio effect. This study endeavors to link ecophysiological and BEF research to better understand why shifts in species composition or environmental change may alter stability of forest function over time.

3.2 Methods

Site characteristics

Black Rock Forest (BRF) is located in the Hudson Highlands region of southeast New York State, USA (41°24′ N, 74°01′ W). Air temperature is seasonal, with mean monthly temperatures ranging from 24 ºC to -2.1 ºC (NOAA, 2020), with the annual mean at 9.7 ºC. Mean annual precipitation is 1.3 m and soils are relatively sloped (10-30º), moderately to excessively draining, shallow, and rocky. Lithic bedrock at 0-60 cm underlays approximately 60% of site with the remainder being fragipan at 35-90 cm (Soil Survey Staff, USDA 2022). BRF is a temperate deciduous forest where oak species (*Quercus spp.*) make up approximately 70% of the canopy trees (Schuster et al., 2008), with other common species being maples (*Acer rubrum* and *A. saccharum*), birch (*Betula lenta*), American beech (*Fagus grandifolia*), and black

gum (*Nyssa sylvatica*). Oak species present include white oak (*Quercus alba*), red oak (*Q. rubra*), chestnut oak (*Q. montana*), and black oak (*Q. velutina*). Before BRF was established as a research forest in 1927, much of the area had been repeatedly logged for approximately the previous 200 years.

Experimental setup

Diversity manipulation

Twelve 75 m by 75 m experimental plots were laid out in a three by four grid on the north slope of Black Rock Mountain in 2006. The layout is a semi-randomized block design grouped by slope position (low, mid and high), where each treatment is repeated once within each of the slope positions. In 2008, each plot received one of four treatments: 0% of the trees girdled (control), 50% (by stem number) of oak trees girdled, 100% of oak trees girdled, and 100% of all non-oak trees girdled. Trees were girdled using a chainsaw cutting 3-5 cm into the bark of the tree to sever phloem transport (Noel, 1970), mimicking the mechanism by which many pathogens block the flow of nutrients through the phloem and cambium. Girdled trees were left standing if greater than 10 cm in diameter at breast height (DBH) and felled if they were smaller. A small number of tree (<5%) continued to leaf out after the girdling in 2008; these were girdled a second time in 2010. Each plot was divided into nine 25 m x 25 m subplots; all trees within the central subplot have been censused annually since 2006 (except for 2014) to establish species identity, record sprouting, assess tree health (alive or dead via leaf presence), and measure the DBH of living trees. New trees were added to the census once they reached 1 cm DBH. Analyses on stability of forest community growth use this central subplot (i.e., forest community). Biomass lost to girdling was calculated from 2007 data as the percentage of total biomass comprising girdled trees (percent girdled).

Environmental variables

In April of 2020, a weather station (METER Group ATMOS 41) measuring VPD and other environmental variables including air temperature, relative humidity, precipitation, and wind speed was installed at the top of the slope containing the experimental treatments.

Dendrometers

In the summer of 2020, automated point dendrometers (Hise Scientific Instrumentation, Somers, New York, USA) were installed on the three trees over 10 cm DBH closest to the soil moisture sensors on the north side of the tree, at 1.3 m from the ground surface (Table 3.1). Dendrometers were attached to the stem with a mounting bracket drilled into the heartwood of the tree to maintain the sensor in a fixed position relative to the non-living xylem. Loose bark was removed with a small rasp and the dendrometer sensor rested on top of the thin bark. An automated data logger recorded sensor readings once an hour. Before installation of each dendrometer was finalized, DBH was taken where the dendrometer sensor would rest.

Analyses

All data processing and statistics were done in R version 4.1.3 (R Core Team, 2022, with extensive use of the *data.table* package (Dowle & Srinivasan, 2021)).

Stability of forest community growth

Within the central 25 m x 25 m subplot, aboveground tree biomass was calculated using species-specific allometric equations based on a living tree's DBH (Brenneman et al. 1978; Monteith, 1979; Whittaker and Woodwell, 1968) and summed for total live tree biomass. Trees which died before 2020 were excluded from the analysis, as were trees less than 10 cm DBH, as the timescale of 10 years was too short for new recruitment to compensate for the death of a single

tree. Relative annual aboveground biomass growth (relative growth) of each central subplot was calculated as:

$$relative\ growth = \frac{\ln(B_{t+\Delta t}) - \ln\ (B_t)}{\Delta t}$$

Where $B_{t+\Delta t}$ equals biomass at the current time, and B_t is the biomass from the previous census. Δt is the difference in years between censuses. Stability of forest community growth was calculated using the coefficient of variation (CV) of relative growth for all years post-girdling (2010-2020):

$$CV_{plot} = \frac{\text{standard deviation of plot relative growth } 2010-2020}{\text{mean plot relative growth } 2010-2020}$$

A lower CV is understood to signify greater stability. To evaluate stability's relationship to diversity, diversity was calculated as the mean number of species for the community between 2010 and 2020. In a separate model, mean biomass of the community from 2010-2020 was also used as a predictor for diversity, to compare whether stability had a stronger relationship to community species richness or biomass.

Complementarity of tree stem growth

As dendrometers periodically failed, due to weather, animal damage, and sensor malfunction, or had to be readjusted, raw output from each dendrometer was manually inspected for jumps and outliers. Data which randomly moved between values or included erroneously high or low measures were removed. Large discontinuities between sections of normal sensor output were adjusted so that the value at the end of earlier section was equal to the beginning value at the later section.

Total tree stem diameter change, which includes both wood and bark growth, was considered as the maximum dendrometer value attained between March and October (end) and

minimum value between March and June (beginning). We used the dates when 10% and 90% of total stem diameter change was reached as the beginning and end, respectively, of the growing season (Eitel et al., 2023; Etzold et al., 2022). While this may not capture the entirety of a tree's seasonal growth, it eliminates potential obfuscation by non-growth related changes such as bark swelling from rain events or winter-induced dehydration that can happen on the shoulders of the seasons (Eitel et al., 2023). We used a two-way ANOVA between day of year (DOY) and the interaction of species and Tukey's Honestly Significant Difference test to examine the differences between beginning, end, and length of growing season. 2020 was excluded from analyses since dendrometers were installed during the middle of the growing season; only 2021 and 2022 were used.

Dendrometer signal was converted to DBH by converting the dendrometer output as follows:

$$D_t = 2cr_t + D_{t0}$$

Where D_t equals the DBH area at the current time, c is a constant which converts millivolts of the dendrometer output to centimeters (c = 3.81083 x 10^{-5}), r_t is the dendrometer reading at the current time in millivolts, and D_{t0} equals the initial DBH. DBH then was converted to species-specific biomass using allometric equations (Brenneman et al. 1978; Monteith, 1979; Whittaker and Woodwell, 1968) and total growth for the entire season was calculated.

To investigate a potential threshold effect for VPD, data were classified into two levels of VPD: high VPD, if VPD was over the 80th percentile for the current year, and low VPD, if they were below the 40th percentile (Fu et al., 2022). Growth was compared on an hourly basis over the course of a day for high and low VPD.

To separate growth from reversable stem-related processes such as dehydration and hydration, we used Zweifel et al.'s (2016) zero-growth model, which assumes growth and stem shrinkage cannot occur simultaneously. Stem diameter excludes shrinkage from a previous maximum and is assumed to be that maximum until the value is exceeded. This difference between the previous and new maximum constitutes growth, which can be converted to biomass using allometric equations. Zero-growth biomass was calculated for each hourly measurement and also by taking the maximum biomass within a day and comparing between days to assess daily growth. Within a tree's growing season, we used the zero-growth model's biomass to calculate tree-relative growth based on Eq. 1 above, where $B_{t+\Delta t}$ equals the biomass of a given tree at the current time and B_t of the same tree at the previous time step. Since, in the zero-growth model, trees stay the same size until new growth, many relative growth values are expected to be zero. All references to tree relative growth are based on the zero-growth model either at the hourly or daily scale.

To examine biomass accumulation based on seasonality, we standardized a tree's biomass at a given point in time by dividing it by the total biomass for that year. This standardization allows us to see which trees grew more and when that growth was occurring.

Linear mixed effects models were used to examine differences in tree relative growth due to VPD. We made two sets of models, one with hourly relative growth and one with daily relative growth as the response variable. Both sets followed the same model selection process, which is as follows: individual tree biomass at the previous time step was always included as a fixed effect as were random effects of dendrometer and plot identity. Previous biomass of the individual tree helps account for size-dependent growth and dendrometer controls for repeated measures. Plot identity serves as a proxy for percent girdled, as the amount of biomass lost to

girdling affects growth rates (as seen in Chapter 1) and is also unique by plot, excepting the controls. Either genus or the interaction between genus and VPD level was included as a random effect. Along with VPD, day of year (DOY) was considered as an additional fixed effect to compare whether growth was responding to environmental conditions correlated with seasonality. When assessing growth at the daily level, maximum VPD per day was used, as high VPD typically exerts more control on growth than lower VPD. The resulting models were compared by Akaike Information Criterion (AIC) to determine parsimony (Supplementary Tables S1 and S2). Models with a difference of over seven from the most parsimonious model (ΔAIC) were not considered further (Burnham & Anderson, 2004). Slope for fixed effects were extracted using the *lme4* package (Bates et al., 2015) and marginal and conditional pseudo R^2 were generated with the *MuMIn* package (Bartoń, 2022).

3.3 Results

Decadal stability of forest community relative growth

From 2010-2020, stability of relative growth increased with the number of species in the forest community (Fig. 3.1). In plots that had greater than 25% of their biomass girdled, this relationship was significant ($p < 0.05$). For plots with less than 25% of their biomass girdled the effect was minimal and not significant ($p > 0.05$), but nonetheless explained 33% of the data. Stability also showed a trend toward increasing with greater biomass when more than 25% of a plot's biomass had been girdled, but the relationship was reversed for plots with less than 25% biomass girdled. Neither trend was significant ($p > 0.05$) and explained the data poorly ($R^2 < 0$).

Complementarity of tree stem phenology

At the seasonal timescale, oaks start growing earlier than maples or birch (mean 22 days; standard deviation 14 days) (Fig. 3.2). Though other species are shown, they are only represented by a single dendrometer per species. No difference existed between different species for end or duration of growth. Red maple grew more than other species (Supplementary Fig. S3.1).

Seasonal complementarity of tree relative growth: high versus low VPD

Over the course of the season, the linear mixed effects model showed no difference between species in relative growth, though this should be interpreted with caution as the linear mixed models were, overall, poor predictors of growth. The fixed effects of the best models explained less that 5% of the data (Table 3.2). The most parsimonious models for growth assessed at the hourly and daily scales both included level of VPD as a random effect (Supplementary Tables S3.1 and S3.2). VPD was not a significant predictor in these models (Table 3.2), possibly because of collinearity or time lags, which were not considered in our analyses. Day of year was negatively related to growth in both models. Species was not an important determinant of relative growth either at low or high VPD, assessed at either the hourly or daily scale. Tree biomass standardized by maximum yearly biomass visually suggests that trees which grow more (i.e., start at lower percentage of total annual mass) are offset over time for different species (Fig. 3.3), but this was not statistically quantified. Relative growth was challenging to visualize in the same way, given its scale and variability (Supplementary Fig. S3.2).

Daily complementarity of tree relative growth: high versus low VPD

Within a day, tree relative growth rate did not differ statistically by species at either low or high VPD (Fig. 3.4). The standard deviation and mean are very similar for all species at low VPDs. During dry conditions (high VPD) the mean for maples and, to a lesser extent, birch, dips

during the afternoon, seemingly more at higher VPD (Supplementary Fig. S3.3). *Carya glabra* and *Nyssa sylvatica* (shown together) have the most erratic behavior during dry conditions, though this is likely a product of fewer readings. Oaks shows the least variation throughout the day, both during low and high VPD.

3.4 Discussion

Over 10 years in our experimental forest communities, more diverse communities were more stable in their relative growth rate (Fig. 3.1), visible as a lower coefficient of variation (CV). Measurements of individual trees via automated point dendrometers suggest complementarity of growth in oaks, maples, and birch over the course of a season as a potential mechanism underpinning the lowered variation over time seen at the larger scale. Oaks started growing earlier and completed a larger portion of their growth early in the season as opposed to maples, birch, and other species (Fig. 3.3), though this also may be a result of an earlier start. Red oaks accumulated more biomass within a season than other species, which was also seen over the past 60 years in long term plots within the same forest (Schuster et al., 2008). These findings are consistent with complementarity observed elsewhere in the same forest, where red oaks have earlier budbreak, earlier onset of radial stem growth, and larger early-season basal area increment compared to red maples (Reinmann et al., 2023).

Whether the complementarity seen in Fig. 3.3 is due to a fundamental physiological difference between oaks and other species at our site, or because oaks make up the majority of canopy species, is unclear. Maples and birch – especially in communities where oaks are present – may be overshadowed by oaks. If this is the case, offset growth between oaks and other species would represent complementarity of different life or successional stages, rather than inherent

physiological differences. Due to the experimental design, however, dendrometers tended to be placed on oaks in communities where oaks dominated. In other naturally occurring communities of red oaks and red maples in the northeast United States, red oaks and red maples differ physiologically, with species-dependent photosynthetic and stomatal conductance rates (Bassow & Bazzaz, 1998), so it is not unreasonable to suppose that this might manifest as different responses to environmental conditions in the radial stem growth. Photosynthetic rates, however, may not translate directly to radial stem growth. In an earlier study within our forest, oaks and maples exhibited differences in respiratory patterns (Turnbull et al., 2001, 2002), so that linking photosynthesis and respiration together resulted in different predictions for carbon gain than either considered independently (Whitehead et al., 2004). Even though radial stem growth at hourly or daily resolution may not yet have a predictable outcome from other well studied physiological processes, it is likely not entirely decoupled from them, as non-synchronous seasonal patterns of photosynthesis and growth likely represent allocation of carbon to differing phases of growth as well as other processes (Krejza et al., 2022).

Contrary to expectations, species did not differ in their growth rates in response to high VPD either over the course of the day or the growing season, potentially due to sufficient water throughout the majority of the growth period or to lag effects, as seen in other studies (Anderegg et al., 2015; Kannenberg et al., 2020; Ogle et al., 2015; Zweifel et al., 2016). Our analyses excluded the end of the growing season, which is typically drier, and did not account for delays in response to VPD, which may result from water exchange between tissues compensating for atmospheric demand (Oberhuber et al., 2023). In our linear mixed-effects models, VPD was either not included in the most parsimonious model or was non-significant as a predictor. Day of year, rather, had a significant, though weak, negative correlation in the most parsimonious

models for relative growth, assessed at both the hourly and daily scale, similar to other studies finding an increased probability of growth with longer day length (Etzold et al., 2022). While both models show a decrease in relative growth rate over the course of the season, these results should be interpreted with caution, as the models overall were a poor fit, suggesting that either we are failing to take into account an important driver of function, or that growth may be aggregated at biologically inappropriate timescales. We used hourly relative growth, as given by the frequency of our dendrometer readings, and daily growth to remove some of the stochasticity within the hourly readings, but evaluating growth based on data from the trees themselves may yield better relationships with environmental drivers (Griffin et al., 2021). The low explanatory power of the model may partially explain why tree relative growth did not respond to VPD, as gross primary production, stomatal conductance, and photosynthetic rates do in other forests globally (Brum et al., 2023; Fu et al., 2022). While coexisting oaks and maples have been shown to have different photosynthetic rates based on VPD and soil water (Bassow & Bazzaz, 1998; Turnbull et al., 2002), this was not reflected in our tree's radial stem growth. Trees allocate carbon to processes other than growth, such as respiration and creation of non-structural carbohydrates, so growth should not be expected to respond directly to photosynthetic rates. Sugar maples (*Acer saccharum*), in particular, store large amounts of non-structural carbohydrates (Muhr et al., 2016), and thus may be buffered against several years of poor carbon accumulation from perturbations such as drought, freezing events, or pest damage (Sala et al., 2012). Alternatively, relative growth's lack of sensitivity to VPD at the seasonal scale might be an artifact of using the zero-growth model as its basis, which excludes contraction of the tree stem due to dehydration.

At the shortest timescale in our study, hourly variations in relative growth did not show complementarity over the of the course of the day either at low or high VPD. VPD may not control radial stem growth at shorter timescales (Zweifel et al., 2006), though this may depend on species (Griffin et al., 2021). While lack of diel complementarity may reflect real physiological processes, the absence of statistical significance could also be a result of experimental design: oaks have the smallest standard deviation overall and also the greatest number of dendrometers associated with them. Though statistical difference between species does not exist at any hour over the course of the day, the mean response of each genus suggests that maples might experience more contraction of their stem at midday than other species, particularly oaks, and this is most apparent at high VPD (Fig 4, Supplementary Fig. S3.3). Maples, however, are generally understood to be more sensitive to VPD than red oak and reduce their transpiration under dry conditions, while transpiration for oaks remain high (Bassow & Bazzaz, 1998; Elliott et al., 2017; Thomsen et al., 2013). Work in our forest, however, showed oaks to be sensitive to VPD (Engel et al., 2002), suggesting an alternate explanation for stem contraction in maples. Relatively greater dehydration of maple stems at midday as compared to oaks could be because oaks are often more deeply rooted than maples, suggesting they may be able to use water at a greater depth within the soil profile during dry conditions (Thomsen et al., 2013). Alternately, another mechanism could be responsible for stem contraction, such as a larger relative portion of non-lignified tissue (Zweifel et al., 2014).

Interestingly, though the percent of biomass girdled in our manipulation was an important predictor of stability of growth at the decadal level as well as annual community growth (as seen in Chapter 1), it was not significant in our linear mixed effects model of individual tree relative growth. When there is little disturbance (girdling), diversity does not play a significant role in the

stability of growth over longer timespans, but when over 25% of biomass is lost, higher diversity is correlated with increased stability in growth over time (Fig. 3.1), which suggests diversity may mediate the effects of disturbance.

3.5 Conclusions

Our study supports three major conclusions. First, more diverse communities had greater stability (i.e., lower variability) in growth, an effect that was strongly dependent on the original experimental manipulation of tree girdling in 2008. Within our forest, oaks are the dominant species, making up anywhere from 58% to 98% of the biomass in un-manipulated plots. Rapid loss of living biomass and associated species is a critical community process, whether this loss occurs through multiple natural stressors, such as pests, pathogens, non-native species, and climate change, or through our experimental manipulation. Thus, while our study focuses on the consequences of variation in tree community diversity, our manipulation sheds light on the future of such forests under multiple global change factors.

Second, the portfolio effect provides an explanation for why stability might influence function within ecosystems or communities (Loreau & de Mazancourt, 2013) and thus offers a way to link mechanism to function across scales. We caution, however, that what constitutes a "mechanism" depends on the scale of inquiry. While diversity might be considered a mechanism for some, it may be insufficient for others, such as those seeking to identify the underlying genetic drivers of growth. Understanding the mechanisms – and at what scales they operate – by which forest ecosystem function responds to changes in community composition is a critical ecological component for predicting the future of our forests and the stability of the ecosystem services they provide. This knowledge would aid forest management in planning for future

climate and disease scenarios, as well as optimizing managed forests for a given function based on human needs.

Finally, in our experimental manipulation of tree community composition, we found that oaks and other species complement each other's growth over the course of the season, but this needs to be more robustly quantified. Complementary growth likely depends on environmental drivers such a day length, warming degree days, soil moisture, and precipitation as well as VPD. As we enter an era of novel species and climate interactions, how this will alter species relationships and complementary timing of growth remains an open question and one of active research. While current empirical work suggests many positive diversity-stability effects, the influence of extrinsic factors, such as temperature (Abbott et al., 2017), nutrients (Niu et al., 2018; H. Yang et al., 2012; Z. Yang et al., 2011), precipitation (Hallett et al., 2014), or perturbation regimes (Grman et al., 2010), may alter the relationship between diversity and stability. Forest ecosystems have adapted to the historic range of variability in climate (Johnstone et al., 2016), and it is unclear how modern changes may affect species composition (Weltzin et al., 2003) and resulting community function. As extreme events such as drought and flooding, already unpredictable in space and time, are expected to increase as human activity alters the climate (Held & Soden, 2006; Tsonis, 1996), the ability of natural systems to function in a consistent way over time may partially depend on species composition. Tree species diversity within forests has the capacity to modulate the impact of disturbance, so that diversity itself may be also understood as a dimension of stability.

3.6 Tables and Figures

Table 3.1 *Number of trees with dendrometers, by species.*

Species	Number of trees with dendrometers
Oaks:	**17 (total)**
Quercus rubra	11
Quercus montana	5
Quercus velutina	1
Maples:	**10 (total)**
Acer rubrum	5
Acer saccharum	5
Birch:	**7 (total)**
Betula lenta	7
Other:	**2 (total)**
Carya glabra (pignut hickory)	1
Nyssa sylvatica (black gum)	1

Table 3.2 *Linear mixed effects models for individual tree relative growth based a zero-growth model for hourly or daily measurements.*

Only models with ΔAIC < 7 from the most parsimonious model are shown. Variables with a significance of p > 0.05 are in grey and slopes with p > 0.05 are not listed. R^2m and R^2c are marginal and conditional R^2, respectively. All predictors have been standardized.

Fixed effects	Random effects	Slope	R^2m	R^2c	ΔAIC
Data aggregation level: hourly					
previous biomass, VPD, DOY	dendrometer ID, plot, genus:VPD level	-4.1×10^{-5}	0.02	0.08	0
Data aggregation level: daily					
previous biomass, DOY	dendrometer ID, plot, genus:VPD level	-2.4	0.04	0.40	0

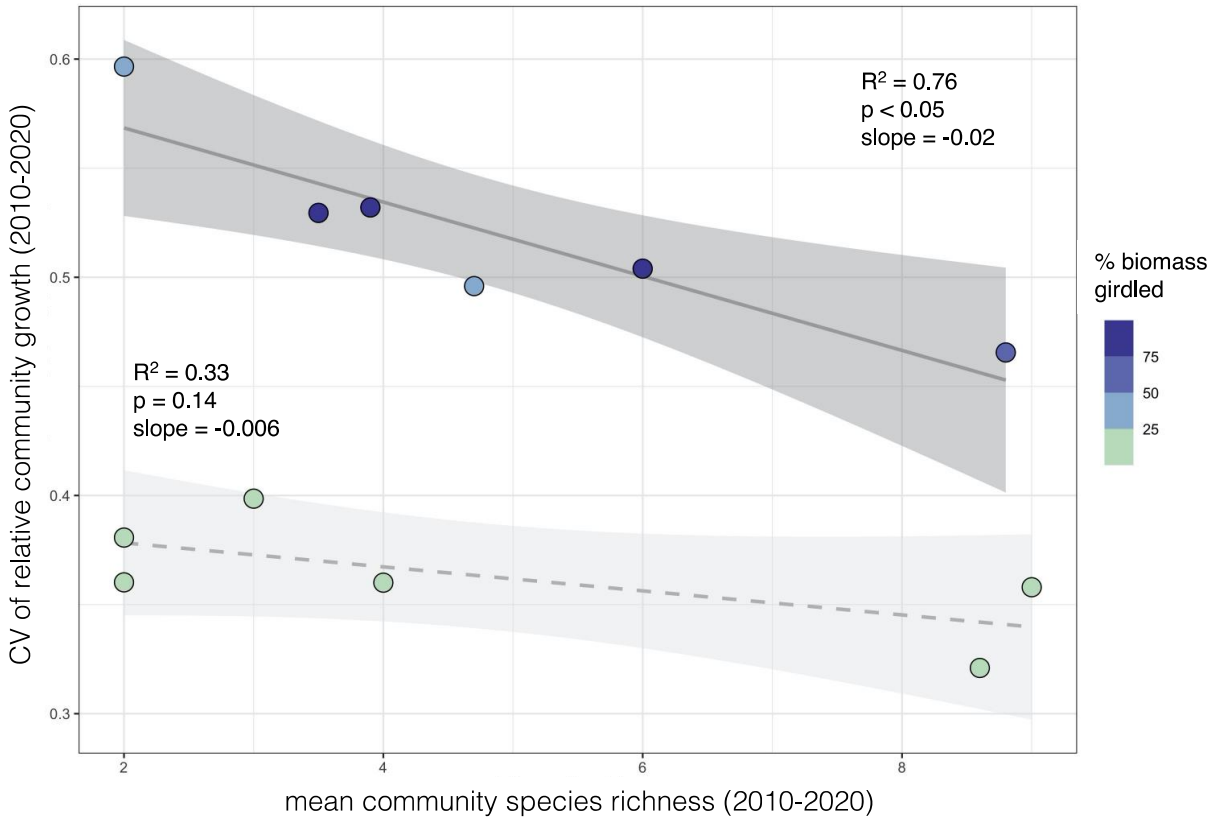

Figure 3.1 Relationship between the coefficient of variation (CV) of a forest communities' annual relative growth and the number of species in the community

For 2010-2020, the relationship between the coefficient of variation (CV) of a forest communities' annual relative growth and the number of species in the community. In 2008, different numbers of trees were girdled in each experimental community. Points are color by the percentage of the original biomass that was girdled.

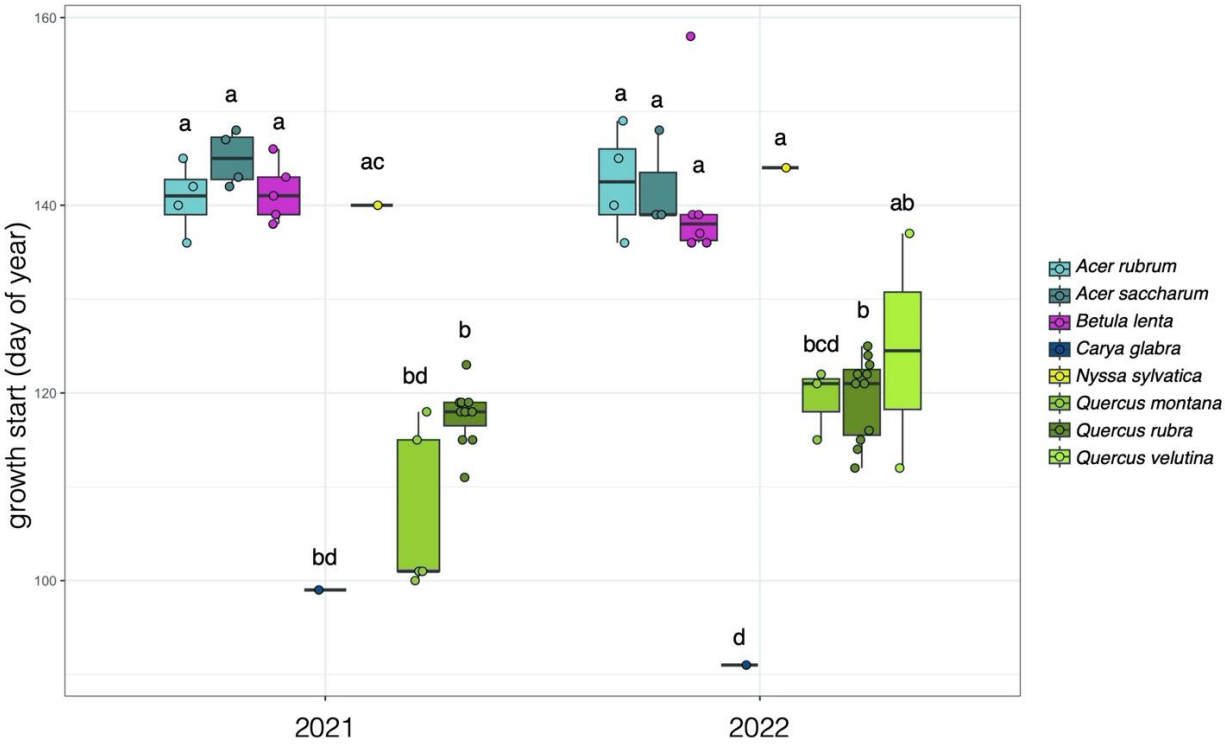

Figure 3.2 Day of year for start of the growing season for each species in 2021 and 2022. Dendrometer determined start of the growing season by species. Start and end were determined at 10% and 90%, respectively, of growth for the entire season. Differences between species were determined by ANOVA and Tukey's Honestly Significant Difference test. Note that the x-axis is categorical and horizontal separation is only for visual purposes.

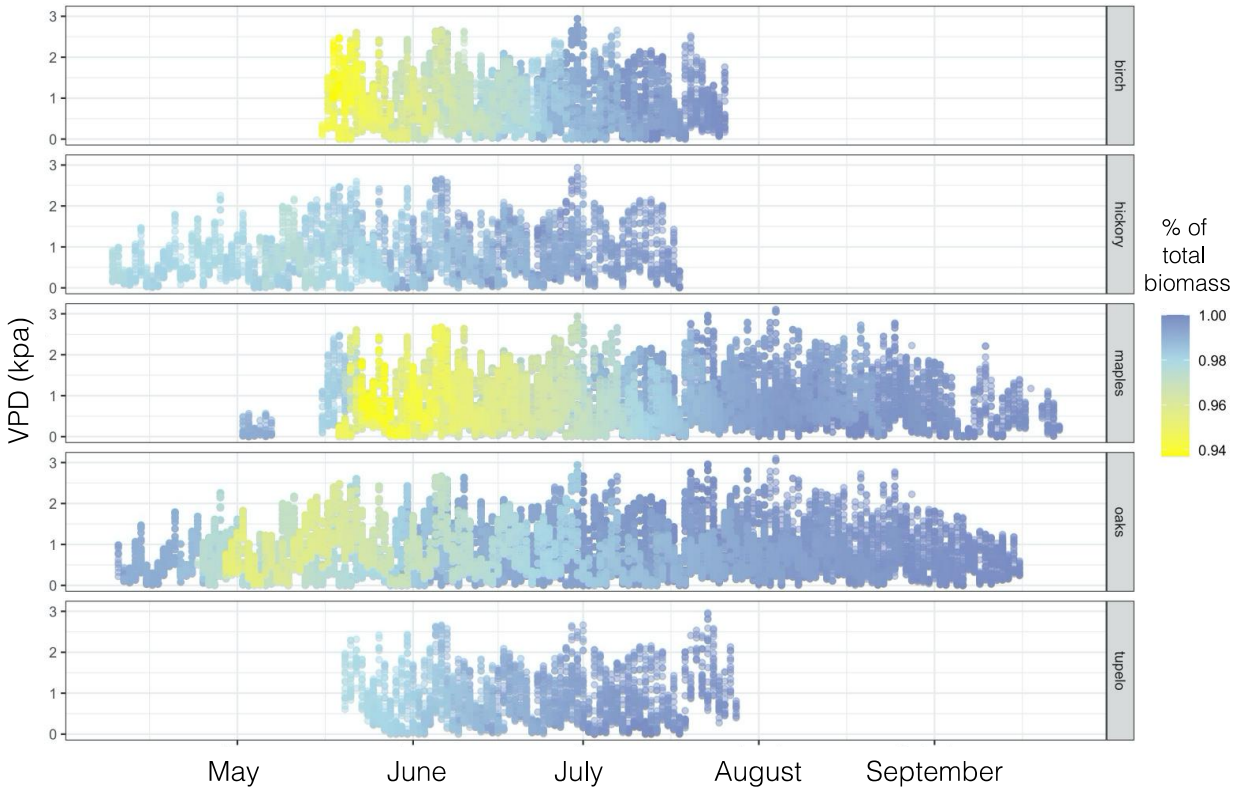

Figure 3.3 Effect of vapor pressure deficit on growth phenology of different species

Biomass of each tree assessed hourly shown by day of year (labelled by month) and vapor pressure deficit (VPD) for two years. Each point is colored by its biomass at that point standardized by its maximum biomass for that year. Note that hickory and tupelo only had a single dendrometer each.

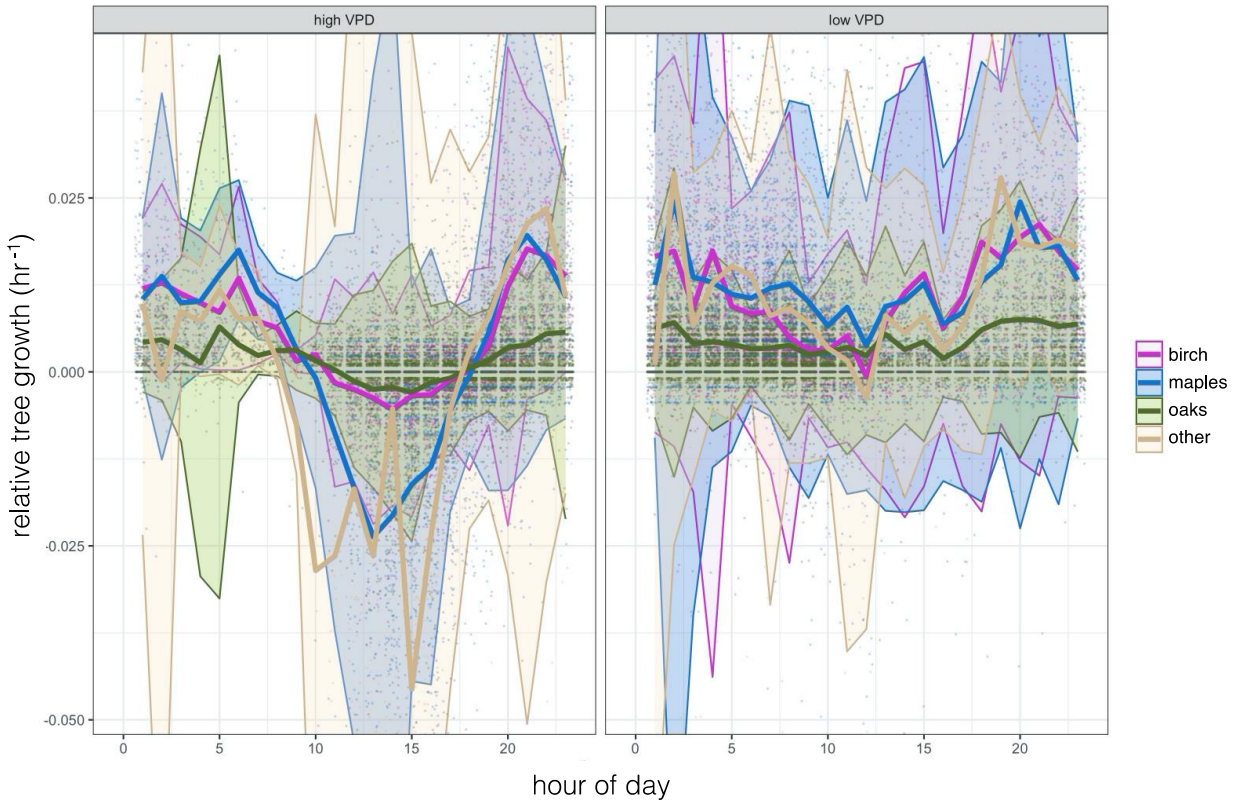

Figure 3.4 Relationship between relative growth and hour of day, by species as measured by automated point dendrometers.

Carya glabra and *Nyssa sylvatica*, which each were represented by a single dendrometer, are grouped as "other" for visual clarity. Lines show the mean value and shaded area is one standard deviation.

References

Abbott, R. E., Doak, D. F., & Peterson, M. L. (2017). Portfolio effects, climate change, and the persistence of small populations: analyses on the rare plant Saussurea weberi. Ecology, 98(4), 1071–1081. https://doi.org/10.1002/ecy.1738

Abrams, M. D. (1998). The Red Maple Paradox. BioScience, 48(5), 355–364. https://doi.org/10.2307/1313374

Adler, P. B., & Bradford, J. B. (2002). Compensation: An alternative method for analyzing diversity-productivity experiments. Oikos, 96(3), 411–420. https://doi.org/10.1034/j.1600-0706.2002.960303.x

Anderegg, W. R. L., Konings, A. G., Trugman, A. T., Yu, K., Bowling, D. R., Karp, D., Pacala, S., Sperry, J. S., & Sulman, B. (2018). Hydraulic diversity of forests regulates ecosystem resilience during drought. Science, In review. https://doi.org/10.1038/s41586-018-0539-7

Anderegg, W. R. L., Schwalm, C., Biondi, F., Camarero, J. J., Koch, G., Litvak, M., Ogle, K., Shaw, J. D., Shevliakova, E., Williams, A. P., Wolf, A., Ziaco, E., & Pacala, S. (2015). Pervasive drought legacies in forest ecosystems and their implications for carbon cycle models. Science, 349(6247), 528–532. https://doi.org/10.1126/science.aab1833

Asner, G. P., Martin, R. E., Keith, L. M., Heller, W. P., Hughes, M. A., Vaughn, N. R., Hughes, R. F., & Balzotti, C. (2018). A spectral mapping signature for the Rapid Ohia Death (ROD) pathogen in Hawaiian forests. Remote Sensing, 10(3). https://doi.org/10.3390/rs10030404

Avolio, M. L., Forrestel, E. J., Chang, C. C., La Pierre, K. J., Burghardt, K. T., & Smith, M. D. (2019). Demystifying dominant species. New Phytologist, 223(3), 1106–1126. https://doi.org/10.1111/nph.15789

Babst, F., Bouriaud, O., Poulter, B., Trouet, V., Girardin, M. P., & Frank, D. C. (2019). Twentieth century redistribution in climatic drivers of global tree growth. Science Advances, 5(1), 1–10. https://doi.org/10.1126/sciadv.aat4313

Bahamondez, C., & Thompson, I. D. (2016). Determining forest degradation, ecosystem state and resilience using a standard stand stocking measurement diagram: Theory into practice. Forestry, 89(3), 290–300. https://doi.org/10.1093/forestry/cpv052

Bakker, L. M., Mommer, L., & Van Ruijven, J. (2018). Can root trait diversity explain complementarity effects in a grassland biodiversity experiment? Journal of Plant Ecology, 11(1), 73–84. https://doi.org/10.1093/jpe/rtw111

Bassow, S. L., & Bazzaz, F. A. (1998). How environmental conditions affect canopy leaf-level photosynthesis in four deciduous tree species. Ecology, 79(8), 2660–2675. https://doi.org/10.1890/0012-9658(1998)079[2660:HECACL]2.0.CO;2

Bonan, G. (2008). Forests and Climate Change: Forcings, Feedbacks, and the Climate Benefits of Forests. Science, 320(5882), 1444–1449. https://doi.org/10.1126/science.1155121

Brasier, C. M., & Buck, K. W. (2001). Rapid evolutionary changes in a globally invading fungal pathogen (Dutch elm disease). Biological Invasions, 3(3), 223–233. https://doi.org/10.1023/A:1015248819864

Bréda, N., Granier, A., & Aussenac, G. (1995). Effects of thinning on soil and tree water relations, transpiration and growth in an oak forest (Quercus petraea (Matt.) Liebl.). Tree Physiology, 15(5), 295–306. https://doi.org/10.1093/treephys/15.5.295

Brenneman, B. B., Frederick, D. J., Gardner, W. E., Schoenhofen, L. H., & Marsh, P. L. (1978). Biomass of species and stands of West Virginia hardwoods. Central Hardwood Forest Conference II, 88(November), 159–178.

Brose, P. H. (2014). Development of prescribed fire as a silvicultural tool for the upland oak forests of the Eastern United States. Journal of Forestry, 112(5), 525–533. https://doi.org/10.5849/jof.13-088

Brum, M., Vadeboncoeur, M., Asbjornsen, H., Puma Vilca, B. L., Galiano, D., Horwath, A. B., & Metcalfe, D. B. (2023). Ecophysiological controls on water use of tropical cloud forest trees in response to experimental drought'. Tree Physiology, 1–19. https://doi.org/10.1093/treephys/tpad070

Buma, B., Hennon, P. E., Harrington, C. A., Popkin, J. R., Krapek, J., Lamb, M. S., Oakes, L. E., Saunders, S., & Zeglen, S. (2017). Emerging climate-driven disturbance processes: widespread mortality associated with snow-to-rain transitions across 10° of latitude and half the range of a climate-threatened conifer. Global Change Biology, 23(7), 2903–2914. https://doi.org/10.1111/gcb.13555

Burnham, K. P., & Anderson, D. R. (2004). Multimodel inference: A Practical Information-Theoretic Approach. In Sociological Methods and Research.

Cardinale, B. J., Duffy, J. E., Gonzalez, A., Hooper, D. U., Perrings, C., Venail, P., Narwani, A., Mace, G. M., Tilman, D., Wardle, D. a, Kinzig, A. P., Daily, G. C., Loreau, M., & Grace, J. B. (2012). Biodiversity loss and its impacton humanity. Nature, 486(7401), 0–9. https://doi.org/10.1038/nature11148

Catovsky, S., Holbrook, N. M., & Bazzaz, F. A. (2002). Coupling whole-tree transpiration and canopy photosynthesis in coniferous and broad-leaved tree species. Canadian Journal of Forest Research, 32(2), 295–309. https://doi.org/10.1139/x01-199

Chan, T., Hölttä, T., Berninger, F., Mäkinen, H., Nöjd, P., Mencuccini, M., & Nikinmaa, E. (2016). Separating water-potential induced swelling and shrinking from measured radial stem variations reveals a cambial growth and osmotic concentration signal. Plant Cell and Environment, 39(2), 233–244. https://doi.org/10.1111/pce.12541

Chaves, F. A., & Smith, M. D. (2021). Resources do not limit compensatory response of a tallgrass prairie plant community to the loss of a dominant species. Journal of Ecology, 109(10), 3617–3633. https://doi.org/10.1111/1365-2745.13741

Chevillat, V. S., Siegwolf, R. T. W., Pepin, S., & Körner, C. (2005). Tissue-specific variation of δ13C in mature canopy trees in a temperate forest in central Europe. Basic and Applied Ecology, 6(6), 519–534. https://doi.org/10.1016/j.baae.2005.04.008

Clark, J. S., Iverson, L., Woodall, C. W., Allen, C. D., Bell, D. M., Bragg, D. C., D'Amato, A. W., Davis, F. W., Hersh, M. H., Ibanez, I., Jackson, S. T., Matthews, S., Pederson, N., Peters, M., Schwartz, M. W., Waring, K. M., & Zimmermann, N. E. (2016). The impacts of increasing drought on forest dynamics, structure, and biodiversity in the United States. Global Change Biology, 22(7), 2329–2352. https://doi.org/10.1111/gcb.13160

Cocozza, C., Tognetti, R., & Giovannelli, A. (2018). High-resolution analytical approach to describe the sensitivity of tree-environment dependences through stem radial variation. Forests, 9(3), 1–18. https://doi.org/10.3390/f9030134

Crowley, K. F., Lovett, G. M., Arthur, M. A., & Weathers, K. C. (2016). Long-term effects of pest-induced tree species change on carbon and nitrogen cycling in northeastern U.S. forests: A modeling analysis. Forest Ecology and Management, 372, 269–290. https://doi.org/10.1016/j.foreco.2016.03.045

D'Odorico, P., Laio, F., Porporato, A., Ridolfi, L., Rinaldo, A., & Rodriguez-Iturbe, I. (2010). Ecohydrology of terrestrial ecosystems. BioScience, 60(11), 898–907. https://doi.org/10.1525/bio.2010.60.11.6

Dallas, T. A., & Kramer, A. M. (2022). Temporal variability in population and community dynamics. Ecology, 103(2), 1–10. https://doi.org/10.1002/ecy.3577

Daly, E., Porporato, A., & Rodriguez-Iturbe, I. (2004). Coupled dynamics of photosynthesis, transpiration, and soil water balance. Part I: Upscaling from hourly to daily level. Journal of Hydrometeorology, 5(3), 546–558. https://doi.org/10.1175/1525-7541(2004)005<0546:CDOPTA>2.0.CO;2

Dayton, P. K. (1972). Toward an understanding of community resilience and the potential effects of enrichment to the benthos at McMurdo Sound, Antarctica. Proceedings of the Colloquium on Conservation Problems in Antarctica, 81–96.

Demeter, L., Molnár, Á. P., Öllerer, K., Csóka, G., Kiš, A., Vadász, C., Horváth, F., & Molnár, Z. (2021). Rethinking the natural regeneration failure of pedunculate oak: The pathogen mildew hypothesis. Biological Conservation, 253. https://doi.org/10.1016/j.biocon.2020.108928

Dey, D. C. (2014). Sustaining oak forests in eastern North America: Regeneration and recruitment, the pillars of sustainability. Forest Science, 60(5), 926–942. https://doi.org/10.5849/forsci.13-114

Dias, F. S., Miller, D. L., Marques, T. A., Marcelino, J., Caldeira, M. C., Orestes Cerdeira, J., & Bugalho, M. N. (2016). Conservation zones promote oak regeneration and shrub diversity in certified Mediterranean oak woodlands. Biological Conservation, 195, 226–234. https://doi.org/10.1016/j.biocon.2016.01.009

Dimitrakopoulos, P. G., & Schmid, B. (2004). Biodiversity effects increase linearly with biotope space. Ecology Letters, 7(7), 574–583. https://doi.org/10.1111/j.1461-0248.2004.00607.x

Doak, Bigger, Harding, Marvier, O'Malley, & Thomson. (1998). The Statistical Inevitability of Stability-Diversity Relationships in Community Ecology. The American Naturalist, 151(3), 264. https://doi.org/10.2307/2463348

Donohue, I., Hillebrand, H., Montoya, J. M., Petchey, O. L., Pimm, S. L., Fowler, M. S., Healy, K., Jackson, A. L., Lurgi, M., McClean, D., O'Connor, N. E., O'Gorman, E. J., & Yang, Q. (2016). Navigating the complexity of ecological stability. Ecology Letters, 19(9), 1172–1185. https://doi.org/10.1111/ele.12648

Donohue, I., Petchey, O. L., Montoya, J. M., Jackson, A. L., Mcnally, L., Viana, M., Healy, K., Lurgi, M., O'Connor, N. E., & Emmerson, M. C. (2013). On the dimensionality of ecological stability. Ecology Letters, 16(4), 421–429. https://doi.org/10.1111/ele.12086

Duffy, J. E., Godwin, C. M., & Cardinale, B. J. (2017). Biodiversity effects in the wild are common and as strong as key drivers of productivity. Nature, 549(7671), 261–264. https://doi.org/10.1038/nature23886

Eitel, J. U. H., Basler, D., Braun, S., Buchmann, N., D'Odorico, P., Etzold, S., Gessler, A., Griffin, K. L., Krejza, J., Luo, Y., Maguire, A. J., Rao, M. P., Vitasse, Y., Walthert, L., & Zweifel, R. (2023). Towards monitoring stem growth phenology from space with high resolution satellite data. Agricultural and Forest Meteorology, 339(June), 109549. https://doi.org/10.1016/j.agrformet.2023.109549

Elliott, K. J., Caldwell, P. V., Brantley, S. T., Miniat, C. F., Vose, J. M., & Swank, W. T. (2017). Water yield following forest-grass-forest transitions. Hydrology and Earth System Sciences, 21(2), 981–997. https://doi.org/10.5194/hess-21-981-2017

Ellison, A. M. (2019). Foundation Species, Non-trophic Interactions, and the Value of Being Common. IScience, 13, 254–268. https://doi.org/10.1016/j.isci.2019.02.020

Ellison, A. M., Bank, M. S., Clinton, B. D., Colburn, E. A., Elliott, K., Ford, C. R., Foster, D. R., Kloeppel, B. D., Knoepp, J. D., Lovett, G. M., Mohan, J., Orwig, D. A., Rodenhouse, N. L., Sobczak, W. V., Stinson, K. A., Stone, J. K., Swan, C. M., Thompson, J., Von Holle, B., & Webster, J. R. (2005). Loss of foundation species: Consequences for the structure and dynamics of forested ecosystems. Frontiers in Ecology and the Environment, 3(9), 479–486. https://doi.org/10.1890/1540-9295(2005)003[0479:LOFSCF]2.0.CO;2

Engel, V. C., Stieglitz, M., Williams, M., & Griffin, K. L. (2002). Forest canopy hydraulic properties and catchment water balance: Observations and modeling. Ecological Modelling, 154(3), 263–288. https://doi.org/10.1016/S0304-3800(02)00068-6

Erwin, D. H. (2008). Macroevolution of ecosystem engineering, niche construction and diversity. Trends in Ecology and Evolution, 23(6), 304–310. https://doi.org/10.1016/j.tree.2008.01.013

Etzold, S., Sterck, F., Bose, A. K., Braun, S., Buchmann, N., Eugster, W., Gessler, A., Kahmen, A., Peters, R. L., Vitasse, Y., Walthert, L., Ziemińska, K., & Zweifel, R. (2022). Number of growth days and not length of the growth period determines radial stem growth of temperate trees. Ecology Letters, 25(2), 427–439. https://doi.org/10.1111/ele.13933

Farquhar, G. D., Ehleringer, J. R., & Hubick, K. T. (1989). Carbon Isotope Discrimination and Photosynthesis. Annual Review of Plant Physiology and Plant Molecular Biology, 40(1), 503–537. https://doi.org/10.1146/annurev.pp.40.060189.002443

Ferrio, J. P., Voltas, J., & Araus, J. L. (2003). Use of carbon isotope composition in monitoring environmental changes. Management of Environmental Quality: An International Journal, 14(1), 82–98. https://doi.org/10.1108/14777830310460405

Foley, J. A., DeFries, R., Asner, G. P., Barford, C., Bonan, G., Carpenter, S. R., Chapin, F. S., Coe, M. T., Daily, G. C., Gibbs, H. K., Helkowski, J. H., Holloway, T., Howard, E. A., Kucharik, C. J., Monfreda, C., Patz, J. A., Prentice, I. C., Ramankutty, N., & Snyder, P. K. (2005). Global consequences of land use. In Science (Vol. 309, Issue 5734, pp. 570–574). https://doi.org/10.1126/science.1111772

Fu, Z., Ciais, P., Prentice, I. C., Gentine, P., Makowski, D., Bastos, A., Luo, X., Green, J. K., Stoy, P. C., Yang, H., & Hajima, T. (2022). Atmospheric dryness reduces photosynthesis along a large range of soil water deficits. Nature Communications, 13(1), 1–16. https://doi.org/10.1038/s41467-022-28652-7

Fu, Z., Li, D., Hararuk, O., Schwalm, C., Luo, Y., Yan, L., & Niu, S. (2017). Recovery time and state change of terrestrial carbon cycle after disturbance. Environmental Research Letters, 12(10). https://doi.org/10.1088/1748-9326/aa8a5c

Garten, C. T., & Taylor, G. E. (1992). Foliar δ13C within a temperate deciduous forest: spatial, temporal, and species sources of variation. Oecologia, 90(1), 1–7. https://doi.org/10.1007/BF00317801

Gaston, K. J. (2000). Global patterns in biodiversity. Nature, 405, 220–227. https://doi.org/10.1038/35012228

Gaston, K. J. (2010). Valuing common species. Science, 327(5962), 154–155. https://doi.org/10.1126/science.1182818

Gentine, P., Green, J. K., Guérin, M., Humphrey, V., Seneviratne, S. I., Zhang, Y., & Zhou, S. (2019). Coupling between the terrestrial carbon and water cycles - A review. Environmental Research Letters, 14(8). https://doi.org/10.1088/1748-9326/ab22d6

Gonzalez, A., Germain, R. M., Srivastava, D. S., Filotas, E., Dee, L. E., Gravel, D., Thompson, P. L., Isbell, F., Wang, S., Kéfi, S., Montoya, J., Zelnik, Y. R., & Loreau, M. (2020). Scaling-up biodiversity-ecosystem functioning research. Ecology Letters, 23(4), 757–776. https://doi.org/10.1111/ele.13456

Gonzalez, A., & Loreau, M. (2009). The Causes and Consequences of Compensatory Dynamics in Ecological Communities. Annual Review of Ecology, Evolution, and Systematics, 40(1), 393–414. https://doi.org/10.1146/annurev.ecolsys.39.110707.173349

Götmark, F., Berglund, Å., & Wiklander, K. (2005). Browsing damage on broadleaved trees in semi-natural temperate forest in Sweden, with a focus on oak regeneration. Scandinavian Journal of Forest Research, 20(3), 223–234. https://doi.org/10.1080/02827580510008383

Gottschall, F., Cesarz, S., Auge, H., Kovach, K. R., Mori, A. S., Nock, C. A., & Eisenhauer, N. (2022). Spatiotemporal dynamics of abiotic and biotic properties explain biodiversity–ecosystem-functioning relationships. Ecological Monographs, 92(1). https://doi.org/10.1002/ecm.1490

Green, J. K., Seneviratne, S. I., Berg, A. M., Findell, K. L., Hagemann, S., Lawrence, D. M., & Gentine, P. (2019). Large influence of soil moisture on long-term terrestrial carbon uptake. Nature, 565(7740), 476–479. https://doi.org/10.1038/s41586-018-0848-x

Griffin, K., Harris, T., Bruner, S., McKenzie, P., & Hise, J. (2021). Is the Radial Growth of Irrigated Urban Trees More Strongly Correlated to Light and Temperature than Water? Arboriculture & Urban Forestry, 47(5), 214–231. https://doi.org/10.48044/jauf.2021.019

Grime, J. P. (1998). Benefits of Plant Diversity to Ecosystems : Immediate , Filter and Founder Effects Author (s): J . P . Grime Published by : British Ecological Society Stable URL : http://www.jstor.org/stable/2648655. Journal of Ecology, 86(6), 902–910.

Grman, E., Lau, J. A., Schoolmaster, D. R., & Gross, K. L. (2010). Mechanisms contributing to stability in ecosystem function depend on the environmental context. Ecology Letters, 13(11), 1400–1410. https://doi.org/10.1111/j.1461-0248.2010.01533.x

Grossiord, C. (2019). Having the right neighbors: how tree species diversity modulates drought impacts on forests. New Phytologist. https://doi.org/10.1111/nph.15667

Grossiord, C., Gessler, A., Granier, A., Berger, S., Bréchet, C., Hentschel, R., Hommel, R., Scherer-Lorenzen, M., & Bonal, D. (2014). Impact of interspecific interactions on the soil water uptake depth in a young temperate mixed species plantation. Journal of Hydrology, 519(PD), 3511–3519. https://doi.org/10.1016/j.jhydrol.2014.11.011

Grossiord, C., Granier, A., Ratcliffe, S., Bouriaud, O., Bruelheide, H., Chećko, E., Forrester, D. I., Dawud, S. M., Finér, L., Pollastrini, M., Scherer-Lorenzen, M., Valladares, F., Bonal, D., & Gessler, A. (2014). Tree diversity does not always improve resistance of forest ecosystems to drought. Proceedings of the National Academy of Sciences, 111(41), 14812–14815. https://doi.org/10.1073/pnas.1411970111

Hagger, V., Wilson, K., England, J. R., & Dwyer, J. M. (2019). Water availability drives aboveground biomass and bird richness in forest restoration plantings to achieve carbon and biodiversity cobenefits. Ecology and Evolution, 9(24), 14379–14393. https://doi.org/10.1002/ece3.5874

Hallett, L. M., Hsu, J. S., Cleland, E. E., Collins, S. L., Dickson, T. L., Farrer, E. C., Gherardi, L. A., Gross, K. L., Hobbs, R. J., Turnbull, L., & Suding, K. N. (2014). Biotic mechanisms of community stability shift along a precipitation gradient. Ecology, 95(6), 1693–1700. https://doi.org/10.1890/13-0895.1

Harrison, J. L., Reinmann, A. B., Maloney, A. S., Phillips, N., Juice, S. M., Webster, A. J., & Templer, P. H. (2020). Transpiration of Dominant Tree Species Varies in Response to Projected Changes in Climate: Implications for Composition and Water Balance of Temperate Forest Ecosystems. Ecosystems, 23(8), 1598–1613. https://doi.org/10.1007/s10021-020-00490-y

Hautier, Y., Seabloom, E. W., Borer, E. T., Adler, P. B., Harpole, W. S., Hillebrand, H., Lind, E. M., MacDougall, A. S., Stevens, C. J., Bakker, J. D., Buckley, Y. M., Chu, C., Collins, S. L., Daleo, P., Damschen, E. I., Davies, K. F., Fay, P. A., Firn, J., Gruner, D. S., … Hector, A. (2014). Eutrophication weakens stabilizing effects of diversity in natural grasslands. Nature, 508(7497), 521–525. https://doi.org/10.1038/nature13014

Held, I. M., & Soden, B. J. (2006). Robust responses of the hydrologic cycle to global warming. J. Clim., 19, 5686–5699. https://doi.org/10.1175/JCLI3990.1

Hillebrand, H., Langenheder, S., Lebret, K., Lindström, E., Östman, Ö., & Striebel, M. (2018). Decomposing multiple dimensions of stability in global change experiments. Ecology Letters, 21(1), 21–30. https://doi.org/10.1111/ele.12867

Hunt, A. G., Sahimi, M., Faybishenko, B. A., Egli, M., Ghanbarian, B., & Yu, F. (2023). Interpreting water demands of forests and grasslands within a new Budyko formulation of evapotranspiration using percolation theory. Science of The Total Environment, 877(February), 162905. https://doi.org/10.1016/j.scitotenv.2023.162905

Isbell, F., Craven, D., Connolly, J., Loreau, M., Schmid, B., Beierkuhnlein, C., Bezemer, T. M., Bonin, C., Bruelheide, H., De Luca, E., Ebeling, A., Griffin, J. N., Guo, Q., Hautier, Y., Hector, A., Jentsch, A., Kreyling, J., Lanta, V., Manning, P., … Eisenhauer, N. (2015). Biodiversity increases the resistance of ecosystem productivity to climate extremes. Nature, 526(7574), 574–577. https://doi.org/10.1038/nature15374

Jia, Z., Ge, S., Li, Y., Kang, D., & Li, J. (2021). Relationship between tree richness and temporary stability of plant communities: A case study of a forest in northeast china. Forests, 12(12). https://doi.org/10.3390/f12121756

Johnstone, J. F., Allen, C. D., Franklin, J. F., Frelich, L. E., Harvey, B. J., Higuera, P. E., Mack, M. C., Meentemeyer, R. K., Metz, M. R., Perry, G. L. W., Schoennagel, T., & Turner, M. G. (2016). Changing disturbance regimes, ecological memory, and forest resilience. Frontiers in Ecology and the Environment, 14(7), 369–378. https://doi.org/10.1002/fee.1311

Jones, C. G., Lawton, J. H., & Shachak, M. (1994). Organisms as Ecosystem Engineers. Oikos, 69(3), 373–386.

Jucker, T., Bouriaud, O., Avacaritei, D., & Coomes, D. A. (2014). Stabilizing effects of diversity on aboveground wood production in forest ecosystems: linking patterns and processes. Ecology Letters, 17(12), 1560–1569. https://doi.org/10.1111/ele.12382

Kannenberg, S. A., Schwalm, C. R., & Anderegg, W. R. L. (2020). Ghosts of the past: how drought legacy effects shape forest functioning and carbon cycling. Ecology Letters, 23(5), 891–901. https://doi.org/10.1111/ele.13485

Kéfi, S., Domínguez-García, V., Donohue, I., Fontaine, C., Thébault, E., & Dakos, V. (2019). Advancing our understanding of ecological stability. Ecology Letters, 22(9), 1349–1356. https://doi.org/10.1111/ele.13340

Kesanakurti, P. R., Fazekas, A. J., Burgess, K. S., Percy, D. M., Newmaster, S. G., Graham, S. W., Barrett, S. C. H., Hajibabaei, M., & Husband, B. C. (2011). Spatial patterns of plant diversity below-ground as revealed by DNA barcoding. Molecular Ecology, 20(6), 1289–1302. https://doi.org/10.1111/j.1365-294X.2010.04989.x

Krejza, J., Haeni, M., Darenova, E., Foltýnová, L., Fajstavr, M., Světlík, J., Nezval, O., Bednář, P., Šigut, L., Horáček, P., & Zweifel, R. (2022). Disentangling carbon uptake and allocation in the stems of a spruce forest. Environmental and Experimental Botany, 196(September 2021). https://doi.org/10.1016/j.envexpbot.2022.104787

Kunz, J., Löffler, G., & Bauhus, J. (2018). Minor European broadleaved tree species are more drought-tolerant than Fagus sylvatica but not more tolerant than Quercus petraea. Forest Ecology and Management, 414(July 2017), 15–27. https://doi.org/10.1016/j.foreco.2018.02.016

Lammerant, R., Rita, A., Borghetti, M., & Muscarella, R. (2023). Water-limited environments affect the association between functional diversity and forest productivity. Ecology and Evolution, 13(8), 1–12. https://doi.org/10.1002/ece3.10406

Laurance, W. F., Lovejoy, T. E., Vasconcelos, H. L., Bruna, E. M., Didham, R. K., Stouffer, P. C., Gascon, C., Bierregaard, R. O., Laurance, S. G., & Sampaio, E. (2002). Ecosystem decay of Amazonian forest fragments: A 22-year investigation. In Conservation Biology (Vol. 16, Issue 3, pp. 605–618). https://doi.org/10.1046/j.1523-1739.2002.01025.x

Leidinger, J., Blaschke, M., Ehrhardt, M., Fischer, A., Gossner, M. M., Jung, K., Kienlein, S., Kózak, J., Michler, B., Mosandl, R., Seibold, S., Wehner, K., & Weisser, W. W. (2021). Shifting tree species composition affects biodiversity of multiple taxa in Central European forests. Forest Ecology and Management, 498(July). https://doi.org/10.1016/j.foreco.2021.119552

Leuning, R. (1995). A critical appraisal of a combined stomatal-photosynthesis model for C3 plants. Plant, Cell & Environment, 18(4), 339–355. https://doi.org/10.1111/j.1365-3040.1995.tb00370.x

Lipoma, M. L., Gurvich, D. E., Urcelay, C., & Díaz, S. (2016). Plant community resilience in the face of fire: experimental evidence from a semi-arid shrubland. Austral Ecology, 41(5), 501–511. https://doi.org/10.1111/aec.12336

Liu, D., Wang, T., Peñuelas, J., & Piao, S. (2022). Drought resistance enhanced by tree species diversity in global forests. Nature Geoscience, 15(10), 800–804. https://doi.org/10.1038/s41561-022-01026-w

Loreau, M., & de Mazancourt, C. (2013). Biodiversity and ecosystem stability: A synthesis of underlying mechanisms. Ecology Letters, 16(SUPPL.1), 106–115. https://doi.org/10.1111/ele.12073

Loreau M., & Hector. A. (2001). Partitioning selection and complementarity in biodiversity experiments. Nature, 412(6842), 72–76.

Lyford, W. . (1980). Development of the Root System of Northern Red Oak Quercus-Rubra. In Harvard Forest Papers (Issue 21, pp. 3–30).

Lyford, W. H., & Wilson, B. F. (1964). Development of the Root System of Acer Rubrum L. In Harvard Forest Paper (Vol. 10, p. 17). https://doi.org/citeulike-article-id:5771996

Majone, B., Viani, F., Filippi, E., Bellin, A., Massa, A., Toller, G., Robol, F., & Salucci, M. (2013). Wireless Sensor Network Deployment for Monitoring Soil Moisture Dynamics at the Field Scale. Procedia Environmental Sciences, 19, 426–435. https://doi.org/10.1016/j.proenv.2013.06.049

Mariotte, P., Vandenberghe, C., Kardol, P., Hagedorn, F., & Buttler, A. (2013). Subordinate plant species enhance community resistance against drought in semi-natural grasslands. Journal of Ecology, 101(3), 763–773. https://doi.org/10.1111/1365-2745.12064

Markowitz, H. (1952). Portfolio Selection. The Journal of Finance, 7(1), 77. https://doi.org/10.1111/j.1540-6261.1952.tb01525.x

Marquard, E., Weigelt, A., Temperton, V. M., Roscher, C., Schumacher, J., Buchmann, N., Fischer, M., Weisser, W. W., & Schmid, B. (2009). Plant species richness and functional composition drive overyielding in a six-year grassland experiment. Ecology, 90(12), 3290–3302. https://doi.org/10.1890/09-0069.1

Mayor, X., & Roda, F. (1993). Growth response of holm oak (Quercus ilex L) to commercial thinning in the Montseny Mountains (NE Spain). Annales Des Sciences Forestieres, 50(3), 247–256. https://doi.org/10.1051/forest:19930303

Meinzer, F. C., Woodruff, D. R., Eissenstat, D. M., Lin, H. S., Adams, T. S., & McCulloh, K. A. (2013). Above-and belowground controls on water use by trees of different wood types in an eastern US deciduous forest. Tree Physiology, 33(4), 345–356. https://doi.org/10.1093/treephys/tpt012

Meli, P., Holl, K. D., Benayas, J. M. R., Jones, H. P., Jones, P. C., Montoya, D., & Mateos, D. M. (2017). A global review of past land use, climate, and active vs. passive restoration effects on forest recovery. PLoS ONE, 12(2), 1–17. https://doi.org/10.1371/journal.pone.0171368

Modrow, T., Kuehne, C., Saha, S., Bauhus, J., & Pyttel, P. L. (2020). Photosynthetic performance, height growth, and dominance of naturally regenerated sessile oak (Quercus petraea [Mattuschka] Liebl.) seedlings in small-scale canopy openings of varying sizes. European Journal of Forest Research, 139(1), 41–52. https://doi.org/10.1007/s10342-019-01238-7

Muhr, J., Messier, C., Delagrange, S., Trumbore, S., Xu, X., & Hartmann, H. (2016). How fresh is maple syrup? Sugar maple trees mobilize carbon stored several years previously during early springtime sap-ascent. New Phytologist, 209(4), 1410–1416. https://doi.org/10.1111/nph.13782

Munson, S. M., & Lauenroth, W. K. (2009). Plant population and community responses to removal of dominant species in the shortgrass steppe. Journal of Vegetation Science, 20(2), 224–232. https://doi.org/10.1111/j.1654-1103.2009.05556.x

Naeem, S., Duffy, J. E., & Zavaleta, E. (2012). The Functions of Biological Diversity in an Age of Extinction. Science, 336(6087), 1401–1406. https://doi.org/10.1126/science.1215855

Naeem, S., Prager, C., Weeks, B., Varga, A., Flynn, D. F. B., Griffin, K., Muscarella, R., Palmer, M., Wood, S., & Schuster, W. (2016). Biodiversity as a multidimensional construct: A review, framework and case study of herbivory's impact on plant biodiversity. Proceedings of the Royal Society B: Biological Sciences, 283(1844). https://doi.org/10.1098/rspb.2015.3005

Nagel, J. M., Griffin, K. L., Schuster, W. S. F., Tissue, D. T., Turnbull, M. H., Brown, K. J., & Whitehead, D. (2002). Energy investment in leaves of red maple and co-occurring oaks within a forested watershed. Tree Physiology, 22(12), 859–867. https://doi.org/10.1093/treephys/22.12.859

Neuwirth, B., Rabbel, I., Bendix, J., Bogena, H. R., & Thies, B. (2021). The european heat wave 2018: The dendroecological response of oak and spruce in western germany. Forests, 12(3), 1–17. https://doi.org/10.3390/f12030283

Niinemets, Ü. (2007). Photosynthesis and resource distribution through plant canopies. Plant, Cell and Environment, 30(9), 1052–1071. https://doi.org/10.1111/j.1365-3040.2007.01683.x

Niu, D., Yuan, X., Cease, A. J., Wen, H., Zhang, C., Fu, H., & Elser, J. J. (2018). The impact of nitrogen enrichment on grassland ecosystem stability depends on nitrogen addition level. Science of the Total Environment, 618(768), 1529–1538. https://doi.org/10.1016/j.scitotenv.2017.09.318

Noel, A. R. A. (1970). The girdled tree. The Botanical Review, 36(2), 162–195. https://doi.org/10.1007/BF02858959

Norden, N., Angarita, H. A., Bongers, F., Martínez-Ramos, M., Cerda, I. G. D. La, Van Breugel, M., Lebrija-Trejos, E., Meave, J. A., Vandermeer, J., Williamson, G. B., Finegan, B., Mesquita, R., & Chazdon, R. L. (2015). Successional dynamics in Neotropical forests are as uncertain as they are predictable. Proceedings of the National Academy of Sciences of the United States of America, 112(26), 8013–8018. https://doi.org/10.1073/pnas.1500403112

Oberhuber, W., Gruber, A., & Wieser, G. (2023). Seasonal and Daily Xylem Radius Variations in Scots Pine Are Closely Linked to Environmental Factors Affecting Transpiration. Biology, 12(9). https://doi.org/10.3390/biology12091251

Ogle, K., Barber, J. J., Barron-Gafford, G. A., Bentley, L. P., Young, J. M., Huxman, T. E., Loik, M. E., & Tissue, D. T. (2015). Quantifying ecological memory in plant and ecosystem processes. Ecology Letters, 18(3), 221–235. https://doi.org/10.1111/ele.12399

Oksanen, J., Blanchet, F., Kindt, R., Legendre, P., Minchin, P. R., O'Hara, R. B., Simpson, G. L., Solymos, P., Stevens, M. H. M., & Wagner, H. (2010). Community ecology package: vegan. In R: A Language and Environment for Statistical Computing.

Orwig, D. A., Foster, D. R., & Mausel, D. L. (2002). Landscape patterns of hemlock decline in New England due to the introduced hemlock woolly adelgid. Journal of Biogeography, 29(10–11), 1475–1487. https://doi.org/10.1046/j.1365-2699.2002.00765.x

Pan, Q., Tian, D., Naeem, S., Auerswald, K., Elser, J. J., Bai, Y., Huang, J., Wang, Q., Wang, H., Wu, J., & Han, X. (2016). Effects of functional diversity loss on ecosystem functions are influenced by compensation. Ecology, 97(9), 2293–2302. https://doi.org/10.1002/ecy.1460

Pellegrini, A. F. A., Hein, A. M., Cavender-Bares, J., Montgomery, R. A., Staver, A. C., Silla, F., Hobbie, S. E., & Reich, P. B. (2021). Disease and fire interact to influence transitions between savanna–forest ecosystems over a multi-decadal experiment. Ecology Letters, 24(5), 1007–1017. https://doi.org/10.1111/ele.13719

Pennekamp, F., Pontarp, M., Tabi, A., Altermatt, F., Alther, R., Choffat, Y., Fronhofer, E. A., Ganesanandamoorthy, P., Garnier, A., Griffiths, J. I., Greene, S., Horgan, K., Massie, T. M., Mächler, E., Palamara, G. M., Seymour, M., & Petchey, O. L. (2018). Biodiversity increases and decreases ecosystem stability. Nature. https://doi.org/10.1038/s41586-018-0627-8

Perez, S. B., Fraterrigo, J. M., & Dalling, J. W. (2022). Interspecific wood trait variation predicts decreased carbon residence time in changing forests. Functional Ecology, 36(3), 674–685. https://doi.org/10.1111/1365-2435.13936

Peters, R. L., Steppe, K., Pappas, C., Zweifel, R., Babst, F., Dietrich, L., von Arx, G., Poyatos, R., Fonti, M., Fonti, P., Grossiord, C., Gharun, M., Buchmann, N., Steger, D. N., & Kahmen, A. (2023). Daytime stomatal regulation in mature temperate trees prioritizes stem rehydration at night. New Phytologist, 239(2), 533–546. https://doi.org/10.1111/nph.18964

Pretzsch, H. (2014). Canopy space filling and tree crown morphology in mixed-species stands compared with monocultures. Forest Ecology and Management, 327, 251–264. https://doi.org/10.1016/j.foreco.2014.04.027

Prieto, I., Armas, C., & Pugnaire, F. I. (2012). Water release through plant roots: New insights into its consequences at the plant and ecosystem level. New Phytologist, 193(4), 830–841. https://doi.org/10.1111/j.1469-8137.2011.04039.x

Rao, M. P., Cook, E. R., Cook, B. I., D'Arrigo, R. D., Palmer, J. G., Lall, U., Woodhouse, C. A., Buckley, B. M., Uriarte, M., Bishop, D. A., Jian, J., & Webster, P. J. (2020). Seven centuries of reconstructed Brahmaputra River discharge demonstrate underestimated high discharge and flood hazard frequency. Nature Communications, 11(1), 1–10. https://doi.org/10.1038/s41467-020-19795-6

Ravenek, J. M., Bessler, H., Engels, C., Scherer-Lorenzen, M., Gessler, A., Gockele, A., de Luca, E., Temperton, V. M., Ebeling, A., Roscher, C., Schmid, B., Weisser, W. W., Wirth, C., De Kroon, H., Weigelt, A., & Liesje, M. J. (2014). Long-term study of root biomass in a biodiversity experiment reveals shifts in diversity effects over time. Oikos, 123(12), 1528–1536. https://doi.org/10.1111/oik.01502

Reinmann, A. B., Bowers, J. T., Kaur, P., & Kohler, C. (2023). Compensatory responses of leaf physiology reduce effects of spring frost defoliation on temperate forest tree carbon uptake. Frontiers in Forests and Global Change, 6(February), 1–13. https://doi.org/10.3389/ffgc.2023.988233

Robertson, W. M., Robinett, M., & McCullough, D. G. (2018). Soil moisture response to white ash mortality following emerald ash borer invasion. Environmental Earth Sciences, 77(9), 1–14. https://doi.org/10.1007/s12665-018-7525-0

Royo, A. A., Peterson, C. J., Stanovick, J. S., & Carson, W. P. (2016). Evaluating the ecological impacts of salvage logging: Can natural and anthropogenic disturbances promote coexistence? Ecology, 97(6), 1566–1582. https://doi.org/10.1890/15-1093.1

Sala, A., Woodruff, D. R., & Meinzer, F. C. (2012). Carbon dynamics in trees: Feast or famine? Tree Physiology, 32(6), 764–775. https://doi.org/10.1093/treephys/tpr143

Salomón, R. L., Peters, R. L., Zweifel, R., Sass-Klaassen, U. G. W., Stegehuis, A. I., Smiljanic, M., Poyatos, R., Babst, F., Cienciala, E., Fonti, P., Lerink, B. J. W., Lindner, M., Martinez-Vilalta, J., Mencuccini, M., Nabuurs, G. J., van der Maaten, E., von Arx, G., Bär, A., Akhmetzyanov, L., … Steppe, K. (2022). The 2018 European heatwave led to stem dehydration but not to consistent growth reductions in forests. Nature Communications, 13(1), 1–11. https://doi.org/10.1038/s41467-021-27579-9

Schindler, D. E., Armstrong, J. B., & Reed, T. E. (2015). The portfolio concept in ecology and evolution. Frontiers in Ecology and the Environment, 13(5), 257–263. https://doi.org/10.1890/140275

Schindler, D. E., Hilborn, R., Chasco, B., Boatright, C. P., Quinn, T. P., Rogers, L. A., & Webster, M. S. (2010). Population diversity and the portfolio effect in an exploited species. Nature, 465(7298), 609–612. https://doi.org/10.1038/nature09060

Schuster, W. S. F., Griffin, K. L., Roth, H., Turnbull, M. H., Whitehead, D., & Tissue, D. T. (2008). Changes in composition, structure and aboveground biomass over seventy-six years (1930-2006) in the Black Rock Forest, Hudson Highlands, southeastern New York State. Tree Physiology, 28, 537–549. https://doi.org/10.1093/treephys/28.4.537

Singh, S. P., Rawat, Y. S., & Garkoti, S. C. (1997). Failure of brown oak (Quercus semecarpifolia) to regenerate in central Himalaya: A case of environmental semisurprise. Current Science, 73(4), 371–374.

Smith, E. A., O'Loughlin, D., Buck, J. R., & St. Clair, S. B. (2011). The influences of conifer succession, physiographic conditions and herbivory on quaking aspen regeneration after fire. Forest Ecology and Management, 262(3), 325–330. https://doi.org/10.1016/j.foreco.2011.03.038

Smith, M. D., & Knapp, A. K. (2003). Dominant species maintain ecosystem function with non-random species loss. Ecology Letters, 6(6), 509–517. https://doi.org/10.1046/j.1461-0248.2003.00454.x

Tague, C. L., Moritz, M., & Hanan, E. (2019). The changing water cycle: The eco-hydrologic impacts of forest density reduction in Mediterranean (seasonally dry) regions. Wiley Interdisciplinary Reviews: Water, 6(4), 1–15. https://doi.org/10.1002/wat2.1350

Telfer, E. S. (1969). Weight–diameter relationships for 22 woody plant species. Canadian Journal of Botany, 47(12), 1851–1855. https://doi.org/10.1139/b69-271

Thomsen, J. E., Bohrer, G., Matheny, A. M., Ivanov, V. Y., He, L., Renninger, H. J., & Schäfer, K. V. R. (2013). Contrasting hydraulic strategies during dry soil conditions in Quercus rubra and Acer rubrum in a sandy site in Michigan. Forests, 4(4), 1106–1120. https://doi.org/10.3390/f4041106

Tilman, D., Lehman, C. L., & Bristow, C. E. (1998). Diversity-Stability Relationships: Statistical Inevitability or Ecological Consequence? The American Naturalist, 151(3), 277–282. https://doi.org/10.1086/286118

Tilman, D., Reich, P. B., & Knops, J. M. H. (2006). Biodiversity and ecosystem stability in a decade-long grassland experiment. Nature, 441(7093), 629–632. https://doi.org/10.1038/nature04742

Tsonis, A. A. (1996). Widespread increases in low-frequency variability over the past century. In Letters to Nature (Vol. 382, pp. 700–702).

Turnbull, M. H., Whitehead, D., Tissue, D. T., Schuster, W. S. F., Brown, K. J., Engel, V. C., & Griffin, K. L. (2002). Photosynthetic characteristics in canopies of Quercus rubra, Quercus prinus and Acer rubrum differ in response to soil water availability. Oecologia, 130(4), 515–524. https://doi.org/10.1007/s00442-001-0842-z

Turnbull, M. H., Whitehead, D., Tissue, D. T., Schuster, W. S. F., Brown, K. J., & Griffin, K. L. (2001). Responses of leaf respiration to temperature and leaf characteristics in three deciduous tree species vary with site water availability. Tree Physiology, 21(9), 571–578. https://doi.org/10.1093/treephys/21.9.571

Valencia, E., de Bello, F., Galland, T., Adler, P. B., Lepš, J., E-Vojtkó, A., van Klink, R., Carmona, C. P., Danihelka, J., Dengler, J., Eldridge, D. J., Estiarte, M., García-González, R., Garnier, E., Gómez-García, D., Harrison, S. P., Herben, T., Ibáñez, R., Jentsch, A., … Götzenberger, L. (2020). Synchrony matters more than species richness in plant community stability at a global

scale. Proceedings of the National Academy of Sciences of the United States of America, 117(39), 24345–24351. https://doi.org/10.1073/pnas.1920405117

van de Gevel, S. L., Hart, J. L., Spond, M. D., White, P. B., Sutton, M. N., & Grissino-Mayer, H. D. (2012). American chestnut (Castanea dentata) to northern red oak (Quercus rubra): forest dynamics of an old-growth forest in the Blue Ridge Mountains, USA. Botany, 90(12), 1263–1276. https://doi.org/10.1139/b2012-100

van der Plas, F. (2019). Biodiversity and ecosystem functioning in naturally assembled communities. Biological Reviews, 94(4), 1220–1245. https://doi.org/10.1111/brv.12499

Wang, S., Isbell, F., Deng, W., Hong, P., Dee, L. E., Thompson, P., & Loreau, M. (2021). How complementarity and selection affect the relationship between ecosystem functioning and stability. Ecology, 102(6), 1–12. https://doi.org/10.1002/ecy.3347

Wang, S., & Loreau, M. (2014). Ecosystem stability in space: α, β and γ variability. Ecology Letters, 17(8), 891–901. https://doi.org/10.1111/ele.12292

Weltzin, J. J. F., Loik, M. E. M., Schwinning, S., Williams, D. G., Fay, P. a., Haddad, B. M., Harte, J., Huxman, T. E., Knapp, A. K., Lin, G., Pockman, W. T., Shaw, M. R., Small, E. E., Smith, M. D., Smith, S. D., Tissue, D. T., & Zak, J. C. (2003). Assessing the Response of Terrestrial Ecosystems to Potential Changes in Precipitation. BioScience, 53(10), 941. https://doi.org/10.1641/0006-3568(2003)053[0941:ATROTE]2.0.CO;2

Werner, C., Schnyder, H., Cuntz, M., Keitel, C., Zeeman, M. J., Dawson, T. E., Badeck, F. W., Brugnoli, E., Ghashghaie, J., Grams, T. E. E., Kayler, Z. E., Lakatos, M., Lee, X., Máguas, C., Ogée, J., Rascher, K. G., Siegwolf, R. T. W., Unger, S., Welker, J., … Gessler, A. (2012). Progress and challenges in using stable isotopes to trace plant carbon and water relations across scales. Biogeosciences, 9(8), 3083–3111. https://doi.org/10.5194/bg-9-3083-2012

Whitehead, D., Griffin, K. L., Turnbull, M. H., Tissue, D. T., Engel, V. C., Brown, K. J., Schuster, W. S. F., & Walcroft, A. S. (2004). Response of total night-time respiration to differences in total daily photosynthesis for leaves in a Quercus rubra L. canopy: Implications for modelling canopy CO2 exchange. Global Change Biology, 10(6), 925–938. https://doi.org/10.1111/j.1529-8817.2003.00739.x

Whittaker, R. H., & Woodwell, G. M. (1968). Dimension and Production Relations of Trees and Shrubs in the Brookhaven Forest, New York. Journal of Ecology, 56(1), 1–25. https://doi.org/10.2307/2258063

Yang, H., Jiang, L., Li, L., Li, A., Wu, M., & Wan, S. (2012). Diversity-dependent stability under mowing and nutrient addition: Evidence from a 7-year grassland experiment. Ecology Letters, 15(6), 619–626. https://doi.org/10.1111/j.1461-0248.2012.01778.x

Yang, Z., van Ruijven, J., & Du, G. (2011). The effects of long-term fertilization on the temporal stability of alpine meadow communities. Plant and Soil, 345(1), 315–324. https://doi.org/10.1007/s11104-011-0784-0

Yi, K., Dragoni, D., Phillips, R. P., Roman, D. T., & Novick, K. A. (2017a). Dynamics of stem water uptake among isohydric and anisohydric species experiencing a severe drought. Tree Physiology, 37(10), 1379–1392. https://doi.org/10.1093/treephys/tpw126

Yi, K., Dragoni, D., Phillips, R. P., Roman, D. T., & Novick, K. A. (2017b). Dynamics of stem water uptake among isohydric and anisohydric species experiencing a severe drought. Tree Physiology, 37(10), 1379–1392. https://doi.org/10.1093/treephys/tpw126

Zavaleta, E. S., Hulvey, K. B., & Fulfrost, B. (2007). Regional patterns of recruitment success and failure in two endemic California oaks. Diversity and Distributions, 13(6), 735–745. https://doi.org/10.1111/j.1472-4642.2007.00384.x

Zweifel, R., Drew, D. M., Schweingruber, F., & Downes, G. M. (2014). Xylem as the main origin of stem radius changes in eucalyptus. Functional Plant Biology, 41(5), 520–534. https://doi.org/10.1071/FP13240

Zweifel, R., Haeni, M., Buchmann, N., & Eugster, W. (2016). Are trees able to grow in periods of stem shrinkage? New Phytologist, 211(3), 839–849. https://doi.org/10.1111/nph.13995

Zweifel, R., Sterck, F., Braun, S., Buchmann, N., Eugster, W., Gessler, A., Häni, M., Peters, R. L., Walthert, L., Wilhelm, M., Ziemińska, K., & Etzold, S. (2021). Why trees grow at night. New Phytologist, 231(6), 2174–2185. https://doi.org/10.1111/nph.17552

Zweifel, R., Zimmermann, L., Zeugin, F., & Newbery, D. M. (2006). Intra-annual radial growth and water relations of trees: Implications towards a growth mechanism. Journal of Experimental Botany, 57(6), 1445–1459. https://doi.org/10.1093/jxb/erj125

Appendix A: Supplementary Information for Chapter 1

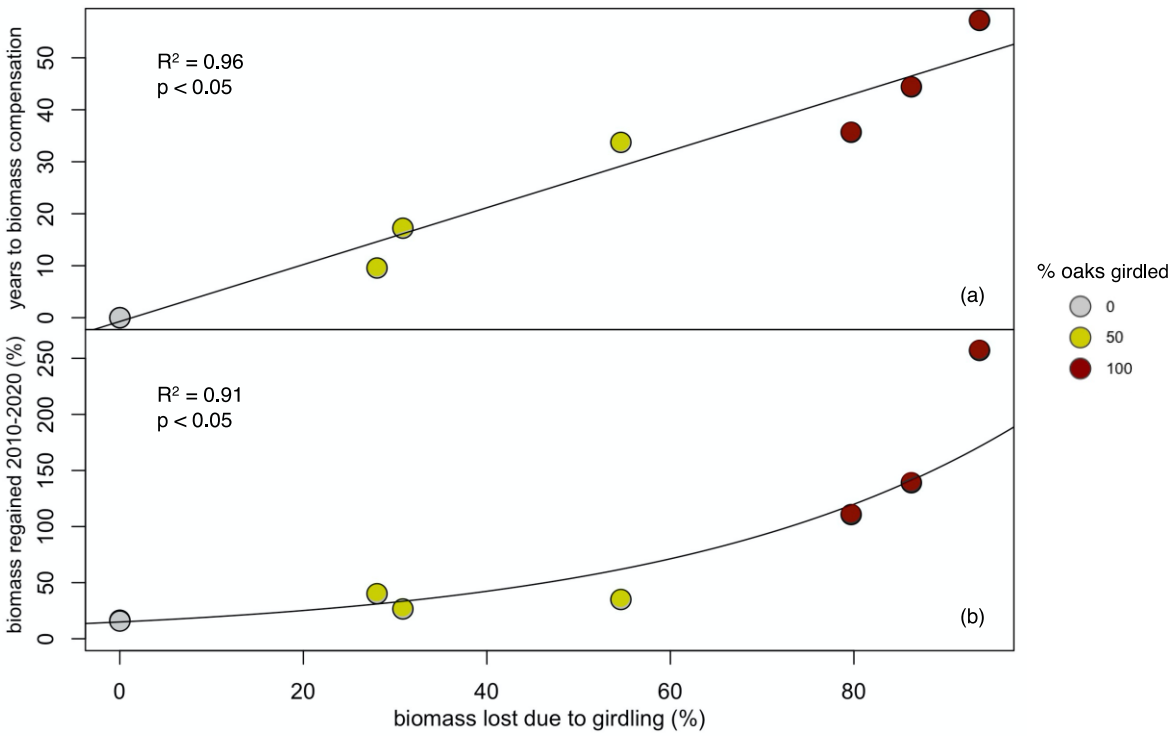

Figure S1.1 Relationships between the percentage of the original plot's biomass lost due to girdling with number of years to biomass compensation and percentage of biomass gained

The relationships between the percentage of the original plot's biomass lost due to girdling with number of years (since 2010) to biomass compensation (a) and percentage of biomass gained 2010-2020 as a percentage of biomass post-girdling (b). In 2008 and 2010, oak trees (*Quercus* spp.) were girdled according to one of three treatments: (1) 100% (red), (2) 50% (yellow), and (3) 0% (grey) of oaks girdled.

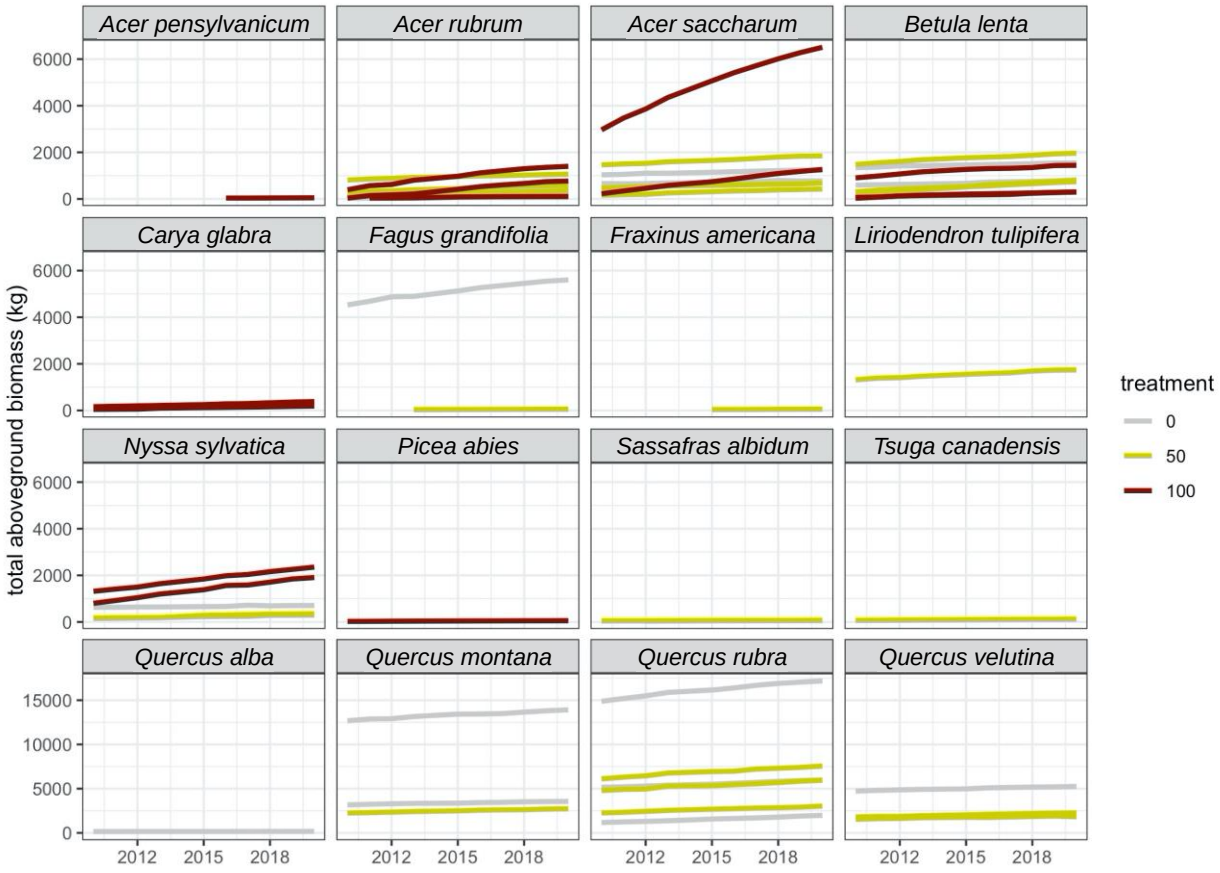

Figure S1.2 Total biomass accumulation for all species in the years following the girdling treatments, 2010-2020.

Each line represents the total aboveground biomass for a given species within a plot; there are three plots per treatment. If no line exists for a given treatment, that species was not present in that plot/treatment. Note *Quercus* species (bottom row) are on a different scale.

Appendix B: Supplementary Information for Chapter 2

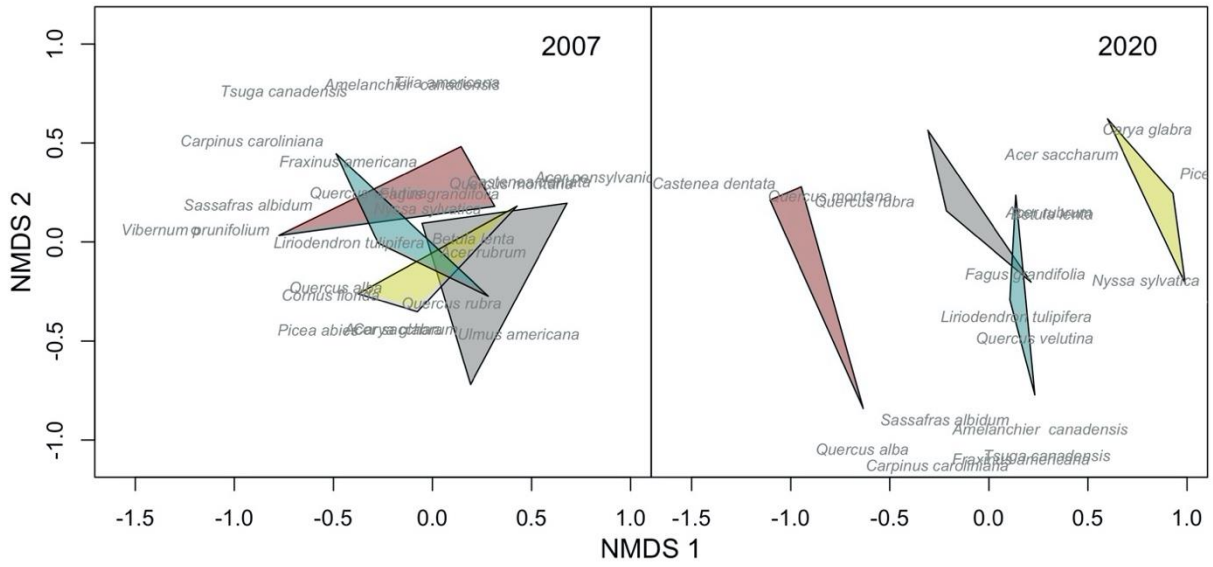

Figure S2.1 Non-metric dimensional scaling (NMDS) for species biomass at the experimental forest plots at Black Rock Forest, NY in 2007 and in 2020

In 2008 and 2010, selective girdling of trees was carried out according to one of three treatments: (1) 100% (red), (2) 50% (yellow), and (3) 0% (grey) of oaks girdled. Each treatment had three plot replicates, which are the corners of each correspondingly colored triangle. In 2007, the colors refer to the treatment that would be applied in 2008 and 2010. As these triangles overlap, no systematic differences exist in the communities prior to the girdling. By 2020, each treatment occupies a distinct space defined by its constituent species' relative biomass. This suggests that the plots' communities have not yet recovered from the girdling treatment.

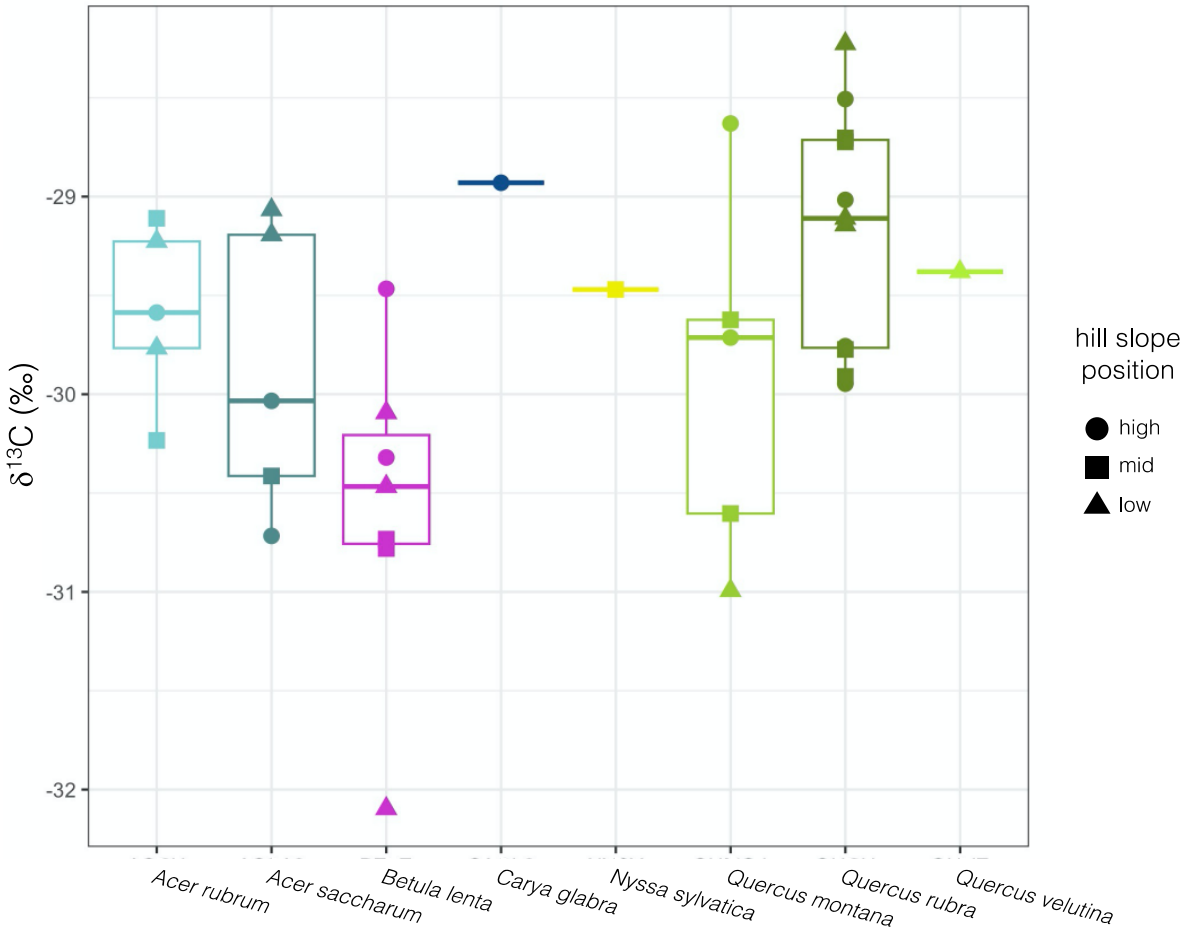

Figure S2.2 Ratio of carbon-13 (^{13}C) to carbon-12 (^{12}C) ($\delta^{13}C$) by species and position on hill slope

Appendix C: Supplementary Information for Chapter 3

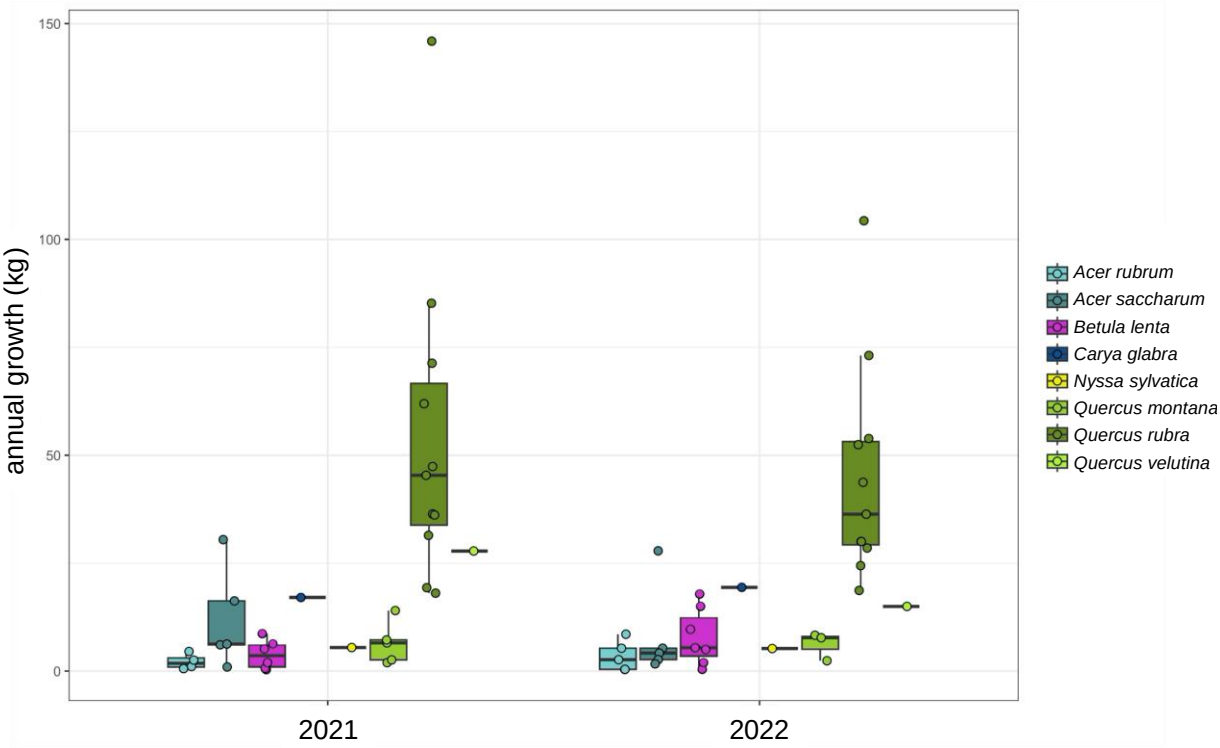

Figure S3.1 Annual growth of different species as measured by dendrometers.

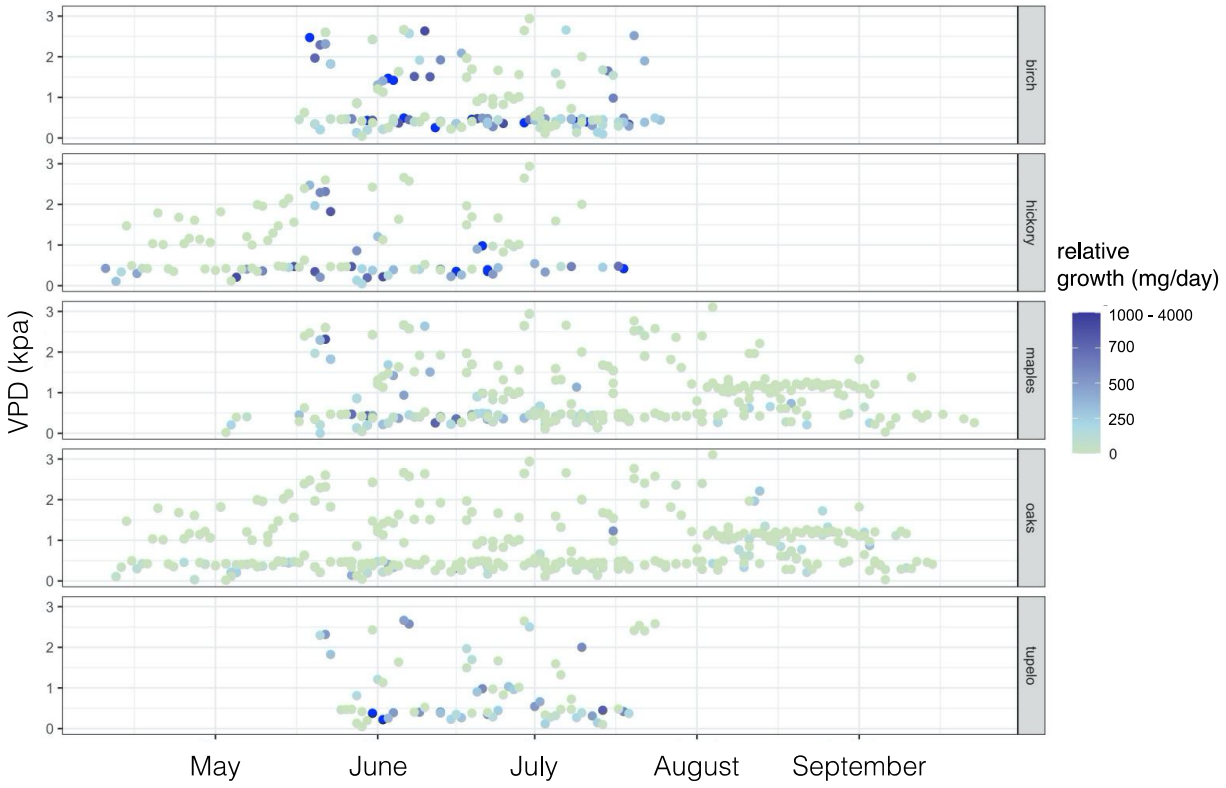

Figure S3.2 Effect of vapor pressure deficit on growth (mg/day) phenology of different species

Growth rate (mg/day) of each tree by day of year (labelled by month) and vapor pressure deficit (VPD) for two years. Each point is colored by its relative growth rate (mg/day), but the scale makes it difficult to see differences. Note that hickory and tupelo only had a single dendrometer each.

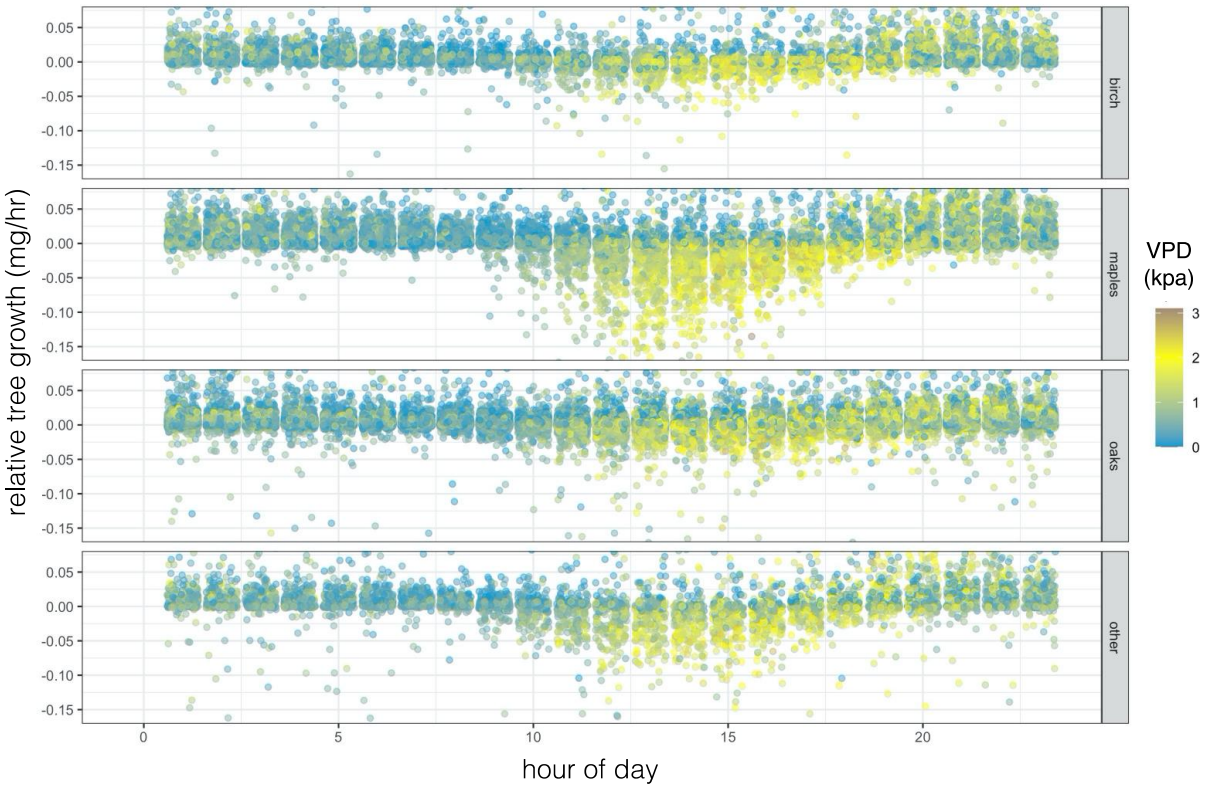

Figure S3.3 Relationship between relative growth, hour of day and VPD, by species, as measured by automated point dendrometers.

Carya glabra and *Nyssa sylvatica*, which each were represented by a single dendrometer, are grouped as "other" for comparison with Fig. 3.4.